ADDIS ABABA UNIVERSITY

ADDIS ABABA INSITUTE OF TECHNOLOGY

SCHOOL OF CIVIL AND ENVIROMENTAL ENGINEERING

Parametric Study of Shear Strength of Reinforced Concrete Beams

A Thesis in Structural Engineering

By Netsanet Bezu

4/19/2018

Addis Ababa

Submitted in Partial Fulfillment of the Requirement for the Degree of Master of Science

ADDIS ABABA UNIVERSITY

ADDIS ABABA INSTITUTE OF TECHNOLOGY

SCHOOL OF CIVIL AND ENVIRONMENTAL ENGINEERING

"Parametric Study of Shear Strength of Reinforced Concrete Beams"

Submmited By

Netsanet Bezu

Approved by the Board of Examiners:

1. Dr. Abreham Gebre	_____	_____
Adviser	**Signature**	**Date**
2. _____	_____	_____
Internal Examiner	**Signature**	**Date**
3. _____	_____	_____
External Examiner	**Signature**	**Date**

AKNOWLEGEMNTS

I would like to thank my families for their support and encouragement throughout my life and career.

I would like to extend my deepest gratitude to my adviser, Dr. Abreham Gebre, for his guidance and support throughout the research work. I appreciate his broad range of expertise and patience.

Table of Contents

AKNOWLEGEMNTS i

LIST OF TABLES v

LIST OF FIGURES vi

ABSTRACT viii

CHAPTER 1 ..... - 1 -

INTRODUCTION ..... - 1 -

1.1 General Background ..... - 1 -
1.2 Research Significance ..... - 2 -
1.3 Objective ..... - 3 -
1.4 Scope and Limitation ..... - 3 -
1.5 Methodology ..... - 3 -
1.6 Organization of the Thesis ..... - 4 -

CHAPTER 2 ..... - 5 -

LITRATURE REVIEW ..... - 5 -

2.1 Previous Size Effect Investigation ..... - 5 -
2.2 Mode of Shear failures and Crack Pattern ..... - 9 -
2.2.1 Diagonal-Tension failure: ..... - 10 -
2.2.2 Shear-Tension Failure: ..... - 10 -
2.2.3 Shear-Compression Failure: ..... - 11 -
2.3 Shear Transfer Mechanisms in Reinforced Concrete Beams ..... - 11 -
2.3.1 Un-Cracked Concrete Zone ..... - 12 -
2.3.2 Interface Shear Transfer ..... - 12 -
2.3.3 Dowel Action of Longitudinal Reinforcement ..... - 13 -
2.3.4 Residual Tensile Stresses across Cracks ..... - 13 -
2.3.5 Beam Action ..... - 14 -
2.3.6 Arch Action ..... - 14 -
2.3.7 Shear Reinforcement ..... - 15 -

2.4 Parameters Influencing the Shear Strength ..... - 16 -
2.4.1 Shear Span to Depth Ratio ..... - 16 -
2.4.2 Size Effect ..... - 17 -
2.4.3 Longitudinal Reinforcement Ratio and Arrangement ..... - 17 -
2.4.4 Axial Force ..... - 17 -
2.4.5 Concrete Strength and Aggregates Size ..... - 17 -
2.4.6 Load Distribution ..... - 18 -
2.4.7 Cross Section Shape ..... - 18 -
2.5 Shear Model for Reinforced Concrete Member ..... - 19 -
2.5.1 Compression Field Approach ..... - 19 -
2.5.2 Truss Model Approaches ..... - 22 -

CHAPTER 3 ..... - 29 -

Shear Design Method ..... - 29 -

3.1 ACI Shear Design Procedure ..... - 29 -
3.2 CSA Simplified Shear Design Procedure ..... - 31 -
3.3 EN 1992:2004 Euro Code 2 ..... - 31 -
3.4 Modified Compression Field Theory Shear Design Procedure ..... - 33 -

CHAPTER 4 ..... - 36 -

NONLINEAR FINITE ELEMENT ANALYSIS OF RC BEAMS ... - 36 -

4.1 General ..... - 36 -
4.2 Material ..... - 37 -
4.3 Model Validation ..... - 38 -
4.3.1 Specimen ..... - 38 -
4.3.2 Materials ..... - 38 -
4.3.3 Modeling ..... - 39 -
4.3.4 Support Condition and Loading ..... - 40 -
4.4 Shear Strength Behavior of Selected RC Beams ..... - 41 -
4.5 Scaling Factor of the Output Parameter Shear Capacity of RC Beams ..... - 44 -
4.6 Load Deflection Analysis ..... - 45 -
4.7 Regression Analysis ..... - 50 -
4.7.1 Partial Least Square Regression Analysis ..... - 50 -

CHARTER 5 ..... - 53 -

PARAMETRIC STUDY ..... - 53 -

5.1 Introduction ..... - 53 -
5.2 Statistical Data Analysis ..... - 53 -
5.2.1 The XLSTAT Approach ..... - 53 -
5.2.2 Sensitivity Analysis ..... - 55 -
5.2.3 The Variable Importance in the Project (VIP) ..... - 57 -
5.2.4 Model Parameters ..... - 58 -
5.2.5 Predictions and Residuals (Variable Shear Force V_u (kN) Analysis): ..... - 59 -
5.2.6 Outliers Analysis: ..... - 60 -

CHAPTER 6 ..... - 63 -

CONCLUSION AND RECOMMENDATION ..... - 63 -

6.1 Conclusion ..... - 63 -
6.2 Recommendation ..... - 63 -

References ..... - 64 -

APPENDIX A ..... - 65 -

Beam Models for Vector -3 Formwork Analysis ..... - 65 -

APPENDIX B ..... - 77 -

Analysis Outputs ..... - 77 -

LIST OF TABLES

Table 4- 1- Specimen Detail ..... - 38 -
Table 4- 2- Material properties and elements used in modelling for concrete ..... - 39 -
Table 4- 3- Material properties and elements used in modelling for reinforcement ... - 39 -
Table 4- 4- Verification of Results ..... - 40 -
Table 4- 5 - Mechanical Properties of Reinforcement Bar ..... - 41 -
Table 4- 6- Mechanical Properties of Concrete ..... - 42 -
Table 4 -7- Statistical Variations of Random Variables ..... - 43 -
Table 4 - 8 -32x7 LHS Layers of Random Variables and Simulation Output ..... - 43 -
Table 4- 9- Results from Nonlinear Finite Element Analysis ..... - 46 -
Table 4-10 - Correlation Matrix Table ..... - 52 -

Table 5 - 1 - Model Quality ..... - 54 -
Table 5 - 2 - Relative Importance of Input Parameters for the Model ..... - 57 -
Table 5 - 3 - Standardized Coefficients (Variable Shear Force Vu VECTOR-3) ..... - 58 -

LIST OF FIGURES

Figure 2- 1- Relative strength (ultimate moment/flexural moment) vs. shear span to depth ratio (a/d) (Kani 1967) ..... - 5 -
Figure 2- 2- Influence of member depth and aggregate size on shear stress at failure for tests carried out by Shioya 1989 ..... - 8 -
Figure 2- 3 - Types of inclined cracks (NCHRP Report 549-2005) ..... - 9 -
Figure 2- 4 - Modes of shear failure of concrete beams (Pillai et. al. 2003) ..... - 11 -
Figure 2 - 5 - Normal and shear stresses over the depth of cracked reinforced concrete beam (WALT 1999) ..... - 12 -
Figure 2- 6 - Schematic distribution of the stresses [CEB 1997] ..... - 13 -
Figure 2- 7 - Different failure mechanisms of the dowel action ..... - 13 -
Figure 2- 8 - Fracture process zone and post-cracking response in tension of normal strength concrete (ASCE1998) ..... - 14 -
Figure 2- 9 - Concrete tooth model and equilibrium (ASCE1998) ..... - 14 -
Figure 2- 10 - Arch action detail ..... - 15 -
Figure 2- 11 - Components of Shear Force Over Crack Plain ..... - 16 -
Figure 2- 12 - The Kani's valley for beams with uniformly distributed load ..... - 18 -
Figure 2- 13 - Compression field theory (Mitchell and Collins 1974) ..... - 21 -
Figure 2- 14 - Truss analogy (MacGregor et al., 2012) ..... - 23 -
Figure 2- 15 - Construction of an analogous plastic truss (MacGregor et al., 2012) .. - 24 -
Figure 2- 16 - Truss Model for design (MacGregor et. al., 2012) ..... - 25 -
Figure 2- 17 - Forces in web reinforcements and compression diagonals ..... - 26 -
Figure 2- 18 - 45 Degree Truss Model (Mahmoud El-Mihilmy et al., 2008) ..... - 28 -

Figure 3 - 1-Determination of strains, εx , for non prestressed beam ..... - 35 -

Figure 4 - 1 - Typical Stress-Strain curve for Concrete ..... - 37 -
Figure 4- 2 - Typical Stress-Strain curve for Reinforcement Bar ..... - 38 -
Figure 4- 3 - Beam Cross Section of the Specimen B1 ..... - 38 -
Figure 4- 4 - Reinforced concrete beam model and cross section in Vector-3 (B1) ... - 40 -
Figure 4- 5 - Load – Deflection diagram of the beam specimen ..... - 41 -
Figure 4 - 6 - Typical Beam Cross Section ..... - 42 -
Figure 4 - 7- Load versus Mid Span Deflection of Selected RC Beams ..... - 45 -

Figure 5 - 1 - Model Quality ..... - 55 -
Figure 5 - 2 - Uncertainty of Random Variables ..... - 56 -
Figure 5 - 3 - Variable Importance of the Project ..... - 58 -
Figure 5 - 4 – Standard Residuals V_s Shear Force V_u (KN) Analysis ..... - 59 -
Figure 5 - 5- Predicted Shear Force V_u (KN) V_s shear Force V_u (KN) Analysis ..... - 59 -
Figure 5 - 6 - Observations Vs Standard Residuals ..... - 60 -
Figure 5 - 7 - Outlier Analysis with respect to input variables ..... - 62 -
Figure 5 - 8 - Outlier Analysis with respect to dependent output variable ..... - 62 -

ABSTRACT

Shear failure of reinforced concrete beam depends upon various parameters. On the basis of various parameters, numerous studies have been done to assure the actual behavior of shear failure. After a long research it is also controversial regarding the exact shear behavior of reinforced concrete structure elements.

The paper presents a parametric study of reinforced concrete beams on shear behavior. A nonlinear finite element analysis using VecTor-3 three dimensional simulation software were conducted to predict the ultimate shear capacity of reinforced concrete beams. A total of thirty two cases of randomly selected input variables namely, shear span to depth ratio (a/d), concrete compressive strength (f_c'), width (b), overall depth (D), longitudinal reinforcement ratio (ρ_l) and web reinforcement ratio (ρ_w) and aggregate size (as) have been analyzed. The random variables selection is done using Latin hypercube sampling method (LHS). The random variables distribution follows normal distribution. And then by taking the ultimate shear strength of the thirty two cases of beam from nonlinear finite element analysis, a statistical data analysis is performed using regression analysis in order to identify the most influential input parameter on the shear capacity of a reinforced concrete beams.

Results of statistical data analysis demonstrates the significance of seven input variables. Overall depth, width and aggregate size are highly influential. It is seen that moderate significance of shear span to depth ratio on shear stress. Shear span to depth ratio has also inverse relationship with shear capacity of beams and all the remaining input variables have direct relationship with shear capacity of reinforced concrete beams. Amount and distribution of reinforcement ratio on shear stress at failure have also moderately influences shear capacity. Finally it is revealed that there is little significance of compressive strength on ultimate shear capacity of a reinforced concrete beams. This will enable to consider factor of safety for the uncertain input parameters on shear design equations. It is helpful to construct empirical equation using large set of data.

Key Word; Shear Strength, Reinforced Concrete Beam, Parametric Study, Nonlinear Finite Element Analysis

CHAPTER 1

INTRODUCTION

1.1 General Background

In spite of the numerous research efforts directed at the shear capacity of reinforced concrete member, there is still great discord concerning the mechanisms that govern shear in reinforced concrete member. The behavior and design of reinforced concrete beam in shear remains an area of much concern. Approximately 40 years after the collapse of U.S. Air force hangar, attributed to inadequate shear design practice, research activities on this area continues. Design codes and procedures are changing continually and generally becoming more stringent. Structures that were designed several decades ago typically do not comply with the requirement of current design codes, with the implication that massive amounts of funds must be spent to rehabilitating and upgrading the infrastructures. It remains a pressing need to establish design and analysis methods that provide realistic assessments the strength, stiffness, and ductility of shear critical elements. [1]

Among the theoretical formulations developed in recent years for this purpose was the modified compression field theory (MCFT), essentially a smeared, rotating crack model for cracked reinforced concrete elements. On the basis of a number of panel tests, constitutive relations were developed describing the behavior of cracked reinforced concrete element in compression and in tension. This behavior, influenced by the mechanisms as compression softening and tension stiffening, is fundamentally different from that of plain concrete. The constitutive models developed were incorporated in to new design procedures that form the basis for the general methods for shear design in Canadian code, CSA A23.3 M94. They were incorporated in formulation of various nonlinear finite element algorithms as well. The resulting analysis procedures have been shown to provide accurate simulation of response for a wide range of structures including beams in flexure, shear and torsion, deep beam, shear walls, columns, and plates and shells. [1]

The use of smeared rotating crack models has gained some degree of acceptance among analysts; thus several alternative, but essentially similar, formulation were developed by a number of researchers. In addition, other researchers opted for smeared, fixed crack model. In general, formulation for both types can be shown to provide good correlation with test data for structures with that are orthogonally reinforced with the reinforcement ratio in the weaker direction being 0.1% or greater. [1]

According to researchers, however, in the application to beams with little or no shear reinforcement, and loaded so as to be critical in shear, the accuracy of the various analysis procedures has shown some deficiencies. Chung and Ahmed concluded that "results indicate that the modified compression field theory (MCFT) is not applicable to lightly reinforced or unreinforced concrete members. These conclusions, however, were based on analyses that were an incomplete adaptation for the theory. [1]

Youb and Filippou, using a model that is an extension of both the MCFT and work by Balakrishnan and Murray, were able to get good results for many structure types except lightly reinforced shear beams. Here, "numerical difficulties were, however, encountered when the crack distribution in the structural element does not satisfy the assumptions of smeared crack model, as in the case of beams without shear reinforcement." Hsu and Zhang also encountered problems in applying their rotating crack model to elements lightly reinforced in one direction. This prompted them to propose fixed crack model for use in such situations. On the other hand, Foster, among others, reported good success in using rotating crack model in the analysis of shear critical beams. [1]

Most smeared, rotating crack models are based on formulation involving average strains and average stresses. Few give consideration to local stress conditions at crack locations, although some incorporate a crack slip check. In the analysis of adequately reinforced structures, the resulting crack are well distributed and the analysis typically provides accurate simulations. In lightly reinforced shear beams, however, behavior is often governed by the formation of a dominant shear crack. Here, a consideration of the local stress conditions adjacent to the crack is critical to a proper analysis, hence the difficulty encountered by some of the previously cited researchers and others. [1]

1.2 Research Significance

Code provisions for shear capacity of reinforced concrete beam equations are conservative. Essentially influencing parameters are Loading and Supporting Conditions, horizontal and vertical web reinforcement, shear span-to-depth ratio, load and support bearing plates, distribution of the reinforcement along depth of the beam's web, tension reinforcement and compressive strength. Least influencing parameters are bottom cover, side cover, and width of the beam, distribution of vertical stirrups in the web, and aggregate size, presence of the web openings. The effect of above factors on the shear capacity and behavior of RC beams have been reviewed. This will enable to consider safety of margin on shear design equations using different codes. [2]

This research paper will address the significance of different influential parameters that affects the shear strength of a reinforced concrete beam which should be considered in shear design equations when designing a structural elements. This can be considered as a starting point for future researches and developments of design codes in the shear design of RC structures subjected to different loading condition.

1.3 Objective

The main objective of present research is to perform a parametric study on some influential input parameters in the design of shear strength of reinforced concrete beams and study their relative effect on shear strength of the reinforced concrete beam using regression analysis. In this study, a nonlinear explicit FE model has been implemented to evaluate the load and deflection capacity of reinforced concrete beams under two point loading as well as their failure modes. An appropriate constitutive material model has been chosen to consider the nonlinear behavior of concrete and steel, stiffness degradation of concrete and strain rate effects. For this purpose, the nonlinear finite element analysis VecTor-3 software, has been used. By taking the ultimate shear strength capacity of each simulated beam a parametric study is performed. And then statistical data evaluation on the predicted shear strength has been conducted.

1.4 Scope and Limitation

The scope of the present research paper is focused only on shear critical beams having a slender and deep shear span. Having a wide, narrow and deep cross section. A normal and high strength concrete, a normal strength steel material properties, balanced and over reinforced longitudinal reinforcement ratio, a minimum web reinforcement and an aggregate size ranging from small to medium size for the scaling factor of the input and output variables data. The input variables data ranges were distributed normal to generate an output data shear force. However it uses limited number of cases for the input data evaluation when modelling the beams. The statistical data analysis accuracy is better when the sampling data range is large set.

1.5 Methodology

Review the existing literature and different design code provision for shear strength capacity in the design of the reinforced concrete beam. In the beginning, scaling factor for the input variables range is established. And then random selection of input variables is done using Latin hyper cube sampling method (LHS). The input variables distribution follows normal distribution. Nonlinear finite element analysis using VecTor-3 simulation software has been conducted on thirty two randomly selected beam data cases in order to determine the ultimate shear strength capacity of

the reinforced concrete beam subjected to two point loading. Program model validation has been done using existing experimental data from literature.

Following this, a parametric study using partial least square regression analysis has been done. The analysis helped to know the most influential input parameters on ultimate shear strength of reinforced concrete beams. Finally statistical data evaluation on predicted shear strength has been performed. The statistical data analysis is performed using XLSTAT tool, 2017. It is working based on visual basic and developed with the C^{++} programming language.

1.6 Organization of the Thesis

Chapter one is the introduction part. A general background of the study is presented. Research significance, objectives of the research, scope and limitation of work and methodology is included. Literature review regarding shear strength capacity of reinforced concrete beams will be presented in chapter two. Chapter three deals with the design procedure for shear strength of reinforced concrete beams using different widely accepted international codes. Chapter four presents scaling factor for the input variables and random distribution of data using Latin hypercube sampling method, beam modelling and simulation using nonlinear finite element analysis three dimensional VecTor-3 program and regression analysis will be presented with result interpretation, load-deflection and crack patterns responses also covered in this chapter. A parametric study using partial least square regression analysis and sensitivity analysis as well as results will be presented in chapter five. Finally, in chapter six conclusion and recommendation will be covered.

Two appendices are added to this document. Appendix A and B, presenting beam model drawings for the analysis and results of the nonlinear finite element analysis program load deflection response diagrams.

CHAPTER 2

LITRATURE REVIEW

2.1 Previous Size Effect Investigation

Limited studies have been reported in the literature on the behavior and strength of deep beams, a fairly common structural element in tall buildings, offshore structures and in foundations systems.

In 1955, the Wilkins Air Force Depot warehouse in Shelby, Ohio, collapsed due to the shear failure of 36 in. (914 mm) deep beams which did not contain any stirrups at the location of failure. These beams had a longitudinal steel ratio of only 0.45%. They failed at a shear stress of only about 0.5MPa whereas the ACI Building Code of the time (ACI Committee 318, 1951) permitted an allowable working stress of 0.62 MPa for the 20 MPa concrete used in the beams. Experiments conducted at the Portland Cement Association on 12 in. (305 mm) deep model beams indicated that the beams could resist about 1.0 MPa. However, the application of an axial tension stress of about 1.4 MPa reduced the shear capacity by about 50%. It was thus concluded that tensile stresses caused by thermal and shrinkage movements were the reason for the beam failures. [3]

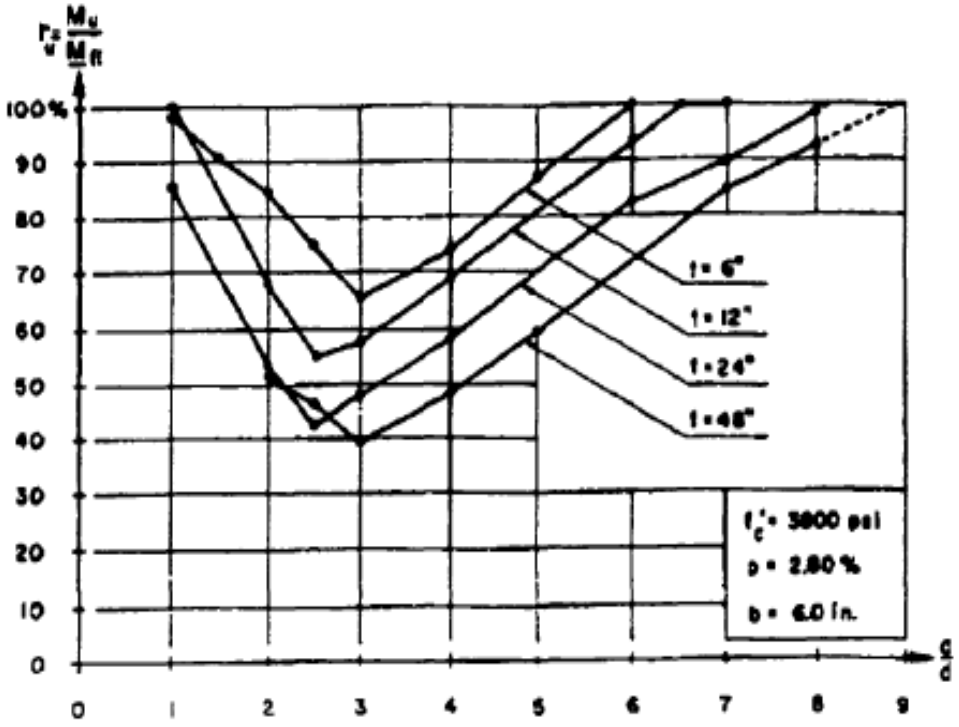

Figure 2- 1- Relative strength (ultimate moment/flexural moment) vs. shear span to depth ratio (a/d) (Kani 1967)

Kani (1966 and 1967) was amongst the first to investigate the effect of absolute member size on concrete shear strength after the dramatic warehouse shear failures of 1955. His work consisted of beams without web reinforcement with varying member depths, d, longitudinal steel

percentages, ρ, and shear span-to-depth ratios, a/d. He determined that member depth and steel percentage had a great effect on shear strength and that there is a transition point at a/d=2.5 at which beams are shear critical (i.e. the value of the bending moment at failure was minimum) (see Fig. 2.1).

Kani found this value of a/d to be the transition point between failure modes and is the same for different member sizes and steel ratios. Below an a/d value of about 2.5 the test beams developed arch action and had a considerable reserve of strength beyond the first cracking point. For a/d values greater than 2.5, failure was sudden, brittle and in diagonal tension soon after the first diagonal cracks appeared. This transition point is more emphasized in test beams containing higher reinforcement ratios and almost disappears in specimens with lower reinforcement ratios. In addition, Kani found a clearly defined envelope bounded by limiting values of ρ and a/d. Inside this envelope diagonal shear failures are predicted to occur and outside of this envelope flexural failures are predicted to occur. These conclusions regarding the influence of both ρ and a/d were similar for all beam depths tested. Kani also looked at the effect of beam width and found no significant effect on shear strength. Kani's work was summarized in the textbook "Kani on Shear in Reinforced Concrete". [3]

More recently, Bazant and Kim (1984) derived a shear strength equation based on the theory of fracture mechanics. This equation accounts for the size effect phenomenon as well as the longitudinal steel ratio and incorporates the effect of aggregate size. This equation was calibrated using 296 previous tests obtained from the literature and was compared with the ACI Code equations. It was noted after the comparison that the practice used in the ACI Code of designing for diagonal shear crack initiation rather than ultimate strength does not yield a uniform safety margin when different beam sizes are considered. It was also found, according to the new equation, that for very large specimen depths the factor of safety in the ACI Code almost disappears. However, no experimental evidence was available yet to confirm that fact as all the tests performed up to that time were on relatively small specimens. This equation was improved by Bazant and Sun (1987) to account for the maximum aggregate size distinctly from the size effect phenomenon and was extended to cover the influence of stirrups. This formula was calibrated using a larger set of test data consisting of 461 test results compiled from the literature. [3]

Later on, Bazant and Kazemi (1991) performed tests on geometrically similar beams with a size range of 1:16 and having a constant a/d ratio of 3.0 and a constant longitudinal steel ratio, ρ.

Beams tested varied in depth from 1 inch (25 mm) to 16 inches (406 mm). The main failure mode of the specimens tested was diagonal shear but the smallest specimen failed in flexure. This study confirmed the size effect phenomenon and helped corroborate the previously published formula. However, the deepest beam tested was relatively small and the authors concluded that for beams larger than 16 inches (406 mm) additional reductions in shear strength due to size effect were likely.

Kim and Park (1994) performed tests on beams with a higher than normal concrete strength (53.7 MPa). Test variables were longitudinal steel ratio, ρ, shear span-to-depth ratio, a/d, and effective depth, d. Beam heights varied from 170 mm to 1000 mm while the longitudinal steel ratio varied from 0.01 to 0.049 and a/d varied from 1.5 to 6.0. Their findings were similar to Kani's from which it was concluded that the behavior of the higher strength concrete is similar to that of normal-strength concrete. However, since only one concrete strength was investigated no general conclusions could be made with respect to concrete strength and shear capacity. [3]

Shioya (1989) conducted a number of tests on large-scale beams in which the influence of member depth and aggregate size on shear strength was investigated. In this study, lightly reinforced concrete beams containing no transverse reinforcement were tested under a uniformly distributed load. The beam depths in this experimental program ranged from 100 mm to 3000 mm. Shioya found that the shear stress at failure decreased as the member size increased and as the aggregate size decreased. It is interesting to note that the beams tested by Shioya contained about the same amount of longitudinal reinforcement as the roof beams of the Air Force warehouse which collapsed in 1955. The warehouse beams had an effective depth of 850 mm and failed at a shear stress of about $0.1\sqrt{f'c}$ MPa. This shear stress level corresponds with the failure shear stress observed in beams having a depth of 1000 mm in the Shioya tests. It is important to mention that there was a tendency for reduced shear stresses at failure even with tests including 3000 mm deep beams. Figure 2.2 illustrates the results obtained by shioya.

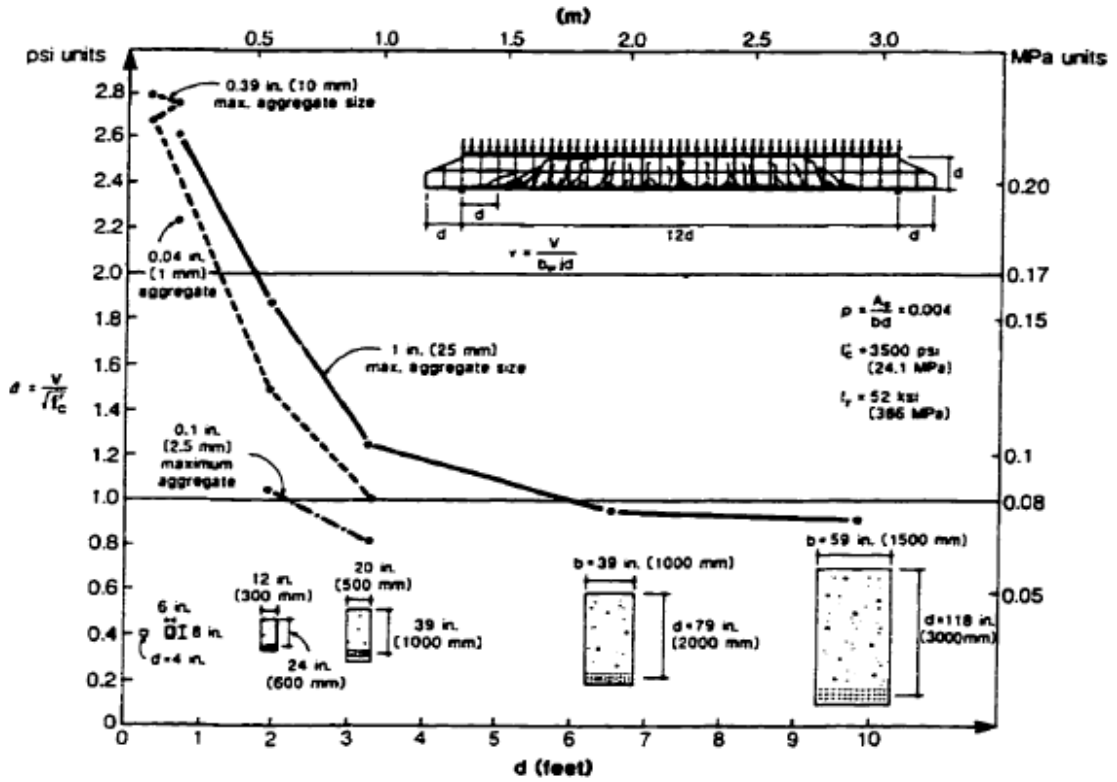

Figure 2- 2- Influence of member depth and aggregate size on shear stress at failure for tests carried out by Shioya 1989

Stanik (1998) performed tests on a wide range of beam specimens at the University of Toronto. The specimens tested had varying depths, d, ranging from 125 mm to 1000 mm, varying amounts of longitudinal steel (0.76% to 1.31%) as well as varying concrete strengths, f'_c, ranging from 37 MPa to 99 MPa. The longitudinal reinforcement was distributed in some specimens along the sides and some specimens contained the minimum amount of transverse reinforcement recommended by the CSA Standard (CSA 1994). In the series with longitudinal bars along the sides, a set of wider beams was also tested. The purpose was to evaluate the influence of the amount, as well as the distribution of the longitudinal steel on the shear strength. Stanik found that the size effect is very pronounced in lightly reinforced deep members. Members containing the minimum amount of transverse reinforcement or side distributed steel performed better than their counterparts with only bottom longitudinal reinforcing bars. Deep members with side distributed reinforcement performed nearly as well as the shallow members containing only bottom longitudinal reinforcement. As well, the wider members containing side distributed steel were weaker than the narrower ones with similar side distributed steel. Stanik concluded that the size effect is more related to measures controlling crack widths and crack spacing rather than the absolute depth of the member. Moreover, Stanik found very little gain in shear strength with the use of higher concrete strengths. In fact, he found that the shear strengths of the beams with 100

MPa concrete were only marginally greater than the shear strength of the 40 MPa beams. Stanik used the modified compression field theory proposed by the CSA Standard (CSA 1994) to predict the response of his test beams. He found good agreement between his experimental results and these predictions. He also proposed to use an effective aggregate size of zero in the modified compression field theory method for the very high-strength concretes in order to account for the insignificant gain in shear strength from the lower concrete strengths. Stanik also performed a comparison between his experimental results and the ACI Code (ACI committee 318-1995) expressions. He found that the ACI expressions substantially overestimate the shear contribution of concrete, notably in the deeper members. [3]

2.2 Mode of Shear failures and Crack Pattern

When the principal tensile stress at any point reaches the tensile strength of concrete, a crack will occur and open normal to the direction of the principal tensile stress or parallel with the direction of the principal compressive stress. Therefore, concrete members subjected to shear forces at ultimate load always have inclined cracks named diagonal cracks or shear cracks. Inclined cracks can be initiated in the web of beams where is proved to be the highest shear stress region and named web shear cracks. Inclined cracks developed from former flexural cracks are called flexure−shear cracks. [4]

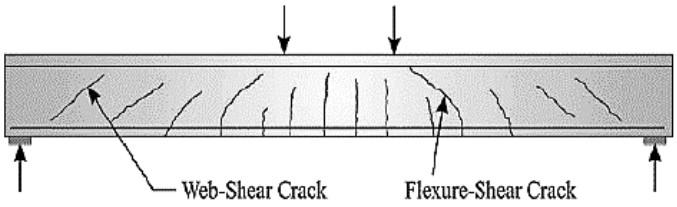

Figure 2- 3 - Types of inclined cracks (NCHRP Report 549-2005)

The type of failure caused by these cracks, usually in a very brittle and abrupt way, is called diagonal failure or shear failure. Normally, there are five different modes of failure caused by diagonal cracks depending on the dimensions, geometries, type of loading, and amount of longitudinal reinforcement and structural properties of concrete members (Fig. 2.4) as follows: (1) Diagonal tension failure (2) Shear compression failure (3) Shear tension failure (4) Web crushing failure and (5) Arch rib failure. Diagonal tension failure usually occurs in concrete members with low amount of stirrups and longitudinal reinforcement. Diagonal cracks may initiate from former flexural cracks and propagate rapidly over the whole cross section of the member until collapse (Fig. 2.4.a). For concrete members with low amount of web reinforcement but adequate longitudinal reinforcement ratio to form a compression zone, shear cracks may easily initiate from former flexural cracks but do not pass through the compression zone. The failure of

structure is caused by the crushing of the concrete in compression zone above the tip of the shear crack and named shear compression failure (Fig. 2.4.b). In cases that the longitudinal reinforcement loses the bond with concrete due to inadequate anchorage of the longitudinal bars or concrete cover, cracks tend to develop along the main bars until they combine with a flexural shear crack to cause shear tension failure as in the figure 2.4.c. Web crushing failure seems to be only identified in I-beams due to slender web thickness while arch rib failure usually occurs in deep beams or short span beams in which the direct force transfer from the loading location to the bearings is dominant (Fig. 2.4.d and 2.4.e). In fact, some normal modes of failure can totally be as a combination of two or more above modes of failure, for example, shear tension failure and shear compression failure. [4]

Failure modes of reinforced concrete beams can be summarized as follow:

2.2.1 Diagonal-Tension failure:

Always in the range of a/d above 2, and sometimes at lower a/d values, the diagonal crack starts from the last flexural crack and turns gradually into a crack more and more inclined under the shear loading, as noted in (Figure 2.4.a). Such a crack does not proceed immediately to failure, although in some of the longer shear spans this either seems almost to be the case or an entirely new and flatter diagonal crack suddenly causes failure. More typically, the diagonal crack encounters resistance as it moves up into the zone of compression, becomes flatter, and stops at some point. Further load; the tension crack extends gradually at a very flat slope until finally sudden failure occurs. The more inclined lower crack will open back, at least to the steel level, and the failure will start at the crack nearer the a/2. [2]

2.2.2 Shear-Tension Failure:

A curved tensile crack in a region of combined moment and shear may also one of two additional modes of failure. A secondary crack may propagate backward along the longitudinal reinforcement from the inclined crack, perhaps because of dowel action in the longitudinal reinforcement. This crack will cause a loss of bond, as the main reinforcement begins to slip, the wedging action of the bar deformations contributes to a splitting of the concrete and a further propagation of the crack, resulting in an anchorage failure of the longitudinal steel as shown in Figure 2.4.c. [2]

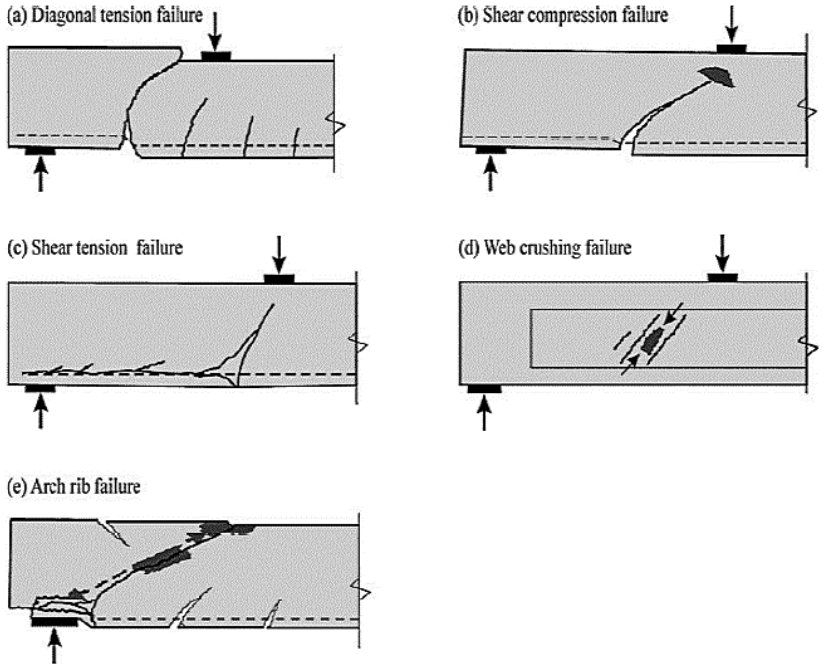

Figure 2- 4 - Modes of shear failure of concrete beams (Pillai et. al. 2003)

2.2.3 Shear-Compression Failure:

The vertical compressive stress under the load reduce the possibility of further tension cracking, and the vertical compressive stresses over the reaction likewise limit the bond splitting and diagonal cracking along the steel. Alternatively, a large shear in short shear spans may initiate approximately a 45° crack (called a web-shear crack) across the neutral axis before a flexural crack appears. Such a crack crowds the shear resistance into a small depth and leads to increasing stresses, and then tends to be self-propagating until stopped by the load or reaction. With either start, a compression failure finally occurs adjacent to the load. Such a failure can be expected to occur when the shear span (a) is less than four times the beam depth, or possibly a little less for very high strength concrete. When shear span is small, the increased shear strength may be significant, with the ultimate shear over twice as much for a = 1.5d as for a = 3.0d. The width of the critical crack, if there is no crack control steel, becomes large as the load increases, sometimes over 3 mm. The concrete above the upper end of the inclined crack fails by crushing in this mode of failure as shown in Figure 2.4.b. Other failure types such as anchorage failure and local crushing failure close to loads or supports are also possible. Such premature failures prevent the development of the full capacity of the beam and can be eliminated by appropriate detailing. [2]

2.3 Shear Transfer Mechanisms in Reinforced Concrete Beams

The reports of the ACI Committee 426 and ASCE-ACI 445 describe in detail the various failure modes and shear transfer mechanisms of members with and without transversal reinforcement. In these reports, the main parameters affecting the shear strength and several empirical formulas

were determined. Currently, these equations are still the basis of shear design rules in several standards.

These reports identify five shear transfer mechanisms of reinforced concrete members; (1) the interface shear transfer, (2) the dowel action of longitudinal reinforcement (3) the residual tensile stress across cracks, (4) the shear carried by the un–cracked concrete and (5) the arch action. Often the first four mechanisms are summarized in the Beam Action. These mechanisms depend on several parameters and in function of the load level influence more or less the shear strength. In reality it is a combination of the different types that allows the transfer of the shear force. The tri-axial state of stress, in the compression zone near the loading point, influences certainly the different failure criteria of the transfer mechanisms. [5]

2.3.1 Un-Cracked Concrete Zone (Shear Transfer by Concrete Shear Stress) (V_c)

In the un-cracked part of the members, the shear force is transferred by inclined principal tensile and compressive stresses, as visualized by the principal stress-trajectories. However, reinforced concrete members are often cracked. The cracks introduce a discontinuity and modify the stress-flow. But in the un-cracked compression zone, depth x, the elastic distribution of the shear stresses is still valid. The integration of the shear stresses over the depth gives a shear force component. The shear transferred by the un-cracked concrete depends on several parameters, like the shape of the cross-section, the member's depth or the presence of an axial force. [5]

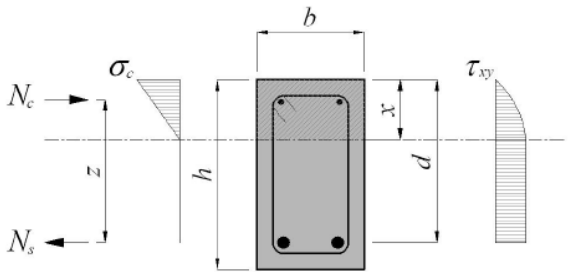

Figure 2 - 5 - Normal and shear stresses over the depth of cracked reinforced concrete beam (WALT 1999)

2.3.2 Interface Shear Transfer (Aggregate Interlock) (V_{av})

The interface shear transfer can be explained by the aggregates protruding from the crack surface that provide a resistance against the slip. This mechanism is often called aggregate interlock. According to several studies, the interface shear transfer is an important mechanism in shear strength of members without stirrups. The important role of this mechanism in the redistribution of diagonal compression fields in members with stirrups is well known. The interface shear

transfer capacity depends principally on the surface roughness, the crack opening and the crack sliding. [5]

2.3.3 Dowel Action of Longitudinal Reinforcement (V_d)

The dowel action is the capacity of the longitudinal reinforcement to carry a part of the shear force (Figure 2.6). This transfer mechanism depends principally on the following parameters: the reinforcement ratio, the diameter of the bars, their space, the stress in the reinforcement, the depth of the concrete cover and the concrete tensile strength. Two failure modes may be distinguished: The first failure mode is the splitting of the concrete cover under the reinforcement (Figure 2.7. a-b). This failure can be directly linked to the concrete tensile strength. The second failure mode is the crushing of the concrete on the bar followed by the yielding of the steel bar (Figure 2.7.c). In a member without transversal reinforcement, the dowel action is relatively low, because the longitudinal reinforcements are not supported by the stirrups.

The dowel action is more important for members with reinforcement implemented on several levels, in both directions or supported by stirrups. [5]

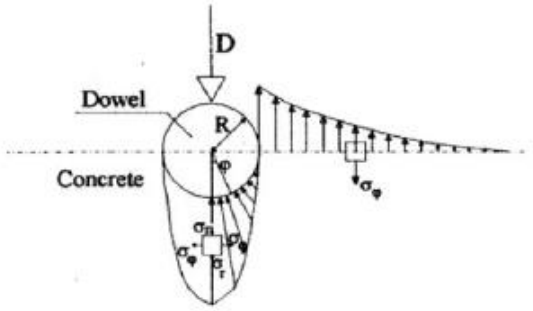

Figure 2- 6 - Schematic distribution of the stresses [CEB 1997]

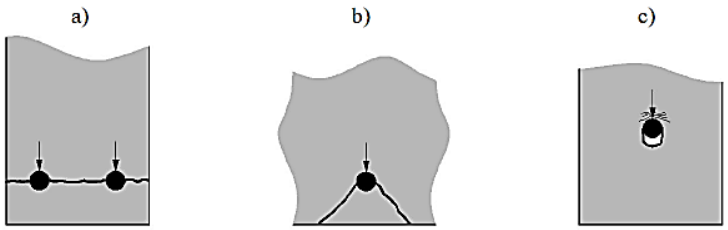

Figure 2- 7 - Different failure mechanisms of the dowel action

2.3.4 Residual Tensile Stresses across Cracks

The tensile behavior of concrete can be characterized by two phases. In the first phase, the behavior is elastic linear until the tensile strength f_{ct} is reached. In the second phase, and after the peak-strength, the stress drops rapidly with a softening branch (Figure 2.8). It exists several "bridges" across the crack for small openings (0.05 to 0.15 mm), thus allowing the transfer of the

tensile stress. In this second phase, the strains are localized in a small region called the fracture process zone. Therefore the response must be expressed in terms of stress – crack opening and not in terms of stress – strain. The application of fracture mechanics to shear design is based on the assumption that residual tensile stress is the principal shear transfer mechanism. [5]

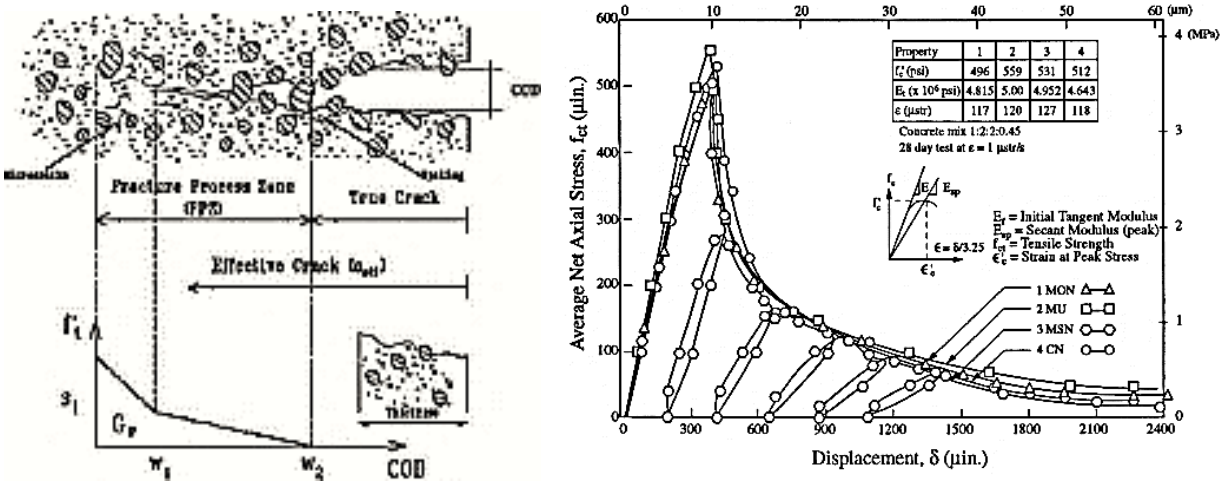

Figure 2- 8 - Fracture process zone and post-cracking response in tension of normal strength concrete (ASCE1998)

2.3.5 Beam Action

In a reinforced concrete member, the flexural cracks divide the tension zone in several blocks as proposed by Kani. These blocks may be assimilated as a cantilever beam fixed in the compression zone where the different mechanisms act. The equilibrium of one concrete tooth gives a horizontal and vertical force and a moment at the support. The external moment is in equilibrium with the internal moment. The beam action is often named cantilever action. The formation of the critical shear crack disables the transfer mechanisms of the beam action. [5]

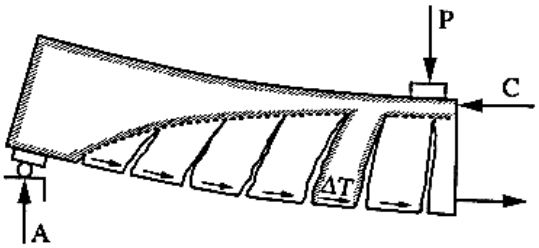

Figure 2- 9 - Concrete tooth model and equilibrium (ASCE1998)

2.3.6 Arch Action

As seen in point 2.3.1, the shear force is transferred from the loading point to the support by inclined principal tensile and compressive stresses. The development of the arch action requires a horizontal reaction at the support. For a simply supported beam, the horizontal reaction is carried by the longitudinal reinforcement. However, for the full development of the arch action, a perfect

anchorage of the reinforcement is required. The arch action depends of on the following parameters: the slenderness or the shear span to depth ratio a/d, the loading arrangement, the concrete strength and the reinforcement ratio. For beams without transverse reinforcement simply supported, the arch action can be seen only if the load is applied on the top and not on the bottom of the beam.

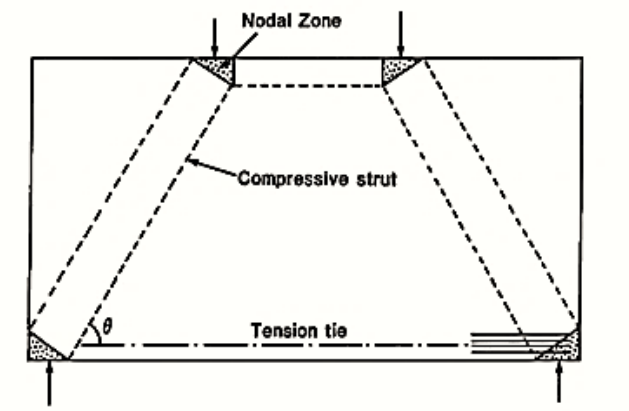

Figure 2- 10 - Arch action detail

Four arch failure modes may be identified: In the first mode, the propagation of the critical shear crack reduces the compression zone. Therefore the failure occurs by the crushing of the concrete at the root of the diagonal shear crack. This type of failure is named shear-compression. In the second mode, the failure occurs by the debonding of the compression zone. In the third mode, the failure occurs by the splitting of the strut. This type takes place for low shear to depth ratios, a/d < 2, and presents large reserve of strength. The last mode is the debonding of the reinforcement at the supports. [5]

2.3.7 Shear Reinforcement

In addition to the shear carried by the stirrup itself, when an inclined crack crosses shear reinforcement, the steel may contribute significantly to the capacity of the member by increasing or maintaining the shear transferred by interfaces shear transfer, dowel action, and arch action. Thus, shear reinforcement restricts the widening of inclined cracks in beams and thus slows the decrease of interfaces shear transfer quite effectively. [2]

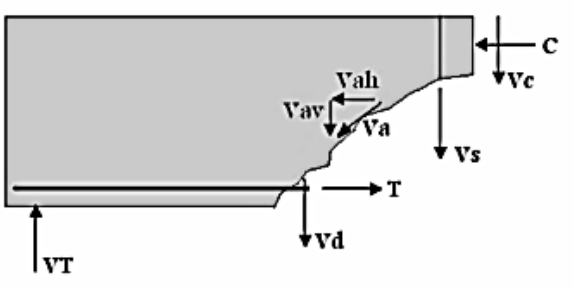

The static equilibrium can express as follows:
$VT = Vc + Vav + Vd + Vs$

Figure 2- 11 - Components of Shear Force Over Crack Plain

2.4 Parameters Influencing the Shear Strength

2.4.1 Shear Span to Depth Ratio

The studies performed by Leonhardt and Walther and Kani highlighted the influence of the slenderness of the members and the presence of different modes governing the shear failure. Kani has performed at University of Toronto 133 tests on beams without stirrups in order to establish the influence on shear strength of the shear span to depth a/d ratio, the concrete compressive strength and the reinforcement ratio. All beams were tested in 4-points bending and have an identical cross-section of 305 mm depth and 152 mm wide. The tests results were represented according to the ratio, moment M on the plastic moment Mu, versus the shear span to depth ratio a/d. This representation highlighted clearly the dependence of the slenderness on the shear strength and the presence of different failure modes. [5]

For $a/d < 1$, the shear strength reaches the flexural capacity and the strength is governed by the yielding of the flexural reinforcement, as diagonal cracks almost do not disturb the compression strut.

For $1 < a/d < 2.5 – 3$, the arch action is dominant. The diagonal shear crack is linear from the loading point to the support. In this configuration, the shear crack progresses in a stable manner and presents large reserve of strength. This regime is called direct strut.

For $2.5 < a/d < 7 – 13$, the diagonal shear crack develops from an inclined flexural crack. The failure develops due to the localization of the strains and limits the strength of the inclined compression strut carrying shear.

For $a/d > 7$, the flexural capacity is dominant.

2.4.2 Size Effect or Depth Effect

The nominal shear strength depends linearly on the member's width and non-linearly on the member's depth. Several tests on shear behavior were performed on relatively small beams h<500 mm. However, some structural members present higher depth like bridge girders. Tests on deep beams h>1000 mm have highlighted that the nominal shear strength is significantly lower compared to small beams (Figure 2.2). [5]

In other words, the shear strength of members without transverse reinforcement decreases as the depth increases. The main reason for this size effect is that deep beams show larger crack width. Therefore, the interface shear transfer in deep beams is smaller. Shear tests performed by Collins and Frosch highlighted that the size effect disappears when beams without stirrups contain well distributed longitudinal reinforcement. In fact, the cracking pattern of these beams showed better distribution and smaller cracks width. [5]

2.4.3 Longitudinal Reinforcement Ratio and Arrangement

The influence of reinforcement ratio on shear capacity was largely investigated by Kani. Members with low reinforcement ratio can fail in shear at low load level. This low shear capacity can be explained by larger flexural crack widths that reduce the size of the compression zone, the dowel action and the interface shear transfer. In other words, the shear strength increases as the reinforcement ratio increases as well, however the deformation capacity decreases and the failure is more brittle and sudden. [5]

2.4.4 Axial Force

Several studies highlighted that the shear strength of members is dependent on axial force. While an axial tension decreases the shear strength, an axial compression, applied by external load or prestressing, increases the shear resistance. But the contribution of axial force on shear capacity is not clearly defined and is still subjected to research programs. A member without transverse reinforcement subjected to high compressive and shear stresses exhibits a sudden failure. Therefore, the shear design is subjected to particular attention. [5]

2.4.5 Concrete Strength and Aggregates Size

For Normal Strength Concrete, the cracks get round the aggregates as the matrix strength is generally lower than the inclusions strength; the contact surface is then irregular. The crack path depends on the maximum aggregate size. Increasing the maximum aggregate size from 10 to 50 mm is making the path of the shear crack rougher and is increasing the failure shear stress of large specimen. However in recent years, several new concrete formulations are largely used in construction as Self Compacting Concrete (SCC), Lightweight Concrete (LC) and High Strength

Concrete (HSC). In comparison of vibrated concrete, SCC is composed of more cement paste. LC and HSC exhibit a matrix strength higher to the aggregate strength. Therefore, these concrete mixes show a smoother contact surface. In this case, the interface shear transfer is lower. [5]

Kani (1966) concluded that the nominal shear strength does not depend on the concrete compressive strength. However, he has only tested beams with concrete compressive strength in a range of 18 to 36 MPa. For these compressive strengths the effect is less noticeable and can present a large scatter. Actually, it's clear that concrete properties have a significant effect on shear capacity. The tensile strength influences the development of the cracking and the interface shear transfer mechanism.

2.4.6 Load Distribution

Loeonhard and Walter have conducted several tests on members similar to the ones tested by Kani with concentrated and distributed loads in order to define the effective shear span. The beams with a uniformly loading distribution showed more favorable results compared to the beams with concentrated loading. The shear span for simply supported beams with a uniformly loading distribution is considered at L/4. [5]

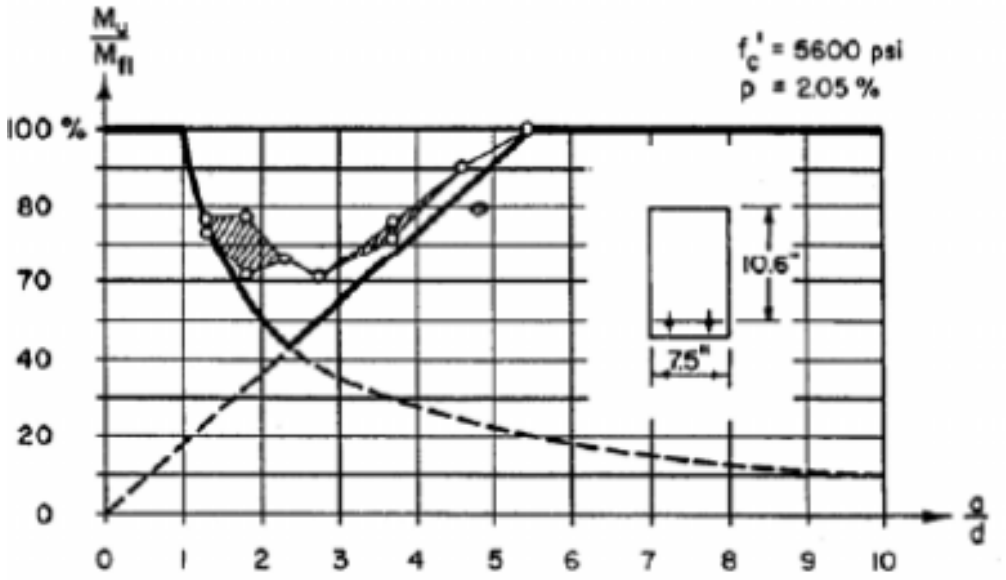

Figure 2- 12 - The Kani's valley for beams with uniformly distributed load (ASCE1998)

2.4.7 Cross Section Shape

The shape of the cross section influences the cracks propagation. Several tests show that diagonal shear cracks stop under the flange of T-beams and I-beams. Therefore, the compressed flange is uncracked and can support a large part of the shear force. The flange allows a redistribution of the diagonal cracks like stirrups. Close to failure, the diagonal crack often may develop horizontally under the flange. Moreover, the uncracked flange can carry a large part of the shear load. [5]

2.5 Shear Model for Reinforced Concrete Member

2.5.1 Compression Field Approach

2.5.1.1 Introduction

The cracked web of a reinforced concrete beam transmits shear in a relatively complex manner. As the load is increased, new cracks form while preexisting cracks spread and change inclination. Because the section resists moment as well as shear, the longitudinal strains and the crack inclinations vary over the depth of the beam. [6]

The early truss models of Ritter (1899) and Mörsch (1920, 1922) approximated this behavior by neglecting tensile stresses in the diagonally cracked concrete and assuming that the shear would be carried by diagonal compressive stresses in the concrete inclined at 45 degree to the longitudinal axis. The diagonal compressive concrete stresses push apart the top and bottom faces of the beam, while the tensile stresses in the stirrups pull them together. Equilibrium requires that these two effects be equal. According to the 45 degree truss model, the shear capacity is reached when the stirrups yield and will correspond to a shear stress of

$$v = \frac{A_v f_y}{b_w S_i} = \rho_v f_y \tag{2.1}$$

One reason why the 45 degree truss equation is often very conservative is that the angle of inclination of the diagonal compressive stresses measured from the longitudinal axis, θ, is typically less than 45 degrees. The general form of Eq. (2-1) is

$$v = \rho_v f_y cot\theta \tag{2.2}$$

Before the general truss equation can be used to determine the shear capacity of a given beam or to design the stirrups to resist a given shear, it is necessary to know the angle θ. Discussing this problem, Mörsch (1922) stated, “It is absolutely impossible to mathematically determine the slope of the secondary inclined cracks according to which one can design the stirrups.” Just seven years after Mörsch made this statement, another German engineer, H. A. Wagner (1929), solved an analogous problem while dealing with the shear design of “stressed-skin” aircraft. Wagner assumed that after the thin metal skin buckled, it could continue to carry shear by a field of diagonal tension, provided that it was stiffened by transverse frames and longitudinal stringers. To determine the angle of inclination of the diagonal tension, Wagner considered the deformations of the system. He assumed that the angle of inclination of the diagonal tensile stresses in the buckled thin metal skin would coincide with the angle of inclination of the principal tensile strain

as determined from the deformations of the skin, the transverse frames, and the longitudinal stringers. This approach became known as the tension field theory.

Shear design procedures for reinforced concrete that, like the tension field theory, determine the angle θ by considering the deformations of the transverse reinforcement, the longitudinal reinforcement, and the diagonally stressed concrete have become known as compression field approaches. With these methods, equilibrium conditions, compatibility conditions, and stress-strain relationships for both the reinforcement and the diagonally cracked concrete are used to predict the load deformation response of a section subjected to shear.

Kupfer (1964) and Baumann (1972) presented approaches for determining the angle θ assuming that the cracked concrete and the reinforcement were linearly elastic. Methods for determining θ applicable over the full loading range and based on Wagner's procedure were developed by Collins and Mitchell (1974) for members in torsion and were applied to shear design by Collins (1978). This procedure was known as CFT. [6]

2.5.1.2 Compression Field Theory

Figure 2.13 summarizes the basic relationships of the CFT. The shear stress ν applied to the cracked reinforced concrete causes tensile stresses in the longitudinal reinforcement f_{sx} and the transverse reinforcement f_{sy} and a compressive stress in the cracked concrete f_2 inclined at angle θ to the longitudinal axis. The equilibrium relationships between these stresses can be derived from Fig. 2.13 (a) and (b) as

$$\rho_v f_{sy} = f_{cy} = \nu tan\theta \tag{2.3}$$

$$\rho_x = f_{sx} = f_{cx} = \nu cot\theta \tag{2.4}$$

$$f_2 = \nu(tan\theta + cot\theta) \tag{2.5}$$

Where ρ_x and ρ_v are the reinforcement ratios in the longitudinal and transverse directions.

If the longitudinal reinforcement elongates by a strain of ε_x , the transverse reinforcement elongates by ε_y , and the diagonally compressed concrete shortens by ε_2 , then the direction of principal compressive strain can be found from Wagner's (1929) equation, which can be derived from Mohr's circle of strain (Fig. 2.13(d)) as

$$\tan^2\theta = \frac{\varepsilon_x + \varepsilon_2}{\varepsilon_y - \varepsilon_2} \tag{2.6}$$

Before this equation can be used to determine θ, however, stress-strain relationships for the reinforcement and the concrete are required. It is assumed that the reinforcement strains are related to the reinforcement stresses by the usual simple bilinear approximations shown in Fig. 2.13(e) and (f). Thus, after the transverse strain ε_y exceeds the yield strain of the stirrups, the stress in the stirrups is assumed to equal the yield stress f_y , and Eq. (2-3) becomes identical to Eq. (2-2).

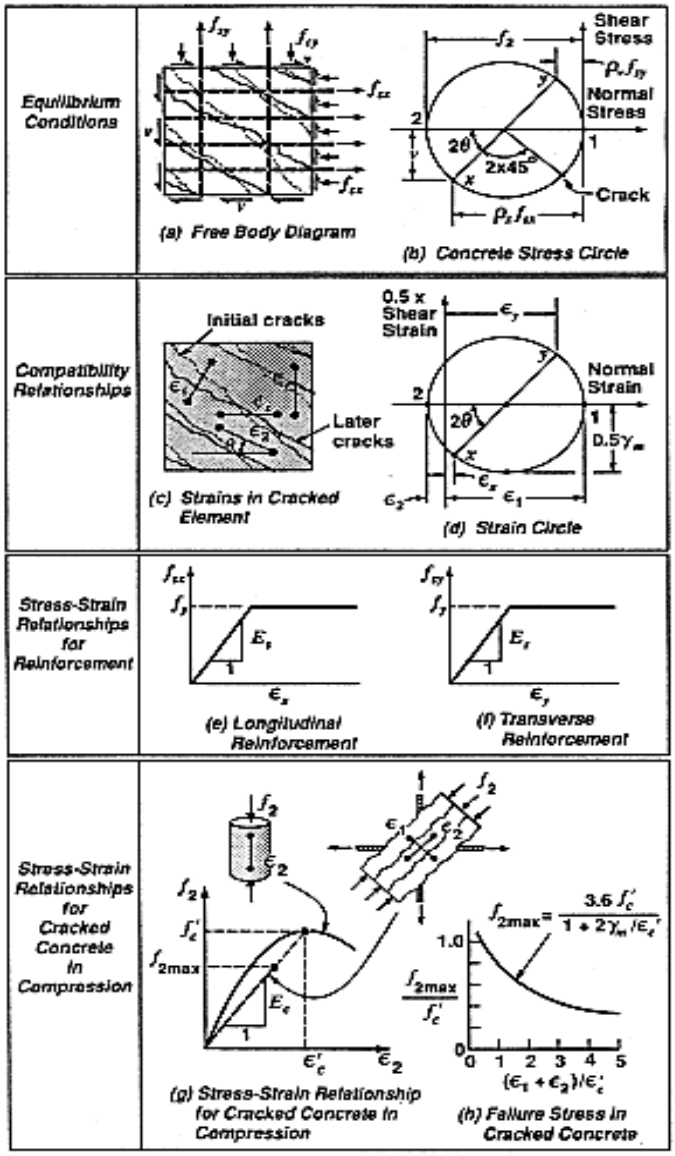

Figure 2- 13 - Compression field theory (Mitchell and Collins 1974)

Based on the results from a series of intensively instrumented beams, Collins (1978) suggested that the relationship between the principal compressive stress f_2 and the principal compressive strain ε_2 for diagonally cracked concrete would differ from the usual compressive stress-strain curve derived from a cylinder test (Fig 2.13(g)). He postulated that as the strain circle becomes

larger, the compressive stress required to fail the concrete f_{2max} becomes smaller (Fig. 2.13(h)). The relationships proposed were

$$f_{2max} = \frac{3.6 f_c'}{1 + 2\frac{\gamma_m}{\epsilon_c'}} \tag{2.7}$$

where

γ_m = diameter of the strain circle (that is, $\varepsilon_1 + \varepsilon_2$); and

ε'_c = strain at which the concrete in a cylinder test reaches the peak stress f'_c

For values of f_2 less than f_{2max}

$$\varepsilon_2 = \frac{f_2}{f_c' \varepsilon_c'} \tag{2.8}$$

It was suggested that the diagonally cracked concrete fails at a low compressive stress because this stress must be transmitted across relatively wide cracks. If the initial cracks shown in Fig. 2.13(a) formed at 45 degrees to the longitudinal reinforcement, and if θ is less than 45 degrees, which will be the case if ρ_v is less than ρ_x, then significant shear stresses should be transmitted across these initial cracks (Fig. 2.13(b)). The ability of the concrete to transmit shear across cracks depends on the width of the cracks, which, in turn, is related to the tensile straining of the concrete. The principal tensile strain ε_1 can be derived from Fig. 2.13(d) as

$$\varepsilon_1 = \varepsilon_x + (\varepsilon_x + \varepsilon_2)\, cot^2\, \theta \tag{2.9}$$

For shear stresses less than that causing first yield of the reinforcement, a simple expression for the angle θ can be derived by rearranging the previous equations to give

$$\tan^4 \theta = \left(1 + \frac{1}{n\rho_x}\right) / \left(1 + \frac{1}{n\rho_v}\right) \tag{2.10}$$

Where

n = modular ratio E_s/E_c ; and E_c is taken as f_c'/ε_c'

2.5.2 Truss Model Approaches

2.5.2.1 Truss model for design of reinforced concrete structures

The behavior of beams failing in shear must be expressed in terms of a mechanical mathematical model before designers can make use of this knowledge in design. MacGregor et al. once stated that the best model for beams with web reinforcement is the truss model. However with the current advances[1] in models for the shear design of reinforced concrete the statement once made by MacGregor can merely be true.

In 1899 and 1902, respectively, the Swiss engineer Ritter and the German engineer Morch, independently, published papers proposing the truss analogy for the design of reinforced concrete beams for shear. These procedures provide an excellent conceptual model to show the forces that exist in a cracked concrete beam. [12]

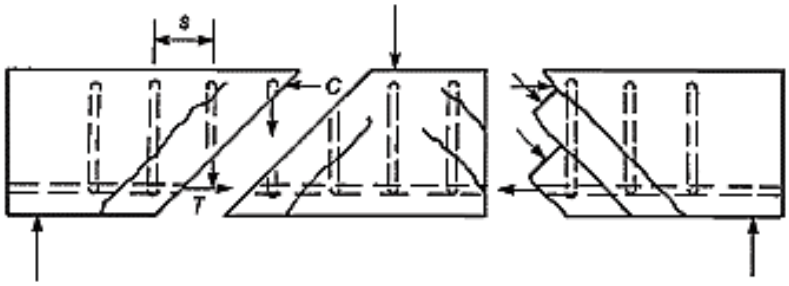

(a) Internal forces in a cracked beam

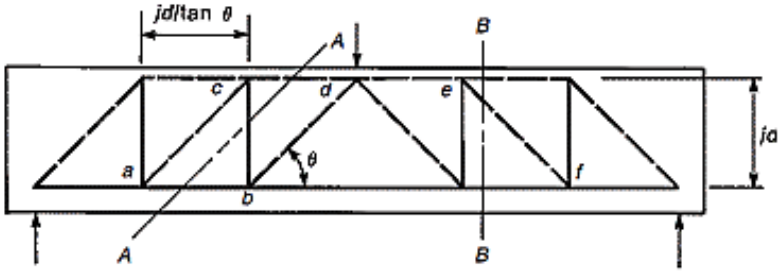

(b) Pin-jointed truss

Figure 2- 14 - Truss analogy (MacGregor et al., 2012)

As shown in Figure 2-14, a beam with inclined cracks develops compressive and tensile forces, C and T, in its top and bottom "flanges," vertical tensions in the web reinforcements, and inclined compressive forces in the concrete "diagonals "between the inclined cracks. This highly indeterminate system of forces can be replaced by an analogous truss. The simplest truss is shown in Figure 2-14b; a more complicated truss is shown in Figure 2-15b.

Several assumptions and simplifications are needed to derive the analogous truss. In Figure 2-14b, the truss has been formed by lumping all of the web reinforcements cut by section A- A into one vertical member b-c and all the diagonal concrete members cut by section B-B into one diagonal member e-f. This diagonal member is stressed in compression to resist the shear on section B-B. The compression chord along the top of the truss is actually a force in the concrete but is shown as a truss member. The compressive members in the truss are shown with dashed lines to imply that they are really forces in the concrete, not separate truss members. The tensile members are shown with solid lines.

Figure 2-15a shows a beam with inclined cracks. The left end of this beam can be replaced by the truss shown in Figure 2-15b.

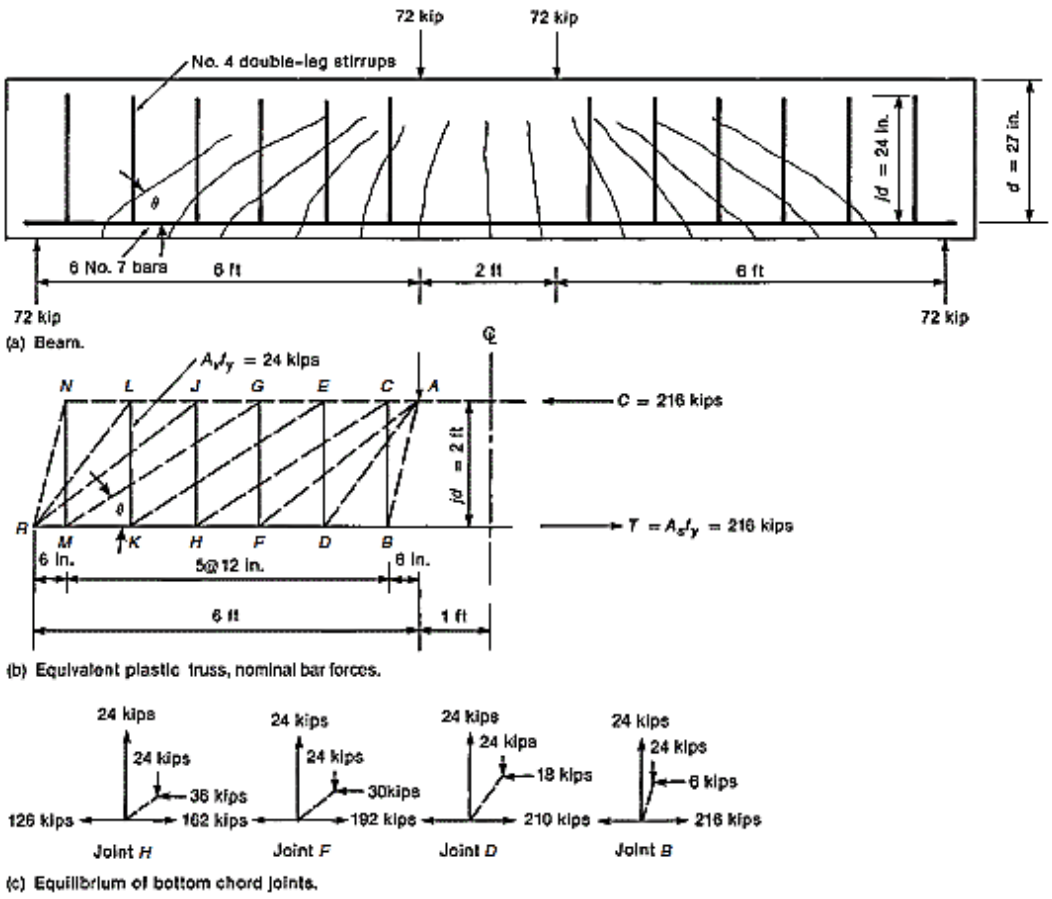

Figure 2- 15 - Construction of an analogous plastic truss (MacGregor et al., 2012)

In design, the ideal distribution of web reinforcements would correspond to all web reinforcements reaching yield by the time the failure load is reached. It will be assumed, therefore, that all the web reinforcements have yielded and that each transmits a force of $A_v f_{yt}$ across the crack, where A_v is the area of the web reinforcement legs and f_{yt} is the yield strength of the transverse reinforcement. When this is done, the truss becomes statically determinate. This truss is referred to as a plastic-truss model, because we are depending on plasticity in the web reinforcements to make it statically determinate. The beam will be proportioned so that the web reinforcements yield before the concrete crushes, so that it will not depend on plastic action in the concrete.

This truss model ignores the shear components V_{cy} , V_d , and V_{ay} . Thus it does not assign any shear "to the concrete."

The compression diagonals originating at the load point A (AB, AD, and AF) are referred to as a compression fan. The number of diagonal struts in the fan must be such that the entire vertical load at A is resisted by the vertical force components in the diagonals meeting at A. A similar compression fan exists at the support R (RN, RL, and RJ). Between the compression fans is a compression field consisting of the parallel diagonal struts CH, EK, and KM. The angle θ of the

compression field is determined by the number of web reinforcements needed to equilibrate the vertical loads in the fans.

Each of the compression fans occurs in a D-region (discontinuity region). The compression field is a B-region (beam region). [12]

2.5.2.2 Simplified Truss analogy

A statically determinate truss analogy can be derived via the method suggested by Marti. Figure 2-16a and b show a uniformly loaded beam with web reinforcements and a truss model incorporating all the web reinforcements and representing the uniform load as a series of concentrated loads at the panel points. This truss in Figure 2-16b is statically indeterminate, but it can be solved if it is assumed that the forces in each web reinforcement cause the web reinforcement to just reach yield. [12]

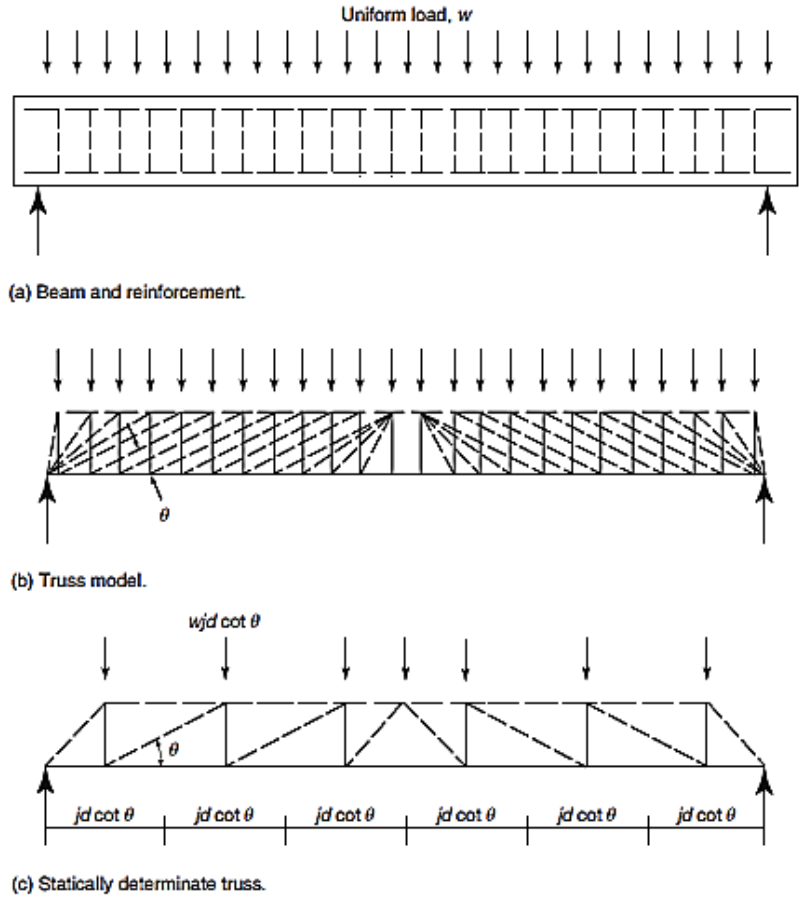

Figure 2- 16 - Truss Model for design (MacGregor et. al., 2012)

For design, it is easier to represent the truss as shown in Figure 2-16c, where the tension force in each vertical member represents the force in all the web reinforcements within a length jd cotθ. Similarly, each inclined compression strut represents a width of web equal to jd cosθ. The uniform load has been idealized as concentrated loads of w(jd cotθ) acting at the panel points. This truss is statically determinate. To draw such a truss, it is necessary to choose θ.

Internal Forces in the Plastic-Truss Model

If we consider the free-body diagram cut by section A-A parallel to the diagonals in the compression field region in Figure 2-17a, the entire vertical component of the shear force is resisted by tension forces in the web reinforcements crossing this section. The horizontal projection of section A-A is jd cotθ, and the number of web reinforcements it cuts is jd cosθ / S. The force in one web reinforcement is $A_v f_{yt}$, which can be calculated from

$$A_v f_{yt} = \frac{V * s}{jd\ cot\theta} \tag{2.11}$$

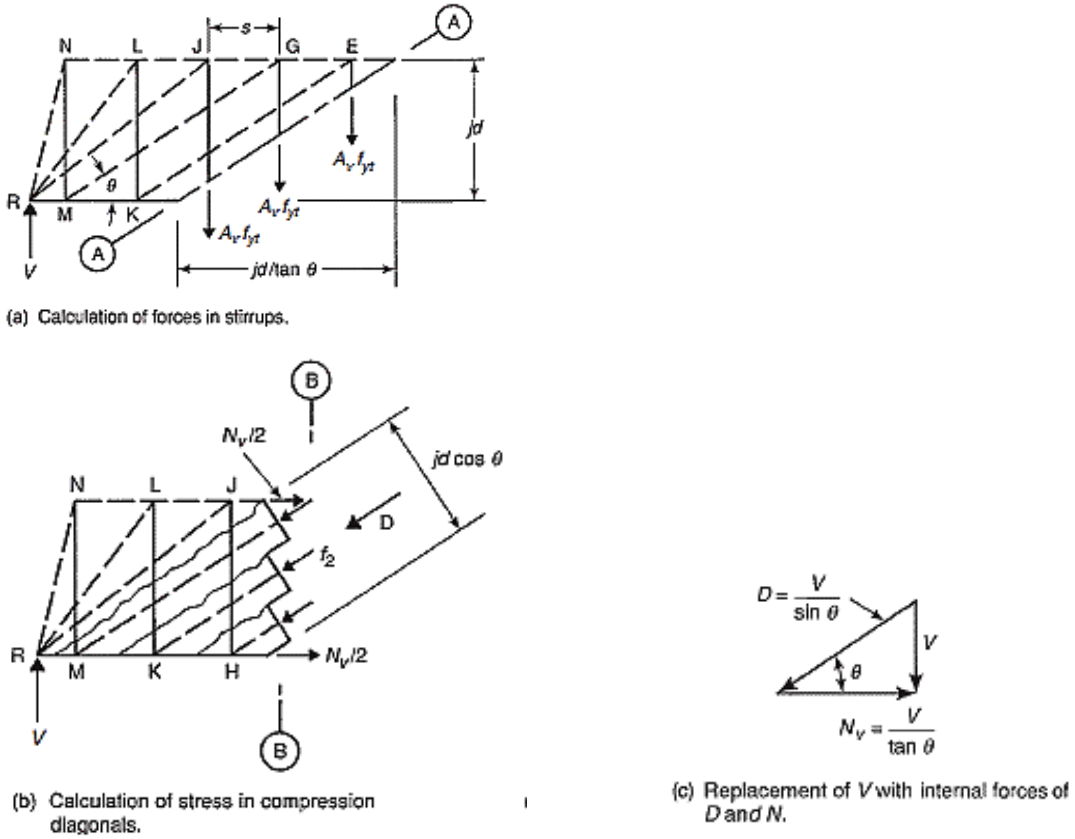

Figure 2- 17 - Forces in web reinforcements and compression diagonals (MacGregor et. al., 2012)

The free body shown in Figure 2-17b is cut by a vertical section between G and J in Figure 2-15b. Here, the vertical force, V, acting on the section is resisted by the vertical component of the diagonal compressive force D (Figure 2-17c). The width of the diagonals is jd cosθ, as shown in Figure 2-17b, and expressing D as V / sinθ, the average compressive stress in the diagonals is

$$f_2 = \frac{V}{b_w jd cos\theta sin\theta} \tag{2.12}$$

With the use of trigonometric identities, this equation becomes

$$f_2 = \frac{V}{b_w jd}\left(tan\theta + \frac{1}{tan\theta}\right) \quad (2.13)$$

Where b_w is the thickness of the web. If the web is very thin, this stress may cause the web to crush.

The shear V on section B-B of Figure 2-17b can be replaced by the diagonal compression force

$$D = \frac{V}{sin\theta} \quad (2.14)$$

And an axial tension force

$$N_v = \frac{V}{tan\theta} \quad (2.15)$$

as shown in Figure 2-17c.

If it is assumed that the shear stress is constant over the height of the beam, the resultants of D and N_v act at mid height. As a result, a tensile force of $N_v/2$ acts in each of the top and bottom chords. This reduces the force in the compression chord and increases the force in the tension chord.

Value of θ in Compression Field Region

When a reinforced concrete beam with web reinforcements is loaded to failure, inclined cracks initially develop at an angle of 35 to 45 degree with the horizontal. With further loading, the angle of the compression stresses may cross some of the cracks. For this to occur, aggregate interlock must exist.

The allowable range of θ is expressed as $0.5 \leq \cot\theta \leq 2.0$ (θ =26 to 64^0) in the Swiss code. This range was selected to limit crack widths. A more restricted range, $\frac{3}{5} \leq cot\theta \leq \frac{5}{3}$ (θ = 31 to 59^0), is allowed in the FIP Design Recommendations.

In design, the value of θ should be in the range $25^0 \leq \theta \leq 65^0$. The choice of a small value of θ reduces the number of web reinforcements required, but increases the compression stresses in the web and increases N_v. The opposite is true for large angles.

In the analysis of a given beam, the angle θ is determined by the number of web reinforcements needed to equilibrate the applied loads and reactions. The angle should be within the limits given, except in compression-fan regions where the angle θ varies. In the design of a beam, the crack angle is a free choice that leads to values of the other unknowns.

Crushing Strength of Concrete in the Web

The web of the beam will crush if the inclined compressive stress, f_2 from , exceeds the strength of the concrete. The compressive strength, f_{2max} , of the concrete in a web that has previously been cracked and that contains web reinforcements stressed in tension at an angle to the cracks will tend to be less than fc' . A reasonable limit is $0.25f_c'$ for $\theta = 30^0$ increasing to $0.45f_c'$ for $\theta = 45^0$.

2.5.2.3 Traditional 45 – Degree Truss Model

Formation of the 45-Degree Truss

Figure 2-18 shows a truss model for a simple beam in which the directions of the diagonal compression stresses are assumed to remain 45 degrees. This truss model of a cracked reinforced concrete beam can be formed by:

- Lumping all of the web reinforcements cut by section A-A into one vertical member.
- Lumping the diagonal concrete members cut by section B-B into one diagonal member with an angle of inclination of 45^0 with respect to the beam axis. This diagonal member is stressed in compression to resist the shear on section B-B.
- Considering the longitudinal tension reinforcement as the bottom chord of the truss.
- Considering the flexural compression zone of the beam acts as the top chord.

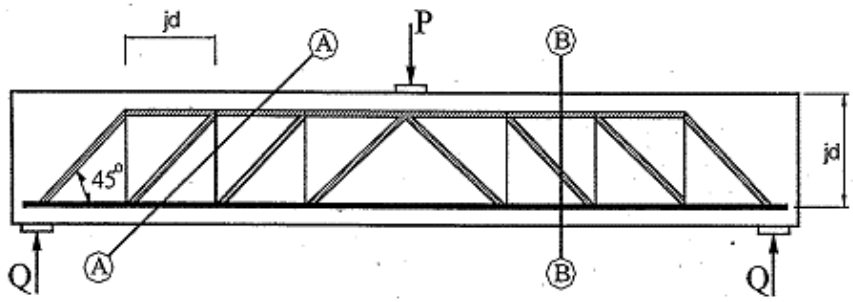

Figure 2- 18 - 45 Degree Truss Model (Mahmoud El-Mihilmy et al., 2008)

Internal Forces in the 45 Degree Truss Model

Internal forces in the 45 degree truss model can easily be found by substituting 45 degree for the value of θ in the equations derived for the variable angle truss analogy. Thus substituting for the value of θ results the force in each web reinforcement, diagonal compressive force in the concrete and additional tensile and compressive forces at the upper and bottom of the truss chord as follows.

$$A_v f_{yt} = \frac{V * s}{jd} \tag{2.16}$$

$$f_2 = \frac{V}{0.5 b_w jd} \tag{2.17}$$

$$D = \frac{V}{\sin 45^0} \tag{2.18}$$

$$N_v = V \tag{2.19}$$

CHAPTER 3

Shear Design Method

3.1 ACI Shear Design Procedure

The ACI Code (ACI Committee 318 - 1995) shear design equations for non-prestressed reinforced concrete beams were derived in 1962 based on tests involving relatively small (d_{avg} = 340 mm) and rather heavily reinforced (ρ_{avg} = 2.2%) beams and do not recognize the size effect on the shear performance. These equations are:

$$v_c = 0.158\sqrt{f_c'}\, b_w \mathrm{d} + 17.24\rho_w \left(\frac{vd}{\mathrm{M}}\right) b_w \mathrm{d} \;\leq 0.29\sqrt{f_c'} b_w \,\mathrm{d} \qquad (3.1)$$

In lieu of equation (3.1), the ACI Code allows the following simpler equation to be used:

$$v_c = 0.166\,\sqrt{f_c'}\, b_w \mathrm{d} \qquad \text{with} \qquad \sqrt{f_c'} \;\leq\; \sqrt{69} \qquad (3.2)$$

These equations for predicting the shear strength of concrete beam elements are based on the shear causing significant diagonal cracking. At the time these expressions were derived, the ACI-ASCE Committee 326 on shear and diagonal tension (ACI-ASCE Committee 326, 1962) concluded that for members without stirrups, any increase in shear capacity beyond the shear which caused significant diagonal cracking was unpredictable due to the great variation in failure mechanisms and should thus be ignored. Bazant et al. (1984, 1987& 1991) criticized this assumption since the diagonal cracking load is not proportional to the ultimate load, and hence a uniform factor of safety against failure is not provided. [3]

Nominal shear strength

$$v_n = v_c + v_s \qquad (3.3)$$

For non prestressed beams

$$v_c = \frac{\sqrt{f_c'}}{6} b_w d \qquad (3.4)$$

For prestressed beams

$$v_c = \left[\frac{\sqrt{f_c'}}{20} + 5\,(v_u\, d/M_u)\right] b_w d \qquad (3.5)$$

$$v_s = \frac{A_v f_y d}{s} \qquad (3.6)$$

The current ACI (ACI 318-2014) design procedure for shear defines the nominal shear strength as the sum of the shear strength provided by shear reinforcement, V_s , and the shear strength provided by concrete, V_c , which is assumed to be the same for beams with and without shear reinforcement and is taken as the shear causing significant inclined cracking.

The value of V_c is defined for members subject to shear and flexure only and for members subject to axial compression separately. Two alternatives are presented for calculation of V_c. The first alternative has a simple formula. Unlike its European counterpart, the ACI provision for calculation of the concrete contribution doesn't contain the longitudinal reinforcement ratio as a factor. It only depends on the compressive strength of the concrete and the size of the member.

The second alternative contains a more detailed calculation. In this case, many factors including ρ_w and $V_u\, d / M_u$ are shown to affect the concrete contribution.

The contribution of the shear reinforcement is based on the modified truss analogy. As it is presented in the commentary, the truss analogy assumes that the total shear is carried by shear reinforcement. However, considerable research has indicated that shear reinforcement needs to be designed to carry only the shear exceeding that which causes inclined cracking, provided the diagonal members in the truss are assumed to be inclined at 45 degrees. Thus, the ACI approach of calculating the shear reinforcement contribution can be generalized as modified 45 degree truss analogy.

$$\nu_c = 2\lambda\sqrt{f_c'}\,b_w d \tag{3.7}$$

$$\nu_s = \frac{A_v f_y d}{s} \tag{3.8}$$

$$\nu_{n,max} = 2\lambda\sqrt{f_c'}\,b_w d + 8\sqrt{f_c'}\,b_w d \tag{3.9}$$

Shear reinforcement restrains the growth of inclined cracking. Ductility is increased and a warning of failure is provided. In an unreinforced web, the sudden formation of inclined cracking might lead directly to failure without warning. Such reinforcement is of great value if a member is subjected to an unexpected tensile force or an overload. Accordingly, due to the reason stated above, a provision for providing minimum shear reinforcement for all members except for solid slabs, footings and joists is stipulated in ACI318. [3]

3.2 CSA Simplified Shear Design Procedure

The simplified expression in the 1994 CSA Standard (CSA 1994) for the evaluation of the contribution of the concrete, v_c , to the shear capacity are given below:

a) For sections having either the minimum amount of transverse reinforcement required in the Standard (CSA 1994), or an effective depth, d, not exceeding 300 mm:

$$v_c = 0.2\phi_c \sqrt{f_c'}\, b_w\, d \qquad (3.10)$$

Where ϕ_c , is the material resistance factor for concrete, equal to 0.60.

The factor of "0.2" in the above equation was artificially increased from that corresponding to the nominal value of 0.166 to account for the low value of ϕ_c. Hence the nominal resistance can be written as:

$$v_c = 0.166\sqrt{f_c'}\, b_w\, d \qquad (3.11)$$

b) For sections with effective depths greater than 300 mm and with less transverse reinforcement than the minimum required:

$$v_c = \left(\frac{260}{1000} + d\right)\phi_c \sqrt{f_c'}\, b_w d \qquad not\ less\ than \quad 0.10\phi_c \sqrt{f_c'}\, b_w d \qquad (3.12)$$

Similarly the nominal resistance can be written as:

$$v_c = \left(\frac{215.8}{1000} + d\right)\phi_c \sqrt{f_c'}\, b_w d \qquad not\ less\ than \quad 0.833\phi_c \sqrt{f_c'}\, b_w d \qquad (3.13)$$

As can be seen from Equation (3.14), the CSA Concrete Standard (CSA 1994) includes a term to account for the size effect in its simplified shear design expression but does not take account of the reinforcing steel ratio, ρ. This shows the concern of this code regarding the size effect phenomenon. However the linear nature of the term added to the shear equation cannot account for the complexity of the problem. More research is needed to adjust this equation to account for higher concrete strengths and amount of longitudinal reinforcement, ρ. Some limitations on the distribution of the longitudinal reinforcement may also be required. [3]

3.3 EN 1992:2004 Euro Code 2

In the current European Code, the shear resistance of a member with shear reinforcement is defined to be the shear resistance offered by the web reinforcements. Shear reinforcement is not necessary if the resulted shear force is less than the member design shear resistance without shear

reinforcement. However minimum shear reinforcement is required except in slabs and members of minor importance.

An empirical formula is given for calculation of the contribution from the concrete in resisting shear. The empirical formula for concrete contribution takes into account the longitudinal reinforcement ratio, the compressive stress capacity of the concrete and the presence of axial force. The calculation of shear force resistance contribution of the transverse reinforcement is based on the variable angle Truss analogy. Unlike the ACI, this code doesn't have a specific value for the crack inclination angle θ.

As per the variable angle truss analogy (section 2.3.1.1), there is an additional tensile stress that will be resulted on the longitudinal reinforcement and European code has a provision to take care of this additional tensile stress as per the analogy.

In the Euro Code 2, 2005, the shear strength for members not requiring transverse reinforcement $\nu_{Rd,c}$ is given by: [3]

$$\nu_{Rd,c} = \left[\frac{0.18}{\gamma_c} k\,(100\rho_l\, f_{ck}\,)^{\left(\frac{1}{3}\right)} + 0.15\sigma_{cp}\right] b_w d \;\geq \left[\nu_{min} + 0.15\sigma_{cp}\right] b_w d \qquad (3.14)$$

This formulation is fully empirical.

Where k is a factor taking into account the size effect,

$$k = 1 + \sqrt{\frac{200}{d}} \leq 2.0 \qquad \text{(d in mm)} \qquad (3.15)$$

ρ_l is the tensile reinforcement ratio, which anchor beyond the section considered,

$$\rho_l = \frac{A_{st}}{b_w\, d} \leq 0.02 \qquad (3.16)$$

σ_{cp} is the compressive stress in the center of gravity of cross-section due to loading or pre-stressing.

The influence of imposed deformation may be ignored,

$$\sigma_{cp} = \frac{N_{Ed}}{A_s} \leq 0.2\, f_{cd} \qquad (3.17)$$

And υ_{min} is the minimum shear strength given by:

$$\nu_{min} = 0.035 k^{3/2}\, f_{ck}^{1/2} \qquad (3.18)$$

The design of members with shear reinforcement is based on a truss model. The recommended value for angle θ should be limited.

$$1 \leq \cot\theta \leq 2.5 \tag{3.19}$$

For members with vertical shear reinforcement, the shear resistance, V_{Rd} is the smaller value of:

$$\nu_{Rd,s} = \frac{A_{sw}}{S} Z f_{ywd} cot\theta \tag{3.20}$$

The design value of the maximum shear force ν_{Rdmax} which can be sustained by the member, limited by crushing of the compression struts is given by:

$$\nu_{Rd,max} = \alpha_{cw} b_w Z \nu_1 f_{cd} / (cot\theta + tan\theta) \tag{3.21}$$

where:

A_{sw} is the cross-sectional area of the shear reinforcement

S is the spacing of the stirrups

f_{ywd} is the design yield strength of the shear reinforcement

ν_1 is a strength reduction factor for concrete cracked in shear

α_{cw} is a coefficient taking account of the state of the stress in the compression chord

3.4 Modified Compression Field Theory Shear Design Procedure

In lieu of the simplified shear design equations, the CSA Standard (CSA 1994) proposes a more rational method of approach to the shear design "problem" based more on fundamental principles than on empirical equations. This method treats the stress-strain characteristics of the cracked concrete using average stresses and strains in the concrete and utilizes equilibrium and compatibility of strains. The crack pattern is also idealized as a series of parallel cracks occurring at an angle θ to the longitudinal direction. The theory considers that the shear strength of concrete at a crack location is dependent on the width of the crack as well as the maximum aggregate size used (i.e., it looks at the crack roughness). This method accounts for the strain softening of the diagonally cracked concrete in compression and also accounts for the tensile stresses in the cracked concrete. The modified compression field theory is explained in detail by Collins and Mitchell (1997) and by Collins et al. (1996) and yields the following design equations for predicting the concrete contribution to the shear strength: [3]

$$\nu_c = \beta \sqrt{f_c'}\, b_w\, d_v \tag{3.22}$$

Where:

b_w = Minimum effective web width within the depth of the section

d_v = Distance measured perpendicular to the neutral axis between the resultants of the tensile and compressive force due to flexure, may be taken as 0.9d for non-prestressed concrete members

β = Tensile stress factor which accounts for the shear resistance of cracked concrete

$$\beta = \left(\frac{0.33cos\theta}{1} + \sqrt{500\varepsilon_1}\right) \leq \left(\frac{0.18}{0.3 + \left(\frac{24w}{a} + 16\right)}\right) \quad (3.23)$$

Where w is the average crack width which is taken as:

$$w = \varepsilon_1 \, s_\theta \quad (3.24)$$

Where:

ε_1 = Principal tensile strain in cracked concrete

S_θ = Crack spacing in the θ direction

And

$$\varepsilon_1 = \varepsilon_x + \left[\varepsilon_x + 0.002\left(1 - \sqrt{1} - \frac{\nu}{f_c'}(tan\theta + cot\theta)(0.8 + 170\varepsilon_1)\right)\right] cot^2\,\theta \quad (3.25)$$

For the case of a non-prestressed beam with bottom chord reinforcement the longitudinal strain of the flexural tension chord can be taken as

$$\varepsilon_x = \frac{\left[\frac{M}{d_v} + 0.5(N + \nu cot\theta)\right]}{E_s A_s} \quad (3.26)$$

Where:

M = Moment at section

N = Axial load at section (positive in tension)

ν = Shear force at section

Es = Modulus of elasticity of longitudinal steel reinforcement

As = Area of longitudinal steel reinforcement in tension zone

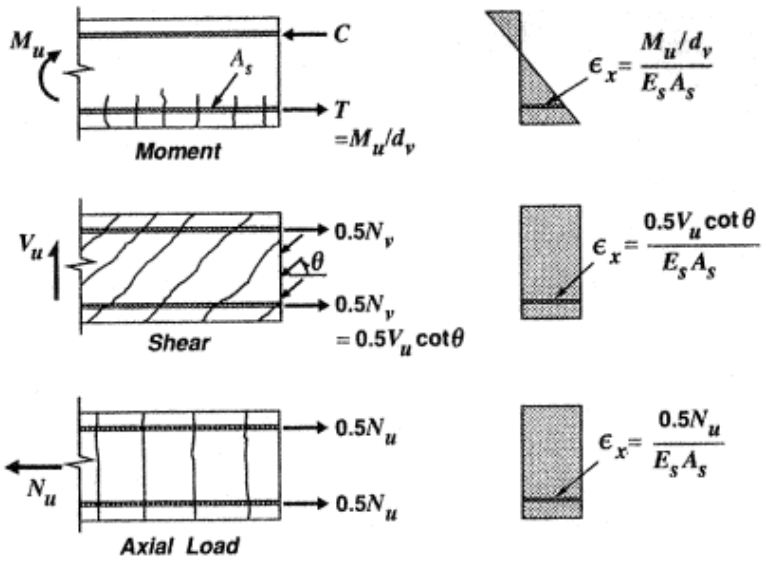

Figure 3 - 1-Determination of strains, εx , for non prestressed beam

Expression for shear strength of a prestressed beam section

$$v_n = v_c + v_s + v_p \tag{3.27}$$

$$v_n = f_1 b_w d_v \cot\theta + A_v \left(\frac{f_y}{s}\right) d_v \cot\theta + v_p \tag{3.28}$$

$$v_n = \beta\sqrt{f_c'}\, b_w\, d_v + A_v \left(\frac{f_y}{s}\right) d_v \cot\theta + v_p \tag{3.29}$$

The shear stress that the web of a beam can resist is a function of the longitudinal straining in the web. The larger this longitudinal straining becomes, the smaller the shear stress required to fail the web. In determining the shear capacity of the beam, it is conservative to use the highest longitudinal strain ε_x occurring within the web. For design calculations, ε_x can be approximated as the strain in the tension chord of the equivalent truss.

$$\varepsilon_x = \frac{\frac{M}{d_v} + 0.5(N + v\cot\theta) - A_{ps} f_{po}}{E_s A_s + E_p A_{ps}} \tag{3.30}$$

CHAPTER 4

NONLINEAR FINITE ELEMENT ANALYSIS OF RC BEAMS

4.1 General

VecTor3 is a nonlinear finite element program for the analysis of three dimensional reinforced concrete solid structural members. The program has been developed at University of Toronto since 1990, when its original version was known as TRIX. This development has coincided with experimental tests to corroborate the ability of VecTor3 to predict the load - deformation response of a variety of reinforced concrete structures exhibiting well distributed cracking when subject to short term static monotonic, cyclic and reverse cyclic loading.

The theoretical bases of VecTor3 are the Modified Compression Field Theory (Vecchio and Collins, 1986) and the Disturbed Stress Field Model (Vecchio, 2000) – analytical models for predicting the response of reinforced concrete solid elements subject to in plane normal and shear stresses. VecTor3 models cracked concrete as an orthotropic material with smeared, rotating cracks. The program utilizes an incremental total load, displacement and iterative secant stiffness algorithm to produce an efficient and robust nonlinear solution.

Originally, VecTor3 employed the constitutive relationships of the MCFT (modified compression field theory). Subsequent developments have incorporated alternative constitutive models for a variety of second order effects including compression softening, tension stiffening, tension softening, and tension splitting. Also, the capabilities of the VecTor3 have been augmented to model concrete expansion and confinement, cyclic loading and hysteretic response, construction and loading chronology for repair applications, bond slip,crack shear slip deformations, reinforcement dowel action, reinforcement buckling, and crack allocation processes.

Finite element models constructed for VecTor3 use a fine mesh of low powered elements. This methodology has advantages of computational efficiency and numerical stability. It is also well suited to reinforced concrete structures, which require a relatively fine mesh to model reinforcement detailing and local crack patterns. The element library includes a six node constant strain triangle, an eight node plane stress regular hexahedral element and an eight node regular hexahedral element for modeling concrete with smeared or discrete reinforcement; a two node uniaxial truss bar for modeling reinforcement; and a two node link and a four node contact element for modeling bond slip mechanisms.

4.2 Material

To determine the concrete tensile strength f_t', cylinder strain e_o and tangent modulus of elasticity E_c, the following formula was used as recommended by the software developer F. J.Vecchio.

$$f_t' = 0.33\sqrt{f_c'} \quad \text{(MPa)} \tag{4.1}$$

$$E_c = 3320\sqrt{f_c'} + 6900 \quad \text{(MPa)} \tag{4.2}$$

$$e_o = 1.8 + 0.0075 f_c' \tag{4.3}$$

A typical stress-strain curve for concrete under compression is shown in Figure 4.1, showing the main material properties required to compile the curve, where f_c and ε_c are the compressive stress and strain in concrete, respectively. 'Poisson's Ratio', μ, and the 'Density', are assigned a values of 0.2 and 2400kg/m^3, respectively. The aggregate size varies from 12.5mm up to 20mm depending on distribution of random variables for the thirty two beam data cases. All the beams compressive strength varies from normal to high strength concrete.

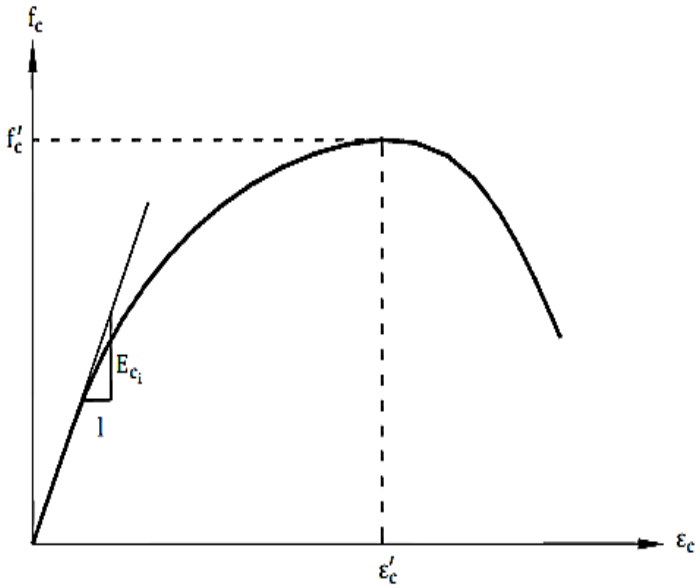

Figure 4 - 1 - Typical Stress-Strain curve for Concrete

Figure 4.2 shows the shape of a typical stress-strain curve for structural steel, showing the main material properties required to compile the curve, where f_s and ε_s are the stress and strain in steel, respectively.

All the reinforcement bars assigned are normal strength rebar with the same tensile strength for both longitudinal and web reinforcement bars. The material properties of the reinforcement bars are shown below.

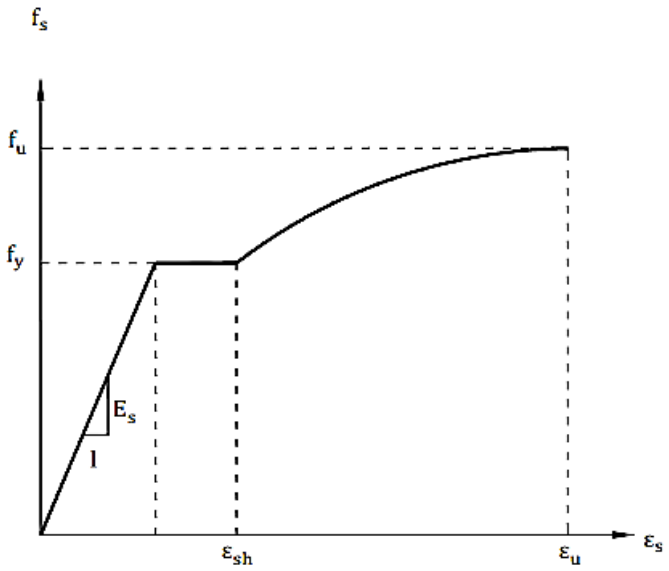

Figure 4- 2 - Typical Stress-Strain curve for Reinforcement Bar

4.3 Model Validation

4.3.1 Specimen

One experimentally tested RC beam is used for model validation. The experimental program consists of a simply supported RC beam specimen with rectangular cross section and a breadth (b) and Depth (D) of 200 mm and 300 mm respectively. Figure 4.3 shows details and reinforcement arrangement of the specimens.

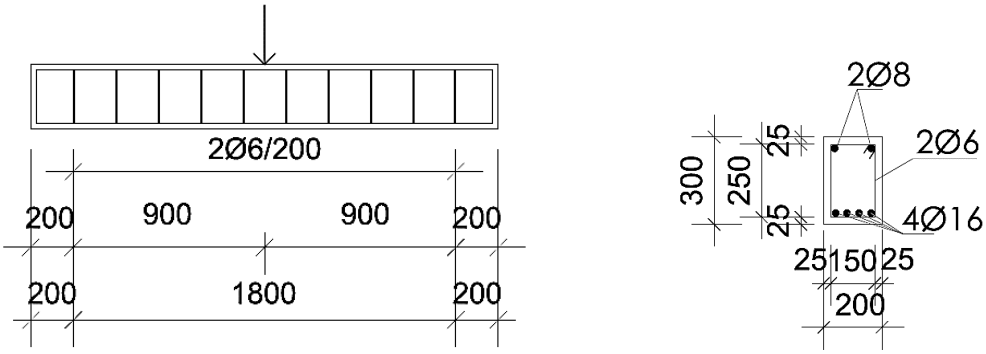

Figure 4- 3 - Beam Cross Section of the Specimen B1

Table 4- 1- Specimen Detail

Specimen	Overall height h, (mm)	Effective depth d, (mm)	Shear span a, (m)	a/d	Side concrete cover to web reinforcement, (mm)	ρ_t (%)	Web reinforcement spacing (mm)
B1	300	262	0.9	3.435	25	0.6	200

4.3.2 Materials

Material properties of the reinforced concrete beam are shown below.

Table 4- 2- Material properties and elements used in modelling for concrete

Material	Compressive strength f_{ck}, (MPa)	Elastic Modulus (MPa)	Tensile strength f'_t (Mpa)	Poison's Ratio	Density (kg/m^3)	Elements used
Concrete	15.29	201,409	1.302	0.2	2500	Hexahedral Element

Table 4- 3- Material properties and elements used in modelling for reinforcement

Bar diameter (mm)	Area (mm^2)	Yeild strength (Mpa)	Ultimate strength (Mpa)	Elastic Modulus (MPa)	Density (kg/m^3)	Poison's Ratio	Elements used
D16	201.062	1847	1992	$201*10^3$	7800	0.2	Truss Bar
D6	28.27	251.11	321.85	$200*10^3$	7800	0.2	Truss Bar
D8	50.266	251.11	321.85	$200*10^3$	7800	0.2	Truss Bar

4.3.3 Modeling

It is proposed to determine the ultimate load and corresponding deflection of the reinforced concrete beam as shown in Figure 4.4 subject to one point loading [11].

The Hognestad model was selected for both the pre and post peak compression response, with the Vecchio 1992-A compression softening model. The Bentz 2003 model was selected for tension stiffening. A crack width limit of 2 mm was imposed and element slip distortions were included with the Hybrid II Vecchio Lai model.

The beam is modeled with hexahedral elements for the concrete, and truss bar elements for the longitudinal reinforcing bars. Two reinforced concrete material types are utilized. One type represents the plain concrete cover. The other type models the web region of the beam with one smeared reinforcement component, which represents the stirrup reinforcement. Three ductile steel reinforcement material types are utilized; tensile reinforcement 4ϕ16mm and 2ϕ8mm bars. For the web reinforcement 2ϕ6mm bars used.

The automatic mesh generation facility with the hybrid discretization type was used to create the mesh shown in Figure 4.4. Each type of longitudinal reinforcing bars was entered as separate reinforcement path with its corresponding material type. One nodal load is applied at the top of the beam. The node at the support is restrained from displacements in both transverse and longitudinal direction. One load case was utilized to impose a downward displacement of 0.2mm

at mid span. The applied displacement was increased monotonically from zero to failure in an increments of 0.2 mm for 80 load stage at mid span. The self-weight of the beam is not included.

4.3.4 Support Condition and Loading

Simply supported beam is considered having overall length of L_1= 2200mm. Size of the beam B-1: 200*300mm. Figure 4.4 shows the beams with boundary conditions used in the analysis. One point loading is applied at mid span of the beam and mid span deflection recorded. To get the accuracy of results mesh size considered is x= 40 mm, y=60mm and z=100mm.

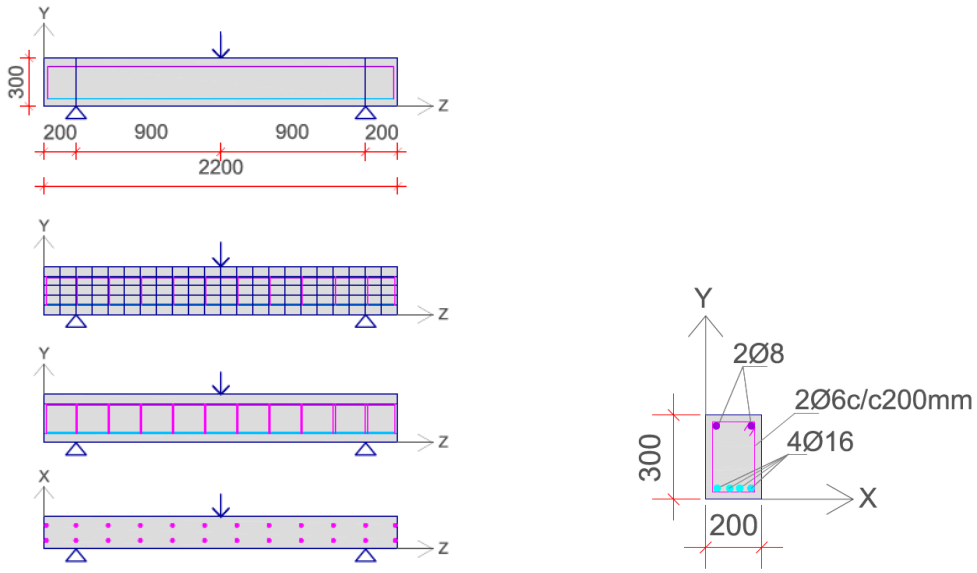

Figure 4- 4 - Reinforced concrete beam model and cross section in Vector-3 (B1)

After simulation of the beam specimen using VecTor-3 software, the ultimate shear strength of reinforced concrete beam determined. And the ultimate load obtained from the analysis and the experiment was 192.74kN at peak displacement of 7.96mm and 193kN at peak displacement of 6.9mm respectively. The difference between the analysis and experimental output has been evaluated below and showed the error is within acceptable limit.

Table 4- 4-Verification of Results

		Maximum Load	Error
Experiment		193	- 0.135%
Numerical Analysis		192.739	

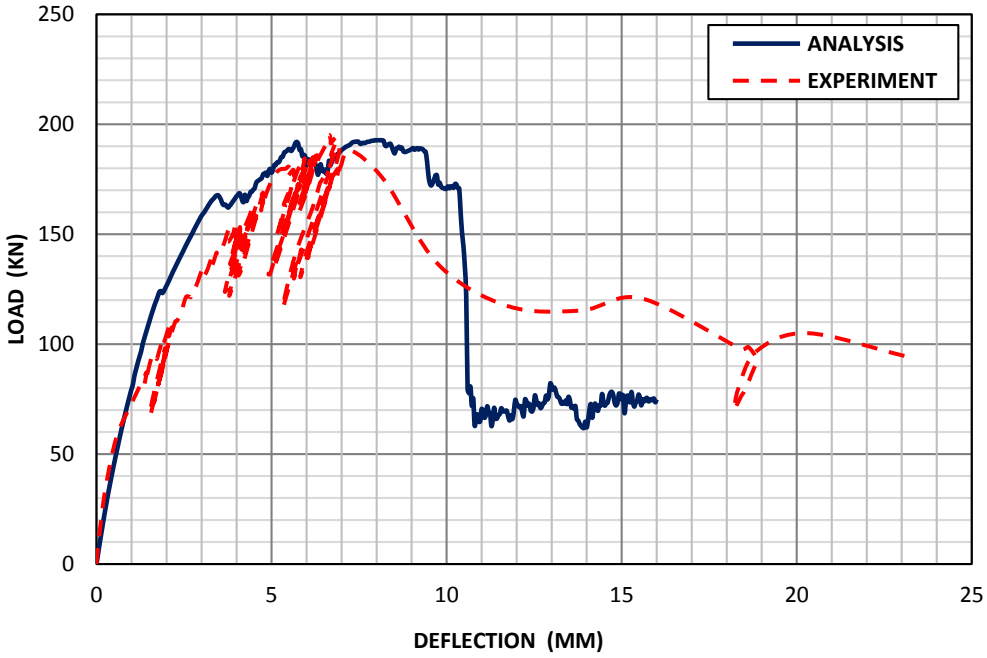

Figure 4- 5 - Load – Deflection diagram of the beam specimen

As a result, it is proved that the analysis software is applicable and reliable for the analysis of solid structural elements.

After model validation, nonlinear finite element analysis for thirty two randomly selected variables of beams data were taken and simulated as a solid element using three dimensional vecTor-3 program. The shear strength of the entire beam was determined and the specimen details are shown below.

4.4 Shear Strength Behavior of Selected RC Beams

Materials used in the simulation

i) Reinforcement bars

Table 4- 5 - Mechanical Properties of Reinforcement Bar

Yield Strength, F_y(MPa)	**Ultimate Strength, F_u(MPa)**	**Elastic Modulus, E_s (MPa)**	**Strain Hardening Strain, e_{sh} (me)**	**Ultimate Strain, e_u (me)**	**Poisson's Ratio, μ**	**Density (kg/m^3)**
435	650	200,000	$5.00*10^{-3}$	$150*10^{-3}$	0.2	78,050

ii) Concrete

Table 4- 6- Mechanical Properties of Concrete

	Concrete Grade (MPa)
	37
Cylindrical Compressive Strength, fc' (MPa)	37
Tensile Strength, f_t' (MPa)	2.0073
Initial Tangent Elastic Modulus, Ec (MPa)	27,094.77
Cylinder Strain at fc', e_o (me)	2.0775
Poisson's Ratio, Mu	0.2
Maximum Aggregate Size, as (mm)	19
Density (kg/m^3)	2,400

iii) Typical Beam Cross Section

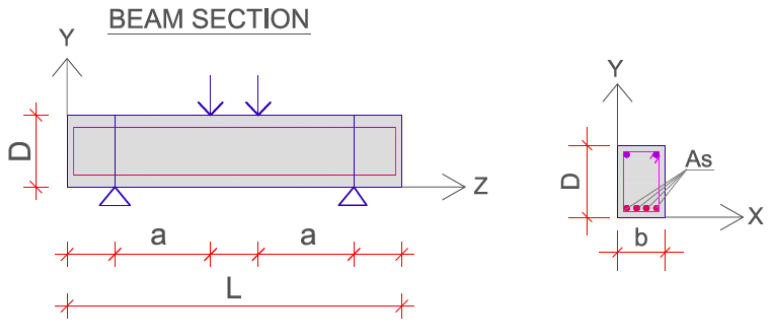

Figure 4 - 6 - Typical Beam Cross Section

Three-dimensional nonlinear finite element analyses were carried out for thirty two cases. The combinations are generated using Latin Hypercube Sampling (LHS) Method. LHS is a sampling method designed to accurately recreate the input distribution through sampling in fewer trails when compared with the Monte Carlo method in which the distribution of each random variable is assumed to be normal. In the LHS sampling method, the cumulative distribution function of each factor is divided into intervals with equal probability, and then sampling is done by only once from each interval [8].

LHS is a sampling method designed to accurately recreate the input distribution through sampling in fewer trails when compared with the Monte Carlo method. LHS, a sampling technique used, forces the samples drawn to correspond more closely with the input distribution and thus converges faster on the true statistics of the input distribution [9].

In this study, the thirty two combinations of random variables of LHS table are found to be sufficient and considered in the simulation. The statistical variations and the 32x7 combinations of random variables are shown in table 4.7 and 4.8, respectively.

In the LHS layers, a range of values with a confidence level of 95% are considered. The minimum and maximum values of each random variable are fixed by considering the actual conditions where a particular RC beam exhibits. That is, materials and dimensions are considered to account the behaviors of different RC beam specimens where conducting of experimental investigation is difficult. These combinations are set systematically using LHS sampling method.

Table 4 - 7- Statistical Variations of Random Variables

Variables	Observation	Minimum	Maximum	Mean	Standard Deviation
fc' (MPa)	32	15.000	60.000	37.084	12.584
b (mm)	32	125.000	500.000	290.469	106.690
D (mm)	32	185.000	1000.000	508.938	219.444
a/d	32	1.540	6.400	3.793	1.315
ρ_l (%)	32	1.420	2.860	1.982	0.407
ρ_w (%)	32	0.670	1.340	1.036	0.180
Aggregate Size (mm)	32	12.500	20.000	16.016	2.551

Table 4 - 8 - 32x7 LHS Layers of Random Variables and Simulation Output

Label	Width b, (mm)	Overall Depth D, (mm)	Compressive Strength $f_{c'}$, (MPa)	Shear Span, a / d	Longitudinal Reinforcement A_{sl} (mm^2)	Web Reinforcement	Aggregate Size a, (mm)
Case-1	325	470	42	5.97	2,513.274	2ϕ6 c/c 250mm	15
Case-2	500	570	30	4.00	3,920.706	2ϕ6 c/c 300mm	20
Case-3	480	980	37	2.94	9,958.850	2ϕ6 c/c 450mm	14
Case-4	250	860	60	3.51	3,216.991	2ϕ6 c/c 400mm	18
Case-5	135	200	58	5.20	307.876	2ϕ6 c/c 210mm	18
Case-6	315	685	38	3.84	3,418.053	2ϕ6 c/c 310mm	17
Case-7	125	510	31	2.90	1,005.309	2ϕ6 c/c 340mm	15
Case-8	360	780	18	4.35	3,820.177	2ϕ6 c/c 370mm	19
Case-9	260	380	29	4.75	1,344.601	2ϕ6 c/c 270mm	15
Case-10	310	700	45	4.24	3,820.177	2ϕ6 c/c 300mm	16
Case-11	250	610	36	5.05	2,412.742	2ϕ6 c/c 280mm	18
Case-12	430	400	27	3.85	2,199.113	2ϕ6 c/c 270mm	14
Case-13	245	575	50	6.00	2,211.679	2ϕ6 c/c 312mm	20
Case-14	390	710	52	3.25	4,574.158	2ϕ6 c/c 350mm	19
Case-15	245	265	56	6.40	1,005.310	2ϕ6 c/c 200mm	16
Case-16	290	480	22	5.67	2,211.680	2ϕ6 c/c 250mm	14

Label	Width b, (mm)	Overall Depth D, (mm)	Compressive Strength $f_{c'}$, (MPa)	Shear Span, a / d	Longitudinal Reinforcement A_{sl} (mm^2)	Web Reinforcement	Aggregate Size a, (mm)
Case-17	200	300	15	1.54	1,256.636	2ϕ6 c/c 200mm	13
Case-18	300	500	25	1.98	3,216.991	2ϕ6 c/c 200mm	20
Case-19	300	400	20	2.50	2,651.504	2ϕ6 c/c 250mm	12.5
Case-20	250	450	35	2.00	2,211.80	2ϕ6 c/c 180mm	19
Case-21	200	265	40.50	2.67	804.248	2ϕ6 c/c 150mm	13
Case-22	150	210	28.90	4.02	603.186	2ϕ6 c/c 86mm	12.5
Case-23	500	1000	32	3.20	9,958.848	2ϕ6 c/c 500mm	20
Case-24	130	350	24.10	3.10	804.248	2ϕ6 c/c 160mm	13
Case-25	450	500	35	3.43	5,629.734	2ϕ6 c/c 250mm	16
Case-26	250	525	37.40	2.50	3,015.929	2ϕ6 c/c 230mm	18
Case-27	320	600	40	3.91	3,015.929	2ϕ6 c/c 300mm	14
Case-28	400	750	33.60	2.18	6,433.982	2ϕ6 c/c 375mm	17
Case-29	305	200	28.60	4.43	924.477	2ϕ6 c/c 100mm	13
Case-30	250	365	43.60	3.07	1,759.291	2ϕ6 c/c 200mm	12.5
Case-31	130	185	60	6.16	402.124	2ϕ6 c/c 100mm	15
Case-32	250	510	57	3.01	3,204.423	2ϕ6 c/c 225mm	16

As a parametric study, extreme and unexpected combinations are also considered to account the actual conditions where material properties are not met due to construction errors and material test failures.

For the different combinations considered, the shear capacity of the reinforced concrete beams are computed using numerical simulation. Two point loading is applied symmetrically on equal shear span along the beam length and a mid-span deflection recorded.

4.5 Scaling Factor of the Output Parameter Shear Capacity of RC Beams

The range of input variables for the model varied by taking in to consideration some essential points which will be helpful on the parametric study on shear strength of a reinforced concrete beams. All the beams are shear critical beams. Shear span to depth ratio (a/d) data for the beams are classified as short and slender, cross section width (b) and overall depth (D) was classified as deep, wide and narrow to study the size effect. The web reinforcement ratio (ρ_w) set larger than the minimum amounts to study the effect of spacing of stirrups and the main reinforcement ratio (ρ_l) categorized as balanced and over reinforced range in order not to fail in flexural capacity plus to see the effects of zone of influence of longitudinal reinforcement on shear strength. The compressive strength (f_c') varied from normal to high strength concrete in order to know the effect of concrete compressive strength on shear capacity of RC beams. To investigate the effects of the aggregate interlock, the aggregate size (as) ranges from small to medium grain size.

4.6 Load Deflection Analysis

Here the deflection of each beam. Nonlinear finite element analysis of beams is done in VecTor-3 program and at mid span deflections an ultimate load carrying capacity of each beam are plotted as below.

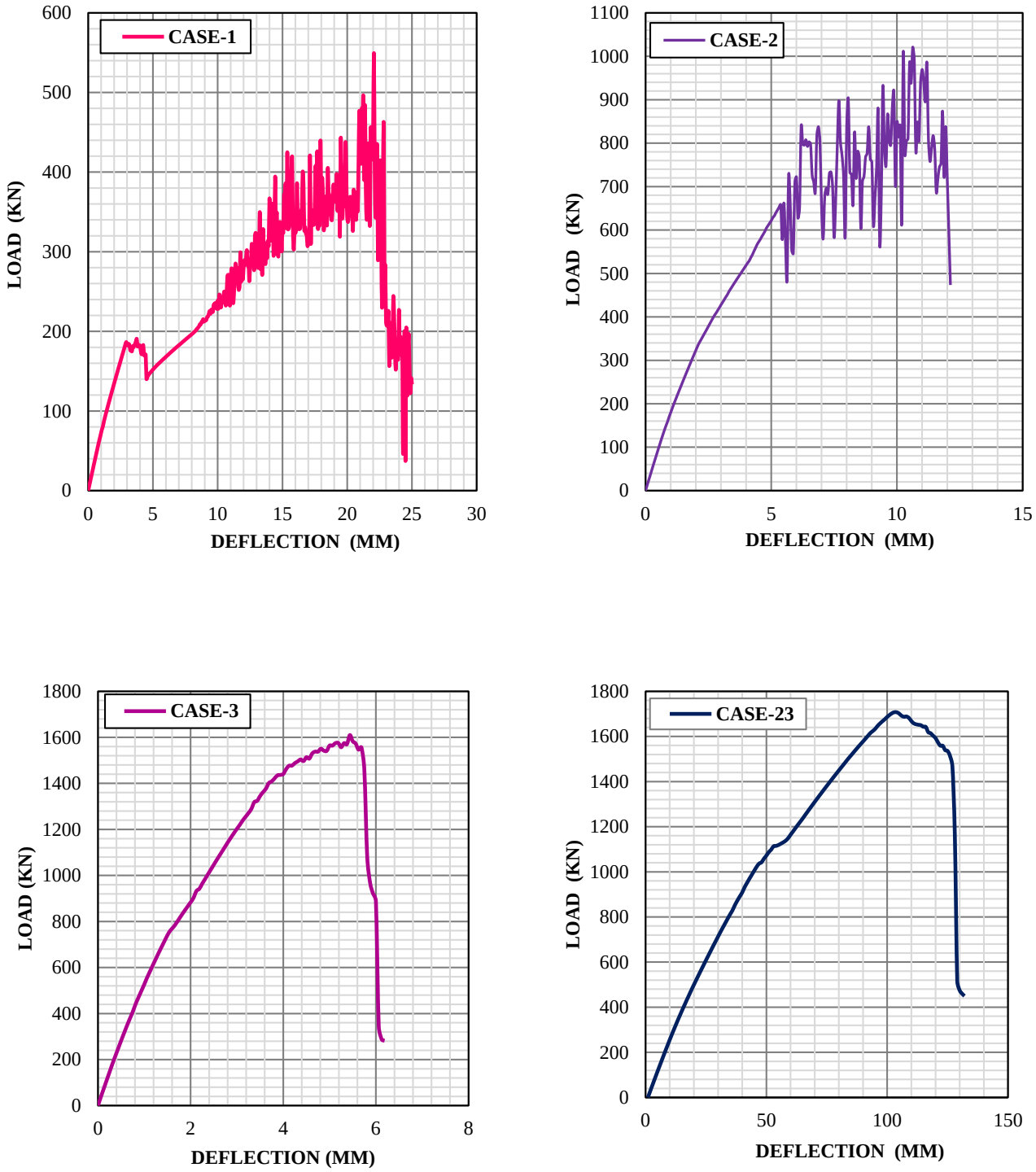

Figure 4 - 7- Load versus Mid Span Deflection of Selected RC Beams

The output of all cases is annexed.

Table 4- 9-Results from Nonlinear Finite Element Analysis

Labels	Ultimate Shear Force V_u, (kN)	Maximum deflection at failure load (mm)	Mode of Failure
Case-1	549.477	22.062	DT
Case-2	1020.969	10.625	DT
Case-3	1610.064	5.438	SC
Case-4	1148.432	9.562	ST + SC
Case-5	212.745	10.188	DT
Case-6	853.289	13.125	DT
Case-7	321.677	7.000	ST + SC
Case-8	581.583	12.375	DT
Case-9	337.634	14.812	DT
Case-10	885.260	11.500	DT
Case-11	446.460	18.062	DT
Case-12	703.206	6.812	ST + SC
Case-13	595.493	20.125	DT
Case-14	1449.404	6.562	SC
Case-15	318.135	12.188	DT
Case-16	364.448	17.750	DT
Case-17	319.404	1.938	SC
Case-18	798.808	4.000	SC
Case-19	462.892	5.562	SC
Case-20	945.675	3.562	SC
Case-21	322.876	2.875	SC
Case-22	419.364	19.500	DT
Case-23	1707.240	6.375	SC
Case-24	238.022	10.938	ST + SC
Case-25	818.562	6.000	SC
Case-26	822.174	6.688	SC
Case-27	712.689	8.500	SC
Case-28	1571.316	4.812	SC
Case-29	244.168	5.500	DT
Case-30	499.805	4.125	SC
Case-31	152.500	6.250	DT
Case-32	795.680	4.125	SC

Where:

SC – Shear Compression

ST - Shear Tension

DT – Diagonal Tension

During the load deflection analysis of the thirty two reinforced concrete beam cases nonlinear behavior of the reinforced concrete beams considered. This enables to investigate further the post cracking behavior of the beams. From the load deflection and crack pattern responses the following specimens behavior observed and discussed.

Case-2, Case-5, Case-6, Case-8, Case-9, Case-10, Case-11 and Case-16

This sample of beams attains its limited shear strength at a maximum deflection of 10.625mm, 10.188mm, 13.125mm, 12.375mm, 14.812mm, 11.500mm, 18.062mm and 17.750mm respectively. It is influenced by shear span to depth ratio ranging from $3.8 \leq a/d \leq 5.7$ and amount of longitudinal reinforcement ranges between ρ_l = 1.5% to 2%. The samples are assigned by adequate cross section and its compressive strength ranges from normal to high strength concrete however this properties does have little significance in gaining shear strength. They are assigned with minimum web reinforcement ratio ranging between ρ_w = 0.7% to 1.3% which contributes to some extent for the shear strength limitation of the beams due to the spacing of the web reinforcement. As it is seen from load deflection and crack pattern responses for most of the samples in the above cases, the diagonal shear crack propagates in unstable manner and is not linear. Diagonal cracking influences the mode of failure for most specimens. It follows diagonal tension mode of failure as it is seen from crack pattern. Their load deflection response of this samples shows their crack does not proceed immediately to failure rather the diagonal crack encounters resistance as it moves up in to the zone of compression, becomes flatter and stops at some point until further loading leads to sudden failure occurrences.

Case-1, Case-13, Case-15 and Case-22

This sample of beams failed in diagonal tension mode of failure due to their slenderness shear span for case-1, case-13, case15 and case-22. Their shear span to depth ratio (a/d) is 5.97, 6.0, 6.4 and 4.02 respectively. They are assigned with normal strength concrete. They have balanced and over reinforcement ratio of longitudinal reinforcement ranging between ρ_l = 1.75% to 2.4% and minimum amounts of web reinforcement ranging between ρ_w = 0.93% to 1.3%. The spacing of the web reinforcement has its own contribution on shear strength limitation of this beams. The samples attained their limited strength at maximum deflection of 22.062mm, 20.125mm, 12.188mm and 19.5mm respectively. As it is seen on the load deflection and crack pattern responses, their crack pattern propagate unstable and it is not linear. As the above sample of beams, this sample of beams doesn't fail immediately rather the diagonal crack encounters resistance as it moves up in to the zone of compression, further loading leads to sudden failure. The type of failure caused by these cracks are very brittle type of failure.

Case-4

The sample attain its ultimate shear strength at a maximum deflection of 9.562mm. . It is influenced by the larger beam cross section 250*860mm. Shear span to depth ratio is a/d = 3.51. The sample is assigned by a longitudinal reinforcement of ρ_l = 1.6% and web reinforcement ratio ρ_w =1.34%. It is assigned with high strength concrete compressive strength of C-60 but it has little gain in shear strength of the beam. The larger depth affected the performance of the beam on shear capacity as a result of the smaller zone of influence of the longitudinal reinforcement on controlling crack width. There is size effect on this sample. In addition to this the spacing of the web reinforcement contributed to the increase of shear stress

on this sample. However the crack pattern propagates in a stable manner as it is seen on the crack pattern responses. Afterward, it follows a combination of shear tension and shear compression mode of failure.

Case-7

The sample attain its ultimate shear strength at a maximum deflection of 7mm. It is influenced by the beams cross section. The shear span to depth ratio is a/d = 2.9. It is assigned by a longitudinal reinforcement ratio of ρ_l = 1.7% and a normal strength concrete. It has narrow beam cross section 125*510mm. As a result, size effect pronounced on this sample. The sample is also influenced by spacing of web reinforcement and distribution of longitudinal reinforcement. As a result, it follows a combination of shear tension and shear compression mode of failure.

Case-24

The sample attain its ultimate shear strength at a maximum deflection of 10.938mm. The shear span to depth ratio is a/d = 3.10. It is assigned by a longitudinal reinforcement ratio of ρ_l = 2% and a normal strength concrete. It has narrow beam cross section 130*350mm. The sample is influenced by spacing of web reinforcement and distribution of longitudinal reinforcement. As a result, it follows a combination of shear tension and shear compression mode of failure.

Case-12

The sample attain it ultimate strength at a maximum deflection of 6.812mm. It has shear span to depth ratio a/d = 3.85 and minimum longitudinal reinforcement ratio ρ_l = 1.4%. It has minimum web reinforcement ratio ρ_w = 0.90%. It is assigned by normal strength concrete. It has wider square cross section 430*400mm. It is influenced by amount and distribution of longitudinal reinforcement. It is also influenced to some extent by shear span to depth ratio and spacing of web reinforcement. As a result, it follows a combination of shear tension and shear compression mode of failure as it is seen from crack pattern response. As it is seen from load deflection response, the sample doesn't resist further loading and failed suddenly.

Case-3, Case-17, Case-18, Case-19, Case-20, Case-21, Case-26, Case-28, Case-30 and Case-32

This sample of beams have shear span to depth ratio ranging from $1.5 \leq$ a/d ≤ 3 and longitudinal reinforcement ratio ranging from ρ_l = 2% to 2.5%. They have minimum amount of web reinforcement which influences the performances of the beams. The concrete compressive strength ranges from normal to high strength which does have little significance for gaining their shear strength. The samples reaches its ultimate shear strength at a maximum deflection of 5.438mm, 1.938mm, 4.0mm, 5.562mm, 3.562mm, 2.875mm, 6.688mm, 4.812mm, 4.125mm and 4.125mm respectively. For this sample of beams arch action is dominant. The diagonal crack is linear from the load point to the support. The shear crack progresses in

stable manner and preserves sufficient amount of strength for some specimens and large reserve of strength for some other beams. Their crack proceeded to failure immediately at a smaller load stages. As a result, it is influenced by shear compression mode of failure as it is seen from load deflection and crack pattern responses.

Case-23 and Case-25

This sample of beams have the same response to failure as the above samples failing in shear compression mode of failure. It reached it ultimate shear strength at a maximum deflection of 6.375mm and 6mm. their shear span to depth ratio is a/d = 3.20 and a/d = 3.43 respectively. Case-23 is large size beam 500*1000mm and Case-25 has wider cross section 450*500mm. They have over reinforcement ratio of longitudinal reinforcement ρ_l = 2.06% for case-23 and ρ_l = 2.86% for case-25. They have minimum web reinforcement which influences the performances of the beams. They have a normal concrete compressive strength. As it is seen on their load deflection and crack pattern responses of the samples, there is size effect on both the samples, as a result it has strength limitation and failed immediately at some load point at less than the shear capacity. In addition to this, sample case-25, the wider beam cross section influences the distribution of the longitudinal reinforcement throughout the cross section which leads to sudden failure. On sample case-23, the larger depth causes reduction in effectiveness of the longitudinal reinforcement on controlling crack width.

Case- 14 and Case- 27

This sample of beams attains its ultimate strength at a maximum deflection of 6.562mm and 8.5mm. Their shear span to depth ratio (a/d) is 3.25 and 3.90 respectively. The samples are assigned with a compressive strength of concrete C-52 for case-14 and C-40 for case-27. Their longitudinal reinforcement ratio ρ_l is 1.8%. Their cross section 390*710mm and 320*600mm, the larger depth has influences the shear stress and decreases the zone of influence of the longitudinal reinforcement on controlling crack width. As a result, size effect pronounced on the samples and limits the shear strength of the sample. Their crack pattern progresses in a stable manner and linear. As a result, the samples crack pattern follow shear compression mode of failure as it is seen from crack pattern responses.

Case- 29

The sample attain its ultimate strength at a maximum deflection of 5.5mm. It is assigned by normal strength concrete, sufficient amount of longitudinal reinforcement ρ_l =1.96% and minimum web reinforcement ρ_w = 0.92%. The shear span to depth ratio a/d = 4.43. It has a cross section 305*200mm. It is influenced by the shear span to depth ratio. The crack pattern of the sample doesn't progress in stable manner and it is not linear. It failed in diagonal tension mode of failure as it is seen on the crack pattern response.

Case- 31

The sample attain its strength at a maximum deflection of 6.25mm. The sample assigned by high strength concrete C-60 which has little significance in gaining shear strength. It is assigned by over reinforcement ratio of longitudinal reinforcement ρ_l = 2.12% and minimum web reinforcement ρ_w =. 1.34%. The shear span to depth ratio a/d = 6.16. It has small cross section 130*185mm. It is evident that the sample influenced by slender shear span to depth ratio. It followed diagonal tension mode of failure.

4.7 Regression Analysis

Any method of fitting equations to data may be called regression. Such equations are valuable for at least two purposes: making predictions and judging the strength of relationships. Because they provide a way of empirically identifying how a variable is affected by other variables, regression methods have become essential in a wide range of fields, including the social sciences, engineering, medical research and business. Of the various methods of performing regression, least squares is the most widely used. In fact, partial least squares regression is by far the most widely used of any statistical technique. [7]

Once the shear strength capacity of the reinforced concrete beams first determined using three dimensional Vector-3 formwork nonlinear finite element analysis software. On thirty two randomly selected beam data samples a partial least square regression analysis were performed to evaluate which parameter has statistically significant influence on shear strength capacity. [7]

4.7.1 Partial Least Square Regression Analysis

Use this module to model and predict the values of one or more dependent quantitative or qualitative variables using a linear combination of one or more explanatory quantitative and/or qualitative variables, without facing the constraints of OLS (ordinary least square regression) on the number of variables versus the number of observations. [7]

This method is quick, efficient and optimal for a criterion based on covariances. It is recommended in cases where the number of variables is high, and where it is likely that the explanatory variables are correlated.

The idea of partial least square (PLS) regression is to create, starting from a table with n observations described by p variables, a set of h components with h < p. The method used to build the components differs from PCA (Principal Components Analysis), and presents the advantage of handling missing data. The determination of the number of components to keep is usually based on a criterion that involves a cross-validation. [7]

The equation of the PLS regression model writes:

$$\begin{aligned} Y &= T_h C_h' + E_h \\ &= X W_h^* C_h^* + E_h \\ &= X W_h (P_h' W_h)^{-1} C_h' + E_h \end{aligned} \quad (4.4)$$

Where Y is the matrix of the dependent variables, X is the matrix of the explanatory variables. T_h, C_h, W^*_h ,W_h and P'_h, are the matrices generated by the Partial Least Square algorithm, and E_h is the matrix of the residuals.

The matrix B of the regression coefficients of Yon X, with h components generated by the PLS regression algorithm is given by:

$$B = W_h (P_h' W_h)^{-1} C_h' \quad (4.5)$$

The coefficient of variation (COV) is the ratio of the standard deviation to the mean. It is dimensionless and it is a particularly useful measure of uncertainty. A small uncertainty would typically be represented by a COV = 0.05 while considerable uncertainty would be indicated by a COV = 0.25.

$$COV = \frac{\sigma}{\mu_x} \quad (4.6)$$

If a pair of random variables (X and Y, for example) depend on each other, the variable X and Y are considered to be correlated, and their covariance is defined by;

$$COV[x, y] = \frac{1}{n} \Sigma (x_i - \mu_x)(y_i - \mu_y) \quad (4.7)$$

This covariance is very similar to the variance. If the covariance is normalized by the standard of the X and Y variable, the correlation coefficient, ρ_{xy}, may be described by COV [X, Y];

$$\rho_{xy} = \frac{COV[x, y]}{\sigma_x , \sigma_y} \quad (4.8)$$

The correlation coefficient ranges in value from -1 to +1. The case $\rho_{xy} = 1$ indicates a perfect positive, linear correlation between the variable X and Y. The case $\rho_{xy} = -1$ indicates a negative, or inverse correlation, where high values of Y occur for low values of X. If the two random variable are linearly independent, then $\rho_{xy} = 0$. [7]

Thus, the general equation for the estimation of shear force is given in the following equation:

$$V_u = a_o + a_1X_1 + a_2X_2 + a_3X_3 + a_4X_4 + a_5X_5 + a_6X_6 + a_7X_7 \quad (4.9)$$

Correlation Matrix

Correlation Matrix table allows visualizing the correlation b/n the explanatory input variables and dependent variables shear force. The matrix is unit and symmetrical.

Table 4 - 10 - Correlation Matrix Table

Variables	**f_c' (MPa)**	**b (mm)**	**D (mm)**	**a / d**	**ρ_l (%)**	**ρ_w (%)**	**Aggregate Size (mm)**	**Shear Force, Vu (KN) Analysis**
f_c' (MPa)	**1.000**	-0.206	0.009	0.401	-0.054	0.995	0.238	**0.092**
b (mm)	-0.206	**1.000**	0.644	-0.138	0.012	-0.175	0.318	**0.740**
D (mm)	0.009	0.644	**1.000**	-0.222	-0.049	0.027	0.504	**0.841**
a / d	0.401	-0.138	-0.222	**1.000**	-0.511	0.396	0.040	**-0.394**
ρ_l (%)	-0.054	0.012	-0.049	-0.511	**1.000**	-0.056	-0.172	**0.181**
ρ_w (%)	0.995	-0.175	0.027	0.396	-0.056	**1.000**	0.241	**0.122**
Aggregate Size (mm)	0.238	0.318	0.504	0.040	-0.172	0.241	**1.000**	**0.484**
Shear Force, Vu (KN) Analysis	**0.092**	**0.740**	**0.841**	**-0.394**	**0.181**	**0.122**	**0.484**	**1.000**

CHARTER 5
PARAMETRIC STUDY

5.1 Introduction

A Parametric study allows to investigate the effect of different random variables and their combinations of selected processing parameter values on part quality. The range of variables will depend on the modelling process being used. In this study, to identify the effect of parameters affecting the capacity of reinforced concrete beams on shear strength, thirty two different cases are considered and sensitivity analysis of random variables has been investigated.

One of the advantage of regression analysis model is that parametric study can be carried out to evaluate the effect of all the influencing input parameters on the shear capacity of a reinforced concrete beams. The parametric study can easily be done by randomly varying input parameters and analyzing the input parameters using Vector-3 formwork program to get an output variable shear force. The error metric can also be easily evaluated using the statistical data analysis. [7]

5.2 Statistical Data Analysis

5.2.1 The XLSTAT Approach

The XLSTAT interface totally relies on Microsoft Excel, whether for inputting the data or for displaying the results. The computations, however, are completely independent of Excel and the corresponding programs relies on Visual Basic Application for the interface and have been developed with the C++ programming language for the mathematical and statistical computations.

In order to guarantee accurate results, the XLSTAT software has been intensively tested and it has been validated by specialists of the statistical methods of interest. [7]

After analyzing the statistical data using partial least square method, the most influential parameters identified with their respective correlation coefficients shown in the following table below. The coefficients of correlation is a measure of how well the independent input variables considered account for the measured dependent variable (ultimate shear force in this study).

Q^2 cumulative index is a measure of global contribution of the first components to the predicted quality of the model. R^2 X cumulative index is a measure of the coefficients of the explanatory power of the first components for the explanatory variables of the model. R^2 Y cumulative index is a measure of the coefficients of the explanatory power of the first components for the dependent variables of the model.

The Q^2 cum (h) index writes:

$$Q^2cum(h) = 1 - \prod_{j-1}^{k} \frac{\sum_{k-1}^{q} PRESS_{kj}}{\sum_{k-1}^{q} SCE_{k(j-1)}} \tag{5.1}$$

The index involves the PRESS statistic (that requires a cross-validation), and the Sum of Squares of Errors (SSE) for a model with one less component (h). The search for the maximum of the Q^2 cum index is equivalent to finding the most stable model.

R^2 (correlation coefficient) helps to determination coefficient for the model. This coefficient, whose value is between 0 and 1, is only displayed if the constant of the model has not been fixed by the user. Its value is defined by:

$$R^2 = 1 - \frac{\sum_{i-1}^{n} w_i(y_i - \hat{y}_i)^2}{\sum_{i-1}^{n} w_i(y_i - \hat{y}_i)^2} \tag{5.2}$$

Where;

$$\hat{Y} = \frac{1}{n}\sum_{i-1}^{n} w_i Y_i \tag{5.3}$$

The R^2 is interpreted as the proportion of the variability of the dependent variable explained by the model. The nearer R^2 is to 1, the better is the model. The problem with the R^2 is that it does not take into account the number of variables used to fit the model.

From the table the correlation coefficient R^2 value is equal to 0.285 for the independent input variable, 0.868 for the dependent variable shear force and 0.833 for the quality index of shear force which is less than 1. It shows the interrelationship between the independent input variables and an output dependent variable shear force. The number showed the model quality is with in an acceptable margin of error.

Table 5 - 1 - Model Quality

Statistic	Component
Q^2 cumulative	0.833
^{2} Y cumulative	0.868
R^2 X cumulative	0.285

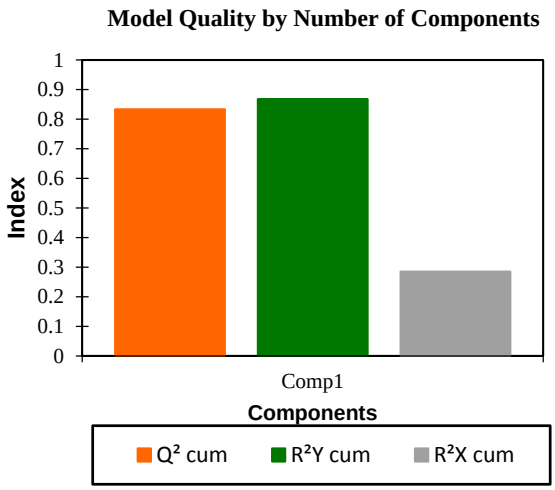

Figure 5 - 1 - Model Quality

5.2.2 Sensitivity Analysis

The sensitivity factor α_i is a kind of an index to estimate the contribution of the uncertainty of x_i to the uncertainty of the function f [8]. Since the objective function f is given, the effects of random variables can be determined as follows:

$$\alpha_i = \frac{\partial f}{\partial x_i}\frac{\bar{x}_i}{\bar{f}} \qquad (i = 1,2,3,\ldots,n) \tag{5.4}$$

$$U_i = \alpha_i (COV)_i \qquad (i = 1,2,3,\ldots,n) \tag{5.5}$$

Where, α_i: sensitivity factor of random variable i

U_i: uncertainty of random variable i

f: function with statistical variations

$\bar{f}$: mean of f

x_i : random variable i

$\bar{x}_i$: mean of x_i

COV$_i$: Coefficient of variation of random variable i

The general model for the shear capacity of a reinforced concrete beams, f, given in Eq. (4.9) is derived using multiple regression analysis. In line with this, the uncertainty of random variables for the shear capacity of a reinforced concrete beams are calculated and plotted in figure 5.2.

5.2.2.1 Uncertainty of Input Variables on Shear Strength

The statistical data analysis using sensitivity analysis gives the most significant variable from all the uncertain input variables. Uncertainty Coefficient allows comparing the relative weight of the variables in the model. The evaluation showed that the cross section of the beams, depth (D) and

width (b) are the most significant parameters from all the uncertain input data analyzed with uncertainty coefficient ratio of 0.429 and 0.378 respectively. The remaining uncertain input parameters have an uncertainty coefficient ratio of 0.247 for aggregate size (as), -0.201 for shear span to depth ratio (a/d), 0.092 for longitudinal reinforcement ratio (ρ_l), 0.062 for web reinforcement ratio (ρ_w) and 0.047 for compressive strength (fc'). The statistical data analysis shows shear span to depth ratio has inverse relationship with shear capacity of a reinforced concrete beams. All the remaining input variables have direct relationship with shear capacity.

As the cross section increases the shear capacity increases linearly however for larger beam size D ≥ 500mm, there is strength limitation. As the aggregate size assigned was fine to medium graded grain size ranging between 12.5-20mm, the influence of aggregate interlock on the thirty two beam cases were in a linear relationship with shear strength. Although the aggregate size increases the shear stress increases. During the analysis beams who doesn't have adequate cross section failed with limited shear capacity even though they are assigned with high compressive strength and sufficient amount of reinforcement as it is proved from analysis result. For beams who have larger beam depth, D ≥ 500mm, size effect pronounced. In addition to this, the zone of influence of the longitudinal reinforcement's decreases on controlling crack width as the depth increase and this influences the shear stresses on the beams. Being assigned with high strength concrete does have a little help for the RC beams in gaining shear capacity. Some other beams who are very slender during data analysis failed before reaching its ultimate capacity as a result of too long shear span to depth ratio (a/d ≥ 6). It is also evident that the amount of longitudinal reinforcement and spacing of web reinforcement has significant effect on some beam cases. Almost all of the beams have larger than the minimum web reinforcement which has influences the shear capacity due to spacing of the web reinforcement.

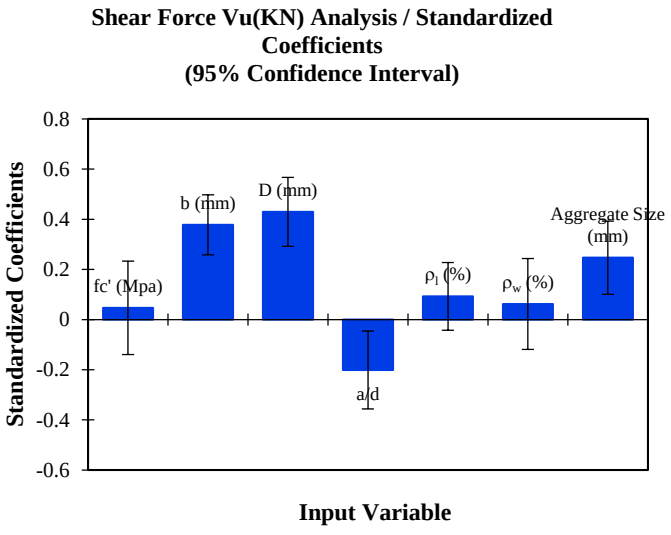

Figure 5 - 2 - Uncertainty of Random Variables

5.2.3 The Variable Importance in the Project (VIP)

The redundancies (Rd) between the input variables (dependent Y and explanatory X) allow evaluating the explanatory power of the components and variables. The redundancy between an X table (n rows and p variables) and a c component is the part of the variance of X explained by c. We define it as the mean of the squares of the correlation coefficients between the variables and the component:

$$Rd\ (X,c) = \frac{1}{P}\sum_{j-1}^{p} R^2(X_j, c) \tag{5.6}$$

From the redundancies one can deduce the VIPs (Variable Importance for the Projection) that measure the importance of an explanatory variable for the building of the t components. The VIP for the j_{th} explanatory variable and the component h is defined by:

$$VIP_{kj} = \sqrt{\frac{P}{\sum_{i-1}^{k}(Y,t_i)}\sum_{i-1}^{k} Rd(Y,t_i)w_{ij}^2} \tag{5.7}$$

The variable importance in the project (VIP) was modeled using partial least square analysis XLSTAT, 2017 program and the results shown in the table below. As shown, the measure important parameter that affects the shear strength of a reinforced concrete beams are overall depth (D) with an importance factor of 1.706, width (b) with an importance factor of 1.502, aggregate size (as) with an importance factor of 0.982, shear span to depth ratio (a/d) with an importance factor of 0.799, longitudinal reinforcement ratio (ρ_l) with an importance factor of 0.367, web reinforcement (ρ_w) with an importance factor of 0.247, and compressive strength (f_c') with an importance factor of 0.186.

Table 5 - 2 - Relative Importance of Input Parameters for the Model

Variables	VIP	Standard Deviation	Lower Bound (95%)	Upper Bound (95%)
D (mm)	1.706	0.157	1.386	2.027
b (mm)	1.502	0.177	1.140	1.864
Aggregate Size (mm)	0.982	0.326	0.316	1.647
a / d	0.799	0.285	0.218	1.380
ρ_l (%)	0.367	0.255	-0.153	0.887
ρ_w (%)	0.247	0.352	-0.471	0.965
f_c' (MPa)	0.186	0.364	-0.556	0.928

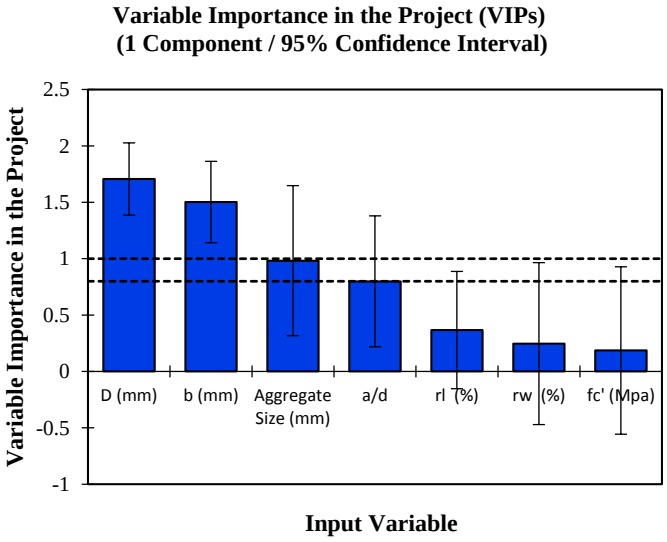

Figure 5 - 3 - Variable Importance of the Project

Figure 5-3 illustrates, variables who lied inside the border line b/n 0.8 ≤ VIP ≤ 1 indicates the variables are moderately influential while variables who lied above one VIP ≥ 1 indicates the variables are highly influential. As a result, overall depth (D), width (b) and aggregate size (as) are highly influential parameters on shear capacity of the beams and the remaining input parameters shear span to depth ratio (a/d), longitudinal reinforcement ratio (ρ_l), web reinforcement (ρ_w) and compressive strength (f_c') are moderately influential on shear strength of a reinforced concrete beams.

5.2.4 Model Parameters

The coefficients of the variables for the model equation is determined using partial least square analysis and given in the following equation.

Equation of the Model:

$$v_u = -994.53 + 1.60f_c' + 1.52\text{b} + 0.84\text{D} + 65.52\frac{a}{d} + 97.28\rho_l + 147.86\rho_w + 41.50\text{as} \quad (5.8)$$

Results for Variable Shear Force Vu (KN) VECTOR-3:

Table 5 - 3 - Standardized Coefficients (Variable Shear Force Vu (KN) VECTOR-3)

Variable	Coefficient	Standard Deviation	Lower bound (95%)	Upper bound (95%)
f_c' (MPa)	0.047	0.092	-0.140	0.233
b (mm)	0.378	0.059	0.258	0.498
D (mm)	0.429	0.067	0.292	0.567
a / d	-0.200	0.076	-0.356	-0.046
ρ_l (%)	0.092	0.066	-0.043	0.227
ρ_w (%)	0.062	0.089	-0.119	0.243
Aggregate Size (mm)	0.247	0.072	0.101	0.393

5.2.5 Predictions and Residuals (Variable Shear Force V_u (kN) Analysis):

The partial least square regression analysis prediction shows that the accuracy of the shear strength estimate is reliable. The ratio of shear force to standard residuals for the thirty two scatter of beam samples lied between 0.828 and -1.041. The distribution of standard residual with respect to shear force Vu of analysis for the observations are shown in figure 5.4. Whereas the comparison of ideal predicted shear force with respect to shear force Vu VecTor-3 analysis on figure 5.5 shows there is only three data case which are outside the ideal boarder line but it is normal to have three data left over outside the limit. The three sample of beams input variables influences the shear capacity of the beams.

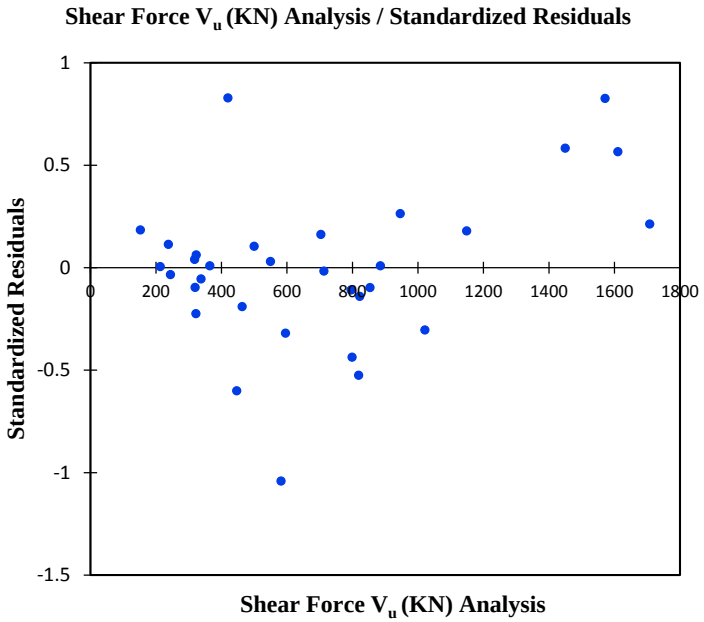

Figure 5 - 4 – Standard Residuals V_s Shear Force V_u (KN) Analysis

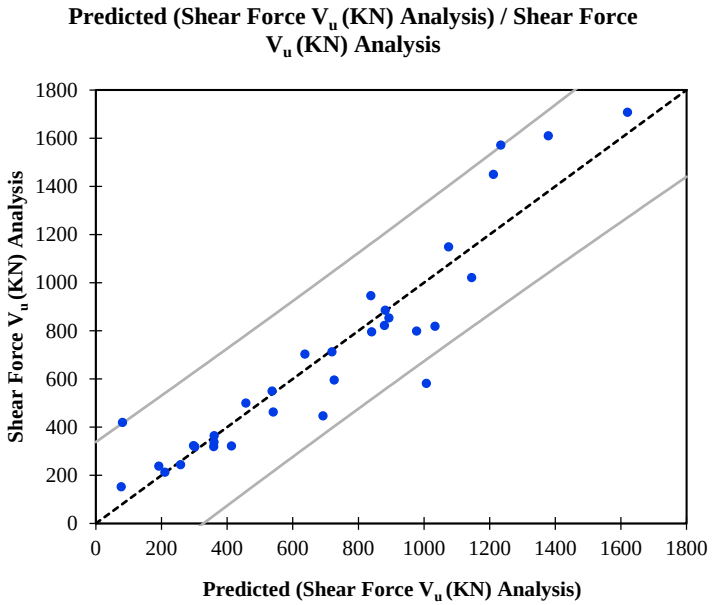

Figure 5 - 5- Predicted Shear Force V_u (KN) V_s shear Force V_u (KN) Analysis

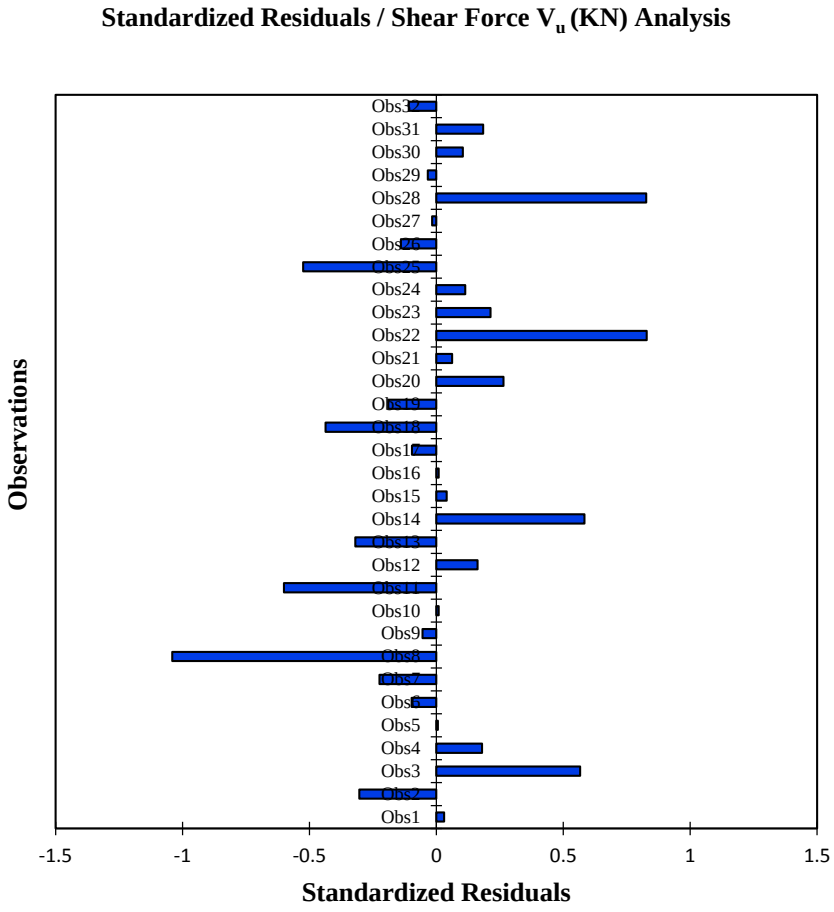

Figure 5 - 6 - Observations Vs Standard Residuals

As it is seen on the standardized residuals of shear force in the above figure, the standard residual for the thirty two data cases sets between -1 and 1. This shows fifteen data cases who have laid in the negative direction have inverse relationship between the dependent (Y) output variables shear force and independent (X) input variables. The remaining seventeen data cases who laid in the positive direction have linear relationship between the dependent variable shear force and independent input variables. In conclusion, fifteen data cases ultimate shear capacity is influenced by their input variables and the other seventeen data cases input variables has significant effect on the ultimate shear capacity of the beams.

5.2.6 Outliers Analysis:

In statistics, an outlier is a value recorded for a given variable that seems unusual and suspiciously lower or greater than the other observed values. An outlier can be reading error or due to typical event. When there are outliers in the data, depending on the stage of the study, we must identify them, possibly with the aid of tests, flag them in the reports, delete or use methods able to treat them as such. [7]

XLSTAT gives an approximation of critical values above which one should reject null (Ho) for a given significant level, α. XLSTAT gives approximation based on Monte Carlo simulations. XLSTAT gives the p-value that corresponds to the computed statistic as well as the conclusion of the test taking into account the significance level given by the user. The acceptance interval is set typically between -1.96 to 1.96 for the critical independent variable and between -1.454 to 1.454 for the dependent variable for 95% confidence interval. Distance from each observation to the model in the space of X variable (DModX) allow identifying outlier for the explanatory variables and distance from each observation to the model in the space of Y (DModY) allow identify outlier for the dependent variables.

The value of the DModX for the i_{th} observation writes:

$$DModX_i = \sqrt{\frac{n}{n-h-1}\frac{\sum_{j-1}^{P} e(X,t)_{ij}^2}{P-h}} \tag{5.9}$$

Where the $e(X,t)_{ij}$ $(i = 1 \dots n)$ are the residuals of the regression of X on the j_{th} component. The value of the DModY for the i_{th} observation writes:

$$DModY_i = \sqrt{\frac{\sum_{j-1}^{q} e(Y,t)_{ij}^2}{q-h}} \tag{5.10}$$

Where q is the number of dependent variables and the $e(Y,t)_{ij}$ $(i = 1 \dots n)$ are the residuals of the regression of Y on the j_{th} component.

For this analytical data cases the values of DModX with respect to DCrit(X) =1.710 for the independent input variables X and DModY with respect to DCrit(Y) =1.393 for the dependent output variable. Any value that is outside is considered suspicious. However if there are large values, it is statistically normal to have some outside this interval. [7]

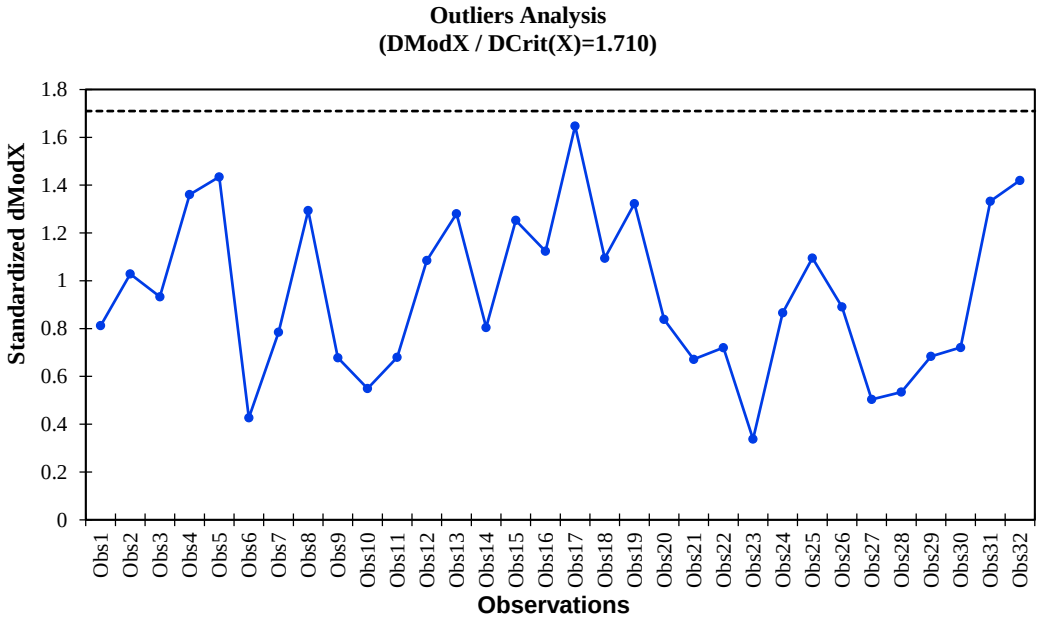

Figure 5 - 7 - Outlier Analysis with respect to input variables

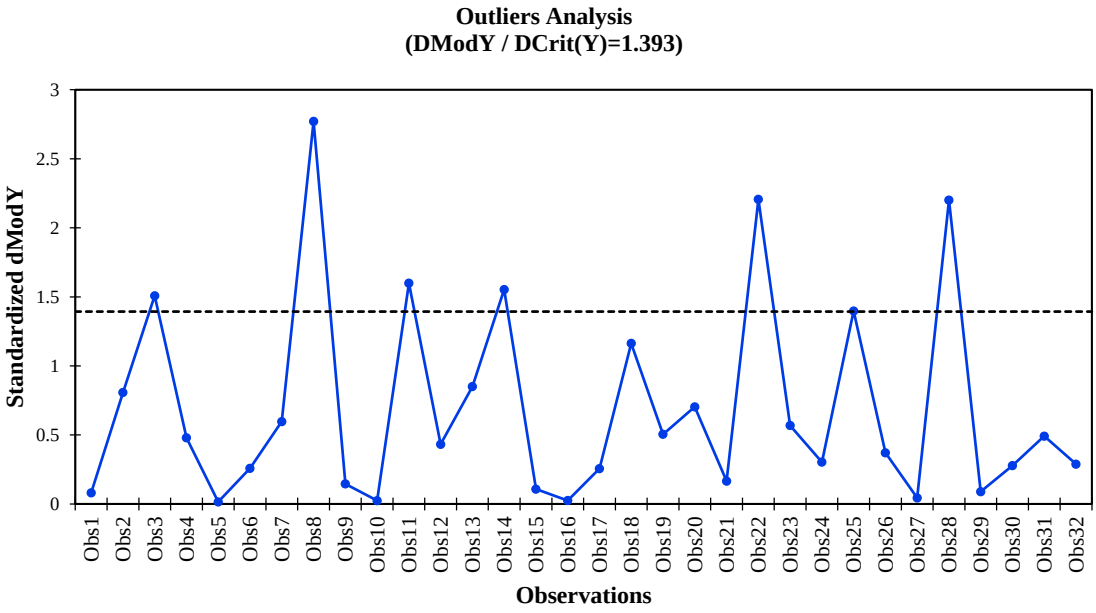

Figure 5 - 8 - Outlier Analysis with respect to dependent output variable

CHAPTER 6

CONCLUSION AND RECOMMENDATION

6.1 Conclusion

A parametric study was carried out on shear strength of reinforced concrete beams after an application of nonlinear finite element analysis using three dimensional VecTor-3 program in predicting the ultimate shear capacity of thirty two simply supported reinforced concrete shear critical beams subjected to symmetrically placed two point loading. Based on the statistical data analysis, the following conclusion can be made:

1. The parametric study have showed the influence of the seven input variables on shear capacity of a reinforced concrete beams. Overall depth (D), width (b) of beam and aggregate size (as) are highly influential whereas shear span to depth ratio (a/d), longitudinal reinforcement ratio (ρ_l), web reinforcement ratio (ρ_w) and compressive strength (f_c') have moderately influences the shear capacity of the beams. The variables importance in the project are 1.706, 1.502, 0.982, 0.799, 0.367, 0.247 and 0.186 respectively.
2. During the sensitivity analysis, it is further verified that overall depth (D), width (b), aggregate size (as), longitudinal reinforcement ratio (ρ_l), web reinforcement ratio (ρ_w) and compressive strength (f_c') have direct relationship with ultimate shear strength of a reinforced concrete beams. Whereas, shear span to depth ratio has inverse relationship with the shear strength of a reinforced concrete beams.
3. It can be concluded from the analysis result, there is size effect. Effects of aggregate interlock on shear stress, influence of shear span to depth ratio on strength limitation, influences of amount and distribution of longitudinal reinforcement. Influences of spacing of web reinforcement. Lastly little significance of compressive strength on gaining shear strength of a reinforced concrete beams.

6.2 Recommendation

This research showed that the ultimate shear capacity of reinforced concrete beams can be influenced by the seven input variables. It is recommended to further investigate both experimentally and analytically the effects of different input variables on shear strength of a reinforced concrete beams specially size effect, influence of shear span to depth ratio, effects of aggregate interlock with a large data set collection. Afterward, factor of safety can be considered and this will enable to construct rational empirical equation in shear design methods.

References

[1] Frank J. Vecchio, "Analysis of Shear-Critical Reinforced Concrete Beams," ACI Structural Journal, vol. 97, January - February 2000.

[2] Yousif Jabbar Lafta, "Specification of Deep Beams Affect the Shear Strength Capacity," Vol.8, No.2, 2016.

[3] Wassim M. Ghannoum,"Size Effect on Shear Strength of Reinforced Concrete Beams," November 1998.

[4] Raju International Journal of Engineering Research and Applications ISSN, "Review on Shear Behavior of Reinforced Concrete Beam without Transverse Reinforcement", ISSN: 2248-9622, Vol. 4, Issue 4(Version 8), April 2014.

[5] Lionel Moreillon,"Shear strength of structural elements in high performance fiber reinforced concrete (HPFRC)". Universite Paris-Est, September, 2013.

[6] ACI-ASCE Committee 445, "Recent Approaches to Shear Design of Structural Concrete" American Society of Civil Engineers, December 1999.

[7] XLSTAT 'Microsoft Excel Statistical Analysis Sheet" 2017.

[8] Tsubaki, T. "Sensitivity Analysis", Transport of the Japan Concrete Institute, Vol. 11, pp. 97-104, 1989.

[9] Appendix A- Sampling Methods: Retrieved from;
http://www.uio.no/studier/emner/matnat/math/STK4400/v05/undervisningsmateriale/Sampling%20methods.pdf

[10] Shirley D.: Statistics for Researchers, 3rd ed, John Wiley and Sons, Inc., 2004.

[11] Mekdes Tadesse,"Effects of spacing and configuration of web reinforcement on shear behavior of reinforced concrete beams", Addis Ababa University Institute of Technology, 2015 E.C.

[12] K. J. Weight and J. G. MacGregor, "Reinforced Concrete Mechanics & Design", 6th ed. New Jersey, US: Pearson Education, 2012.

[13] Vecchio, F.J., and Collins, M.P., "Predicting the Response of Reinforced Concrete Beams Subjected to Shear Using the Modified Compression Field Theory ". ACI Structural Journal, Vol.85 No.3, p. 258-268, May-June 1988.

[14] American Concrete Institute Committee 318, "Building Code Requirements for Structural Concrete", ACI 318-08, American Concrete Institute , Detroit, MI, 2008

[15] ACI Committee 318, "Building Code Requirements for Structural Concrete (AC1 318-95) and Commentary (AC1 318R-95) ". American Concrete Institute. Detroit, 1995, 369 pp.

APPENDIX A

Beam Models for Vector -3 Formwork Analysis

Beam Models for Vector -3 Formwork Analysis

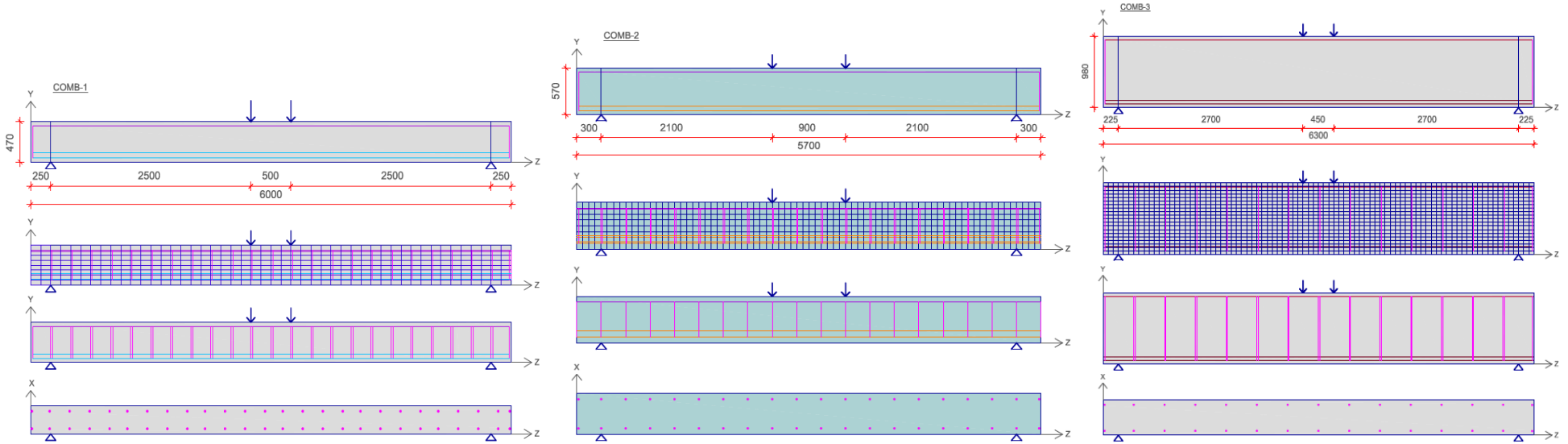

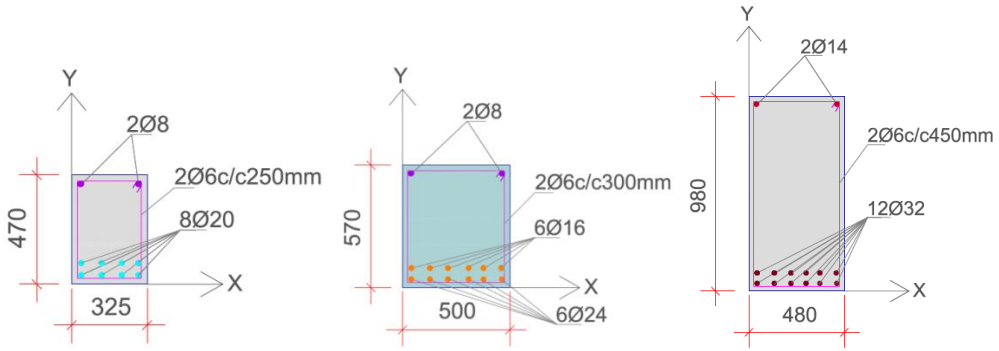

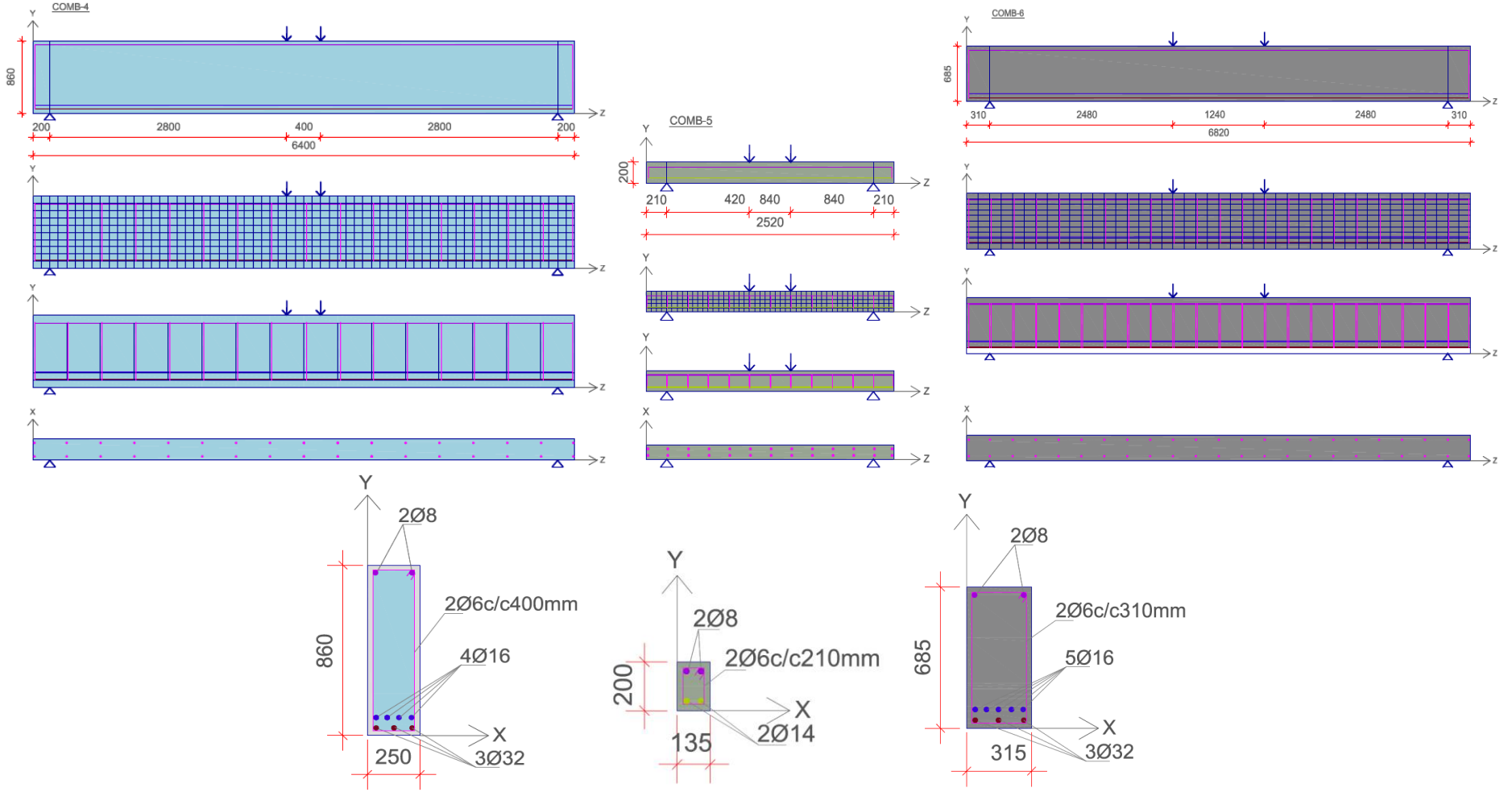
COMB-4
860
200
2800
400
2800
200
6400
COMB-5
200
210
420
840
840
210
2520
COMB-6
685
310
2480
1240
2480
310
6820
2Ø8
2Ø6c/c400mm
4Ø16
860
250
3Ø32
2Ø8
2Ø6c/c210mm
200
135
2Ø14
2Ø8
2Ø6c/c310mm
5Ø16
685
315
3Ø32

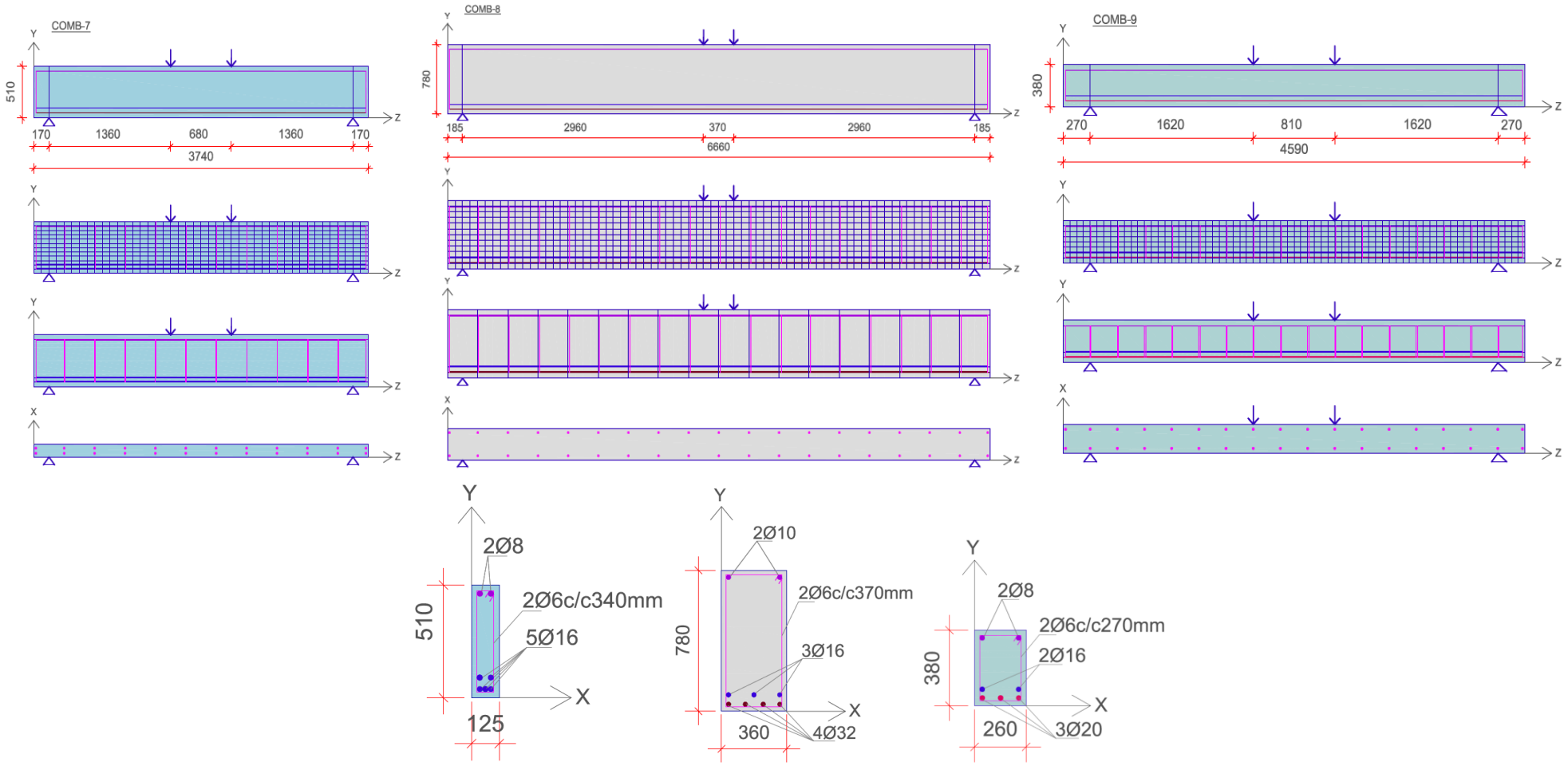
COMB-7
510
170
1360
680
1360
170
3740
COMB-8
780
185
2960
370
2960
185
6660
COMB-9
380
270
1620
810
1620
270
4590
2Ø8
2Ø6c/c340mm
5Ø16
510
125
2Ø10
2Ø6c/c370mm
3Ø16
780
360
4Ø32
2Ø8
2Ø6c/c270mm
2Ø16
380
260
3Ø20

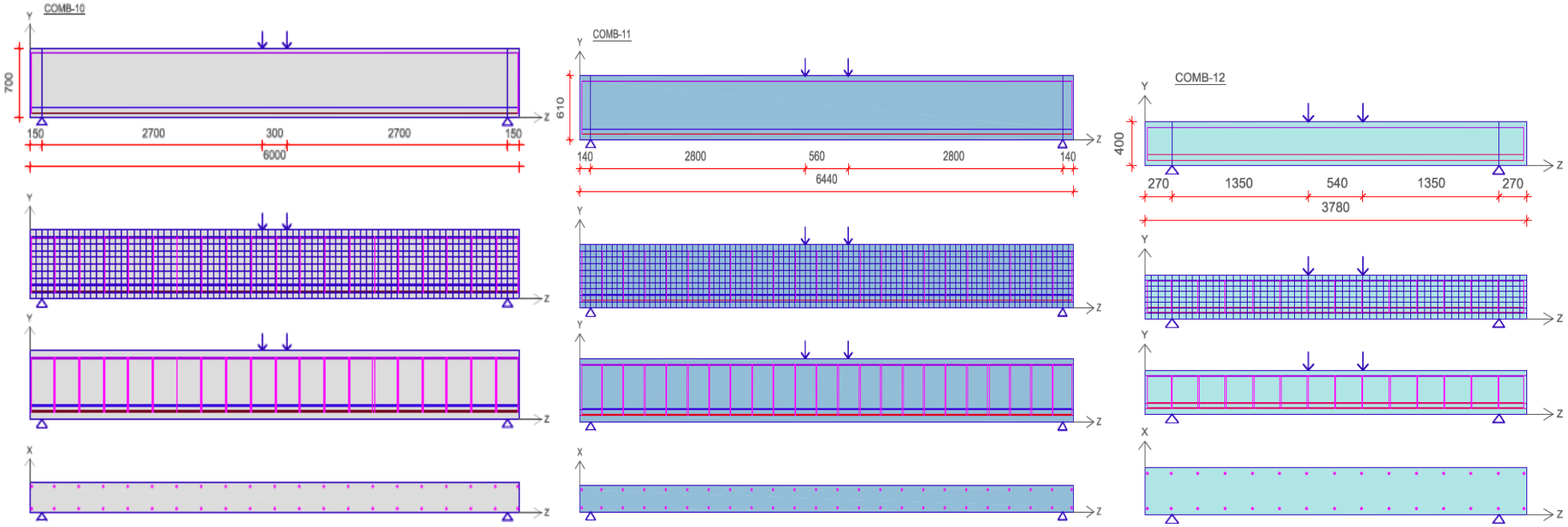
COMB-10
700
150
2700
300
2700
150
6000
COMB-11
610
140
2800
560
2800
140
6440
COMB-12
400
270
1350
540
1350
270
3780

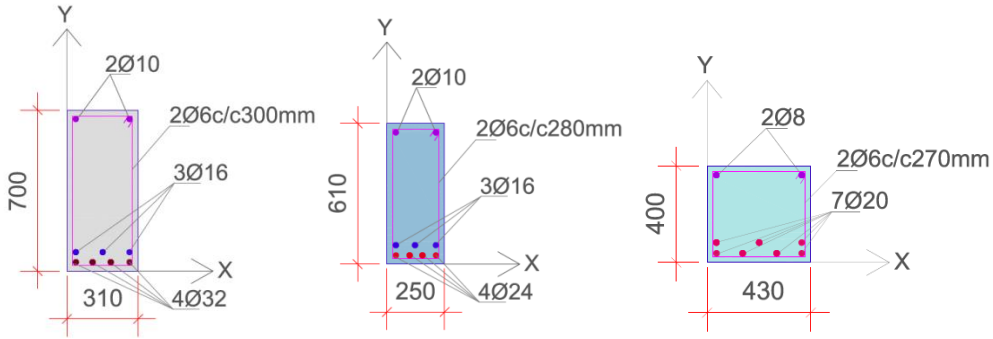
2Ø10
2Ø6c/c300mm
3Ø16
700
310
4Ø32
2Ø10
2Ø6c/c280mm
3Ø16
610
250
4Ø24
2Ø8
2Ø6c/c270mm
7Ø20
400
430

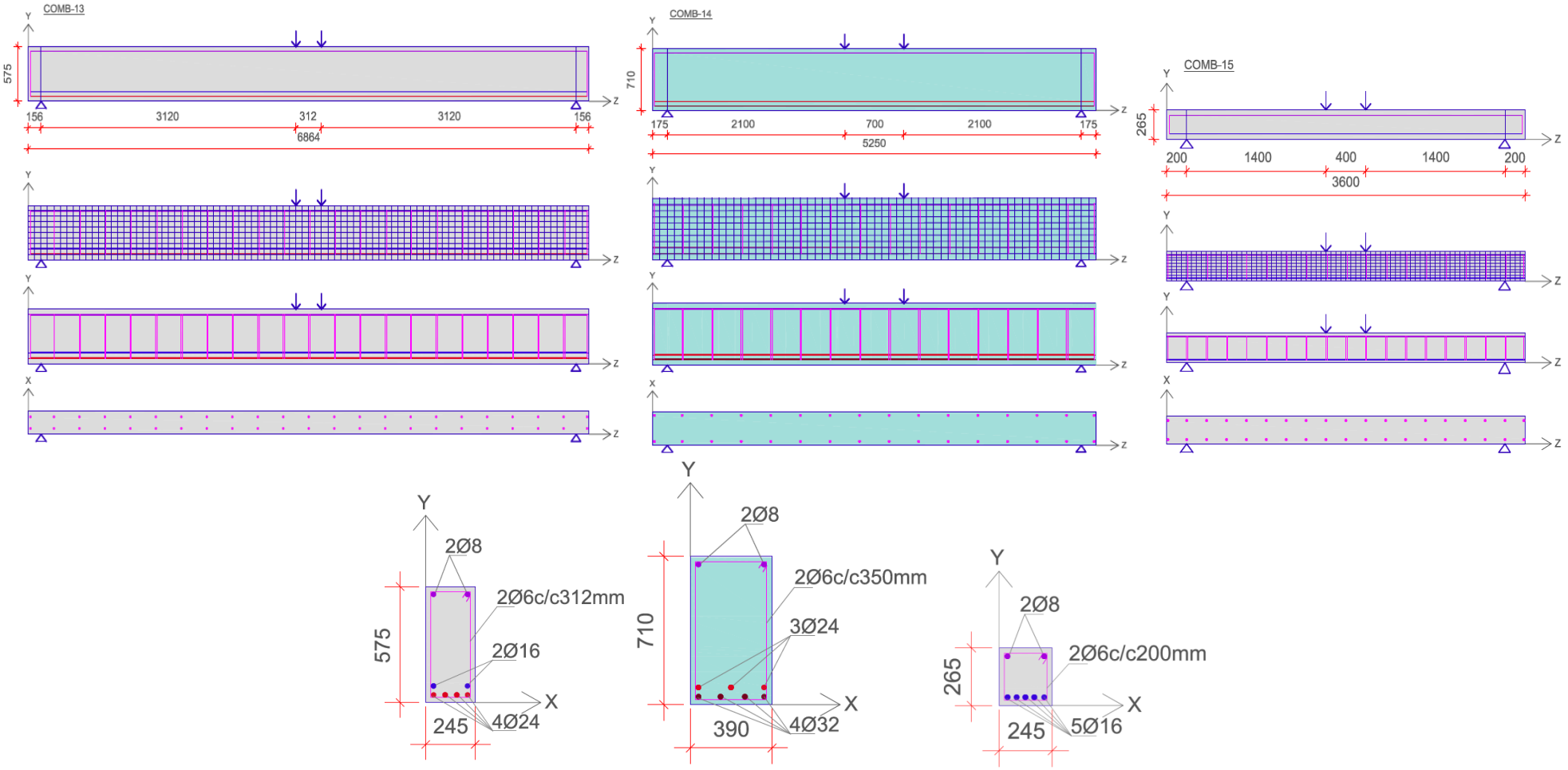
COMB-13
575
156
3120
312
3120
156
6864
COMB-14
710
175
2100
700
2100
175
5250
COMB-15
265
200
1400
400
1400
200
3600
Y
Z
X
2Ø8
2Ø6c/c312mm
2Ø16
575
245
4Ø24
2Ø8
2Ø6c/c350mm
3Ø24
710
390
4Ø32
2Ø8
2Ø6c/c200mm
265
245
5Ø16

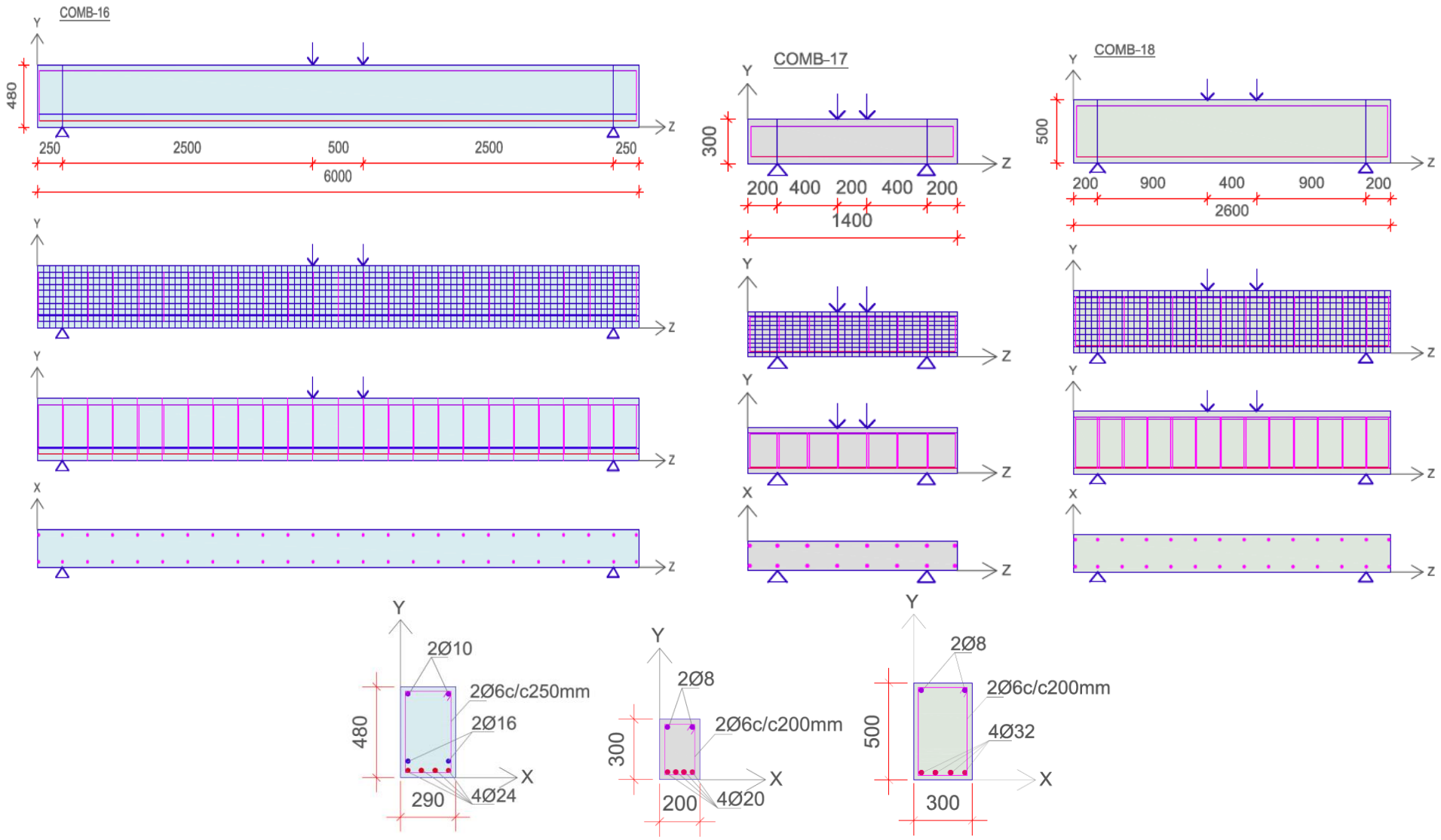
COMB-16
480
250
2500
500
2500
250
6000
COMB-17
300
200
400
200
400
200
1400
COMB-18
500
200
900
400
900
200
2600
2Ø10
2Ø6c/c250mm
2Ø16
480
290
4Ø24
2Ø8
2Ø6c/c200mm
300
200
4Ø20
2Ø8
2Ø6c/c200mm
4Ø32
500
300

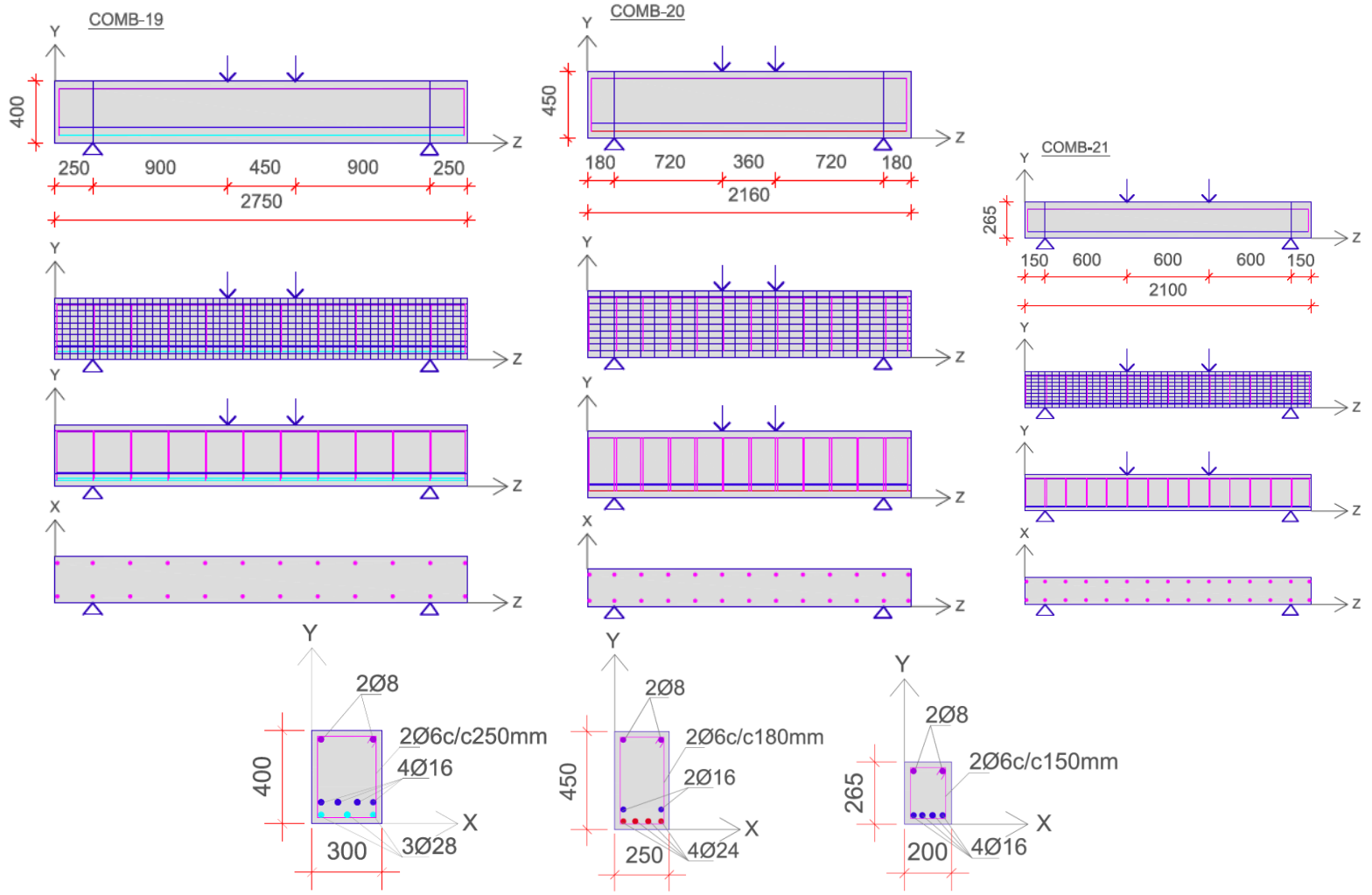
COMB-19
400
250
900
450
900
250
2750
COMB-20
450
180
720
360
720
180
2160
COMB-21
265
150
600
600
600
150
2100
Y
Z
X
2Ø8
2Ø6c/c250mm
4Ø16
3Ø28
400
300
2Ø6c/c180mm
2Ø16
4Ø24
450
250
2Ø6c/c150mm
4Ø16
265
200

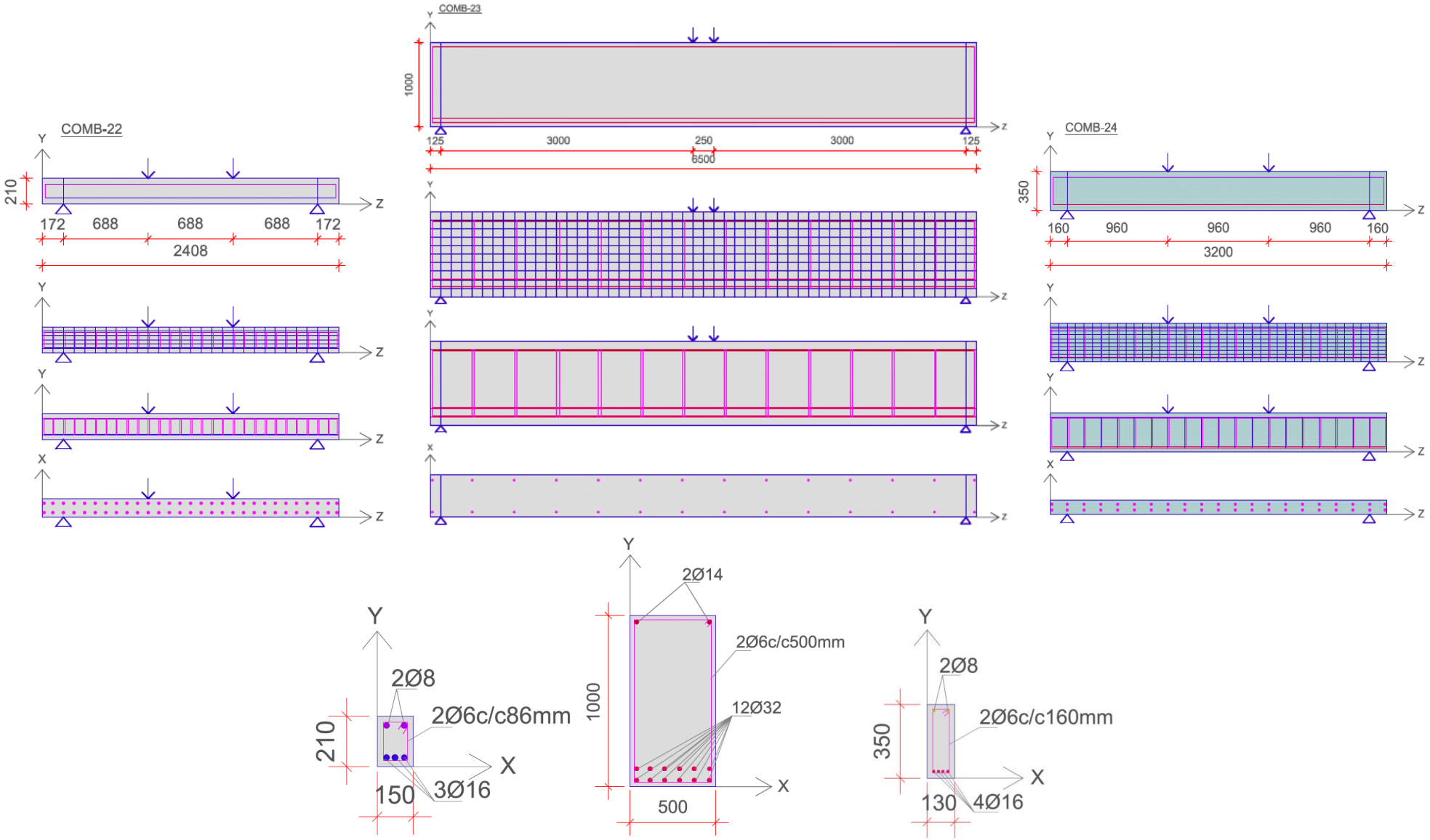
COMB-22
210
172
688
688
688
172
2408
COMB-23
1000
125
3000
250
3000
125
6500
COMB-24
350
160
960
960
960
160
3200
Y
Z
X
2Ø8
2Ø6c/c86mm
210
150
3Ø16
2Ø14
2Ø6c/c500mm
12Ø32
1000
500
2Ø8
2Ø6c/c160mm
350
130
4Ø16

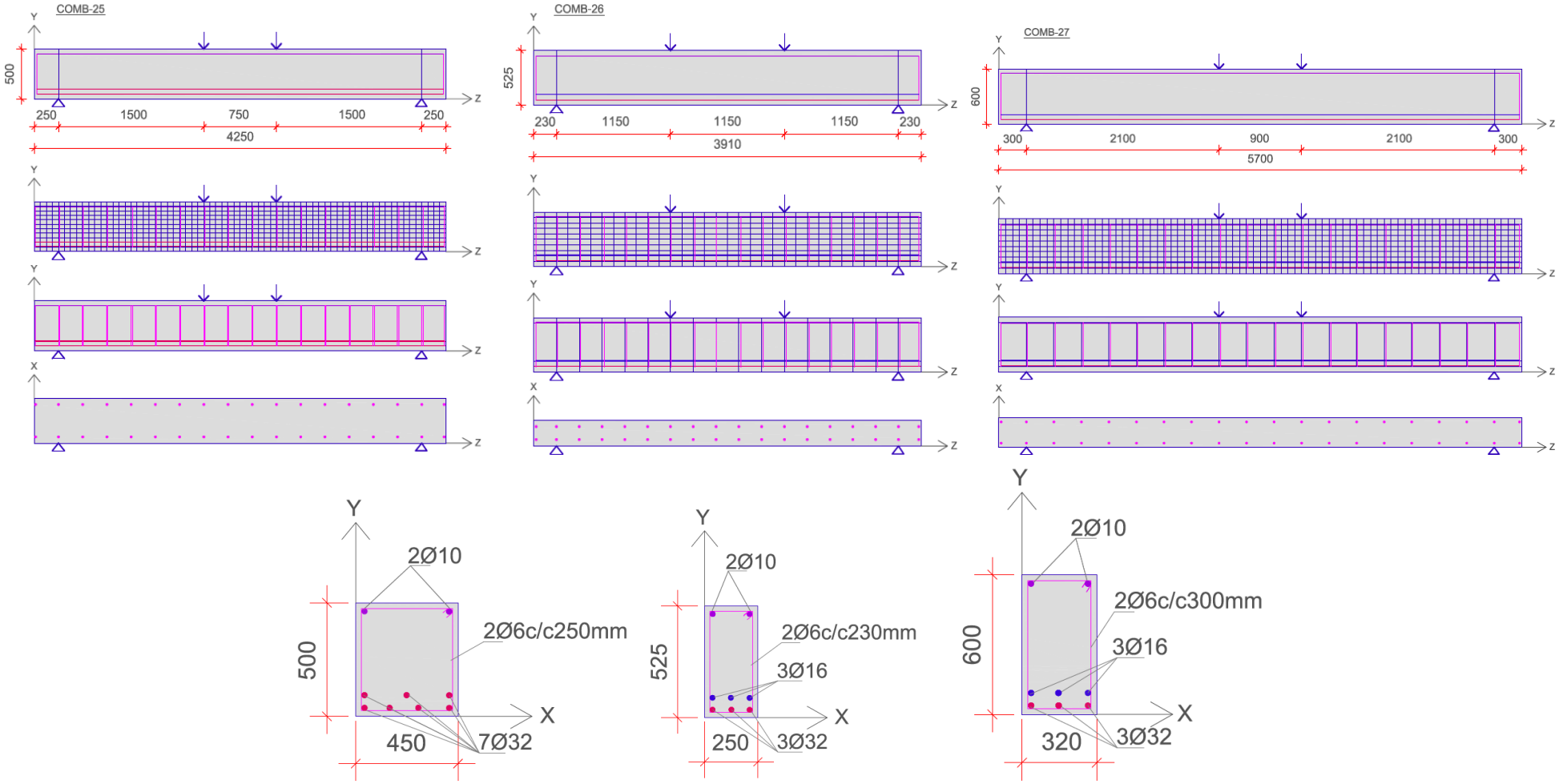
COMB-25
500
250
1500
750
1500
250
4250
COMB-26
525
230
1150
1150
1150
230
3910
COMB-27
600
300
2100
900
2100
300
5700
Y
Z
X
2Ø10
2Ø6c/c250mm
500
450
7Ø32
2Ø10
2Ø6c/c230mm
3Ø16
525
250
3Ø32
2Ø10
2Ø6c/c300mm
3Ø16
600
320
3Ø32

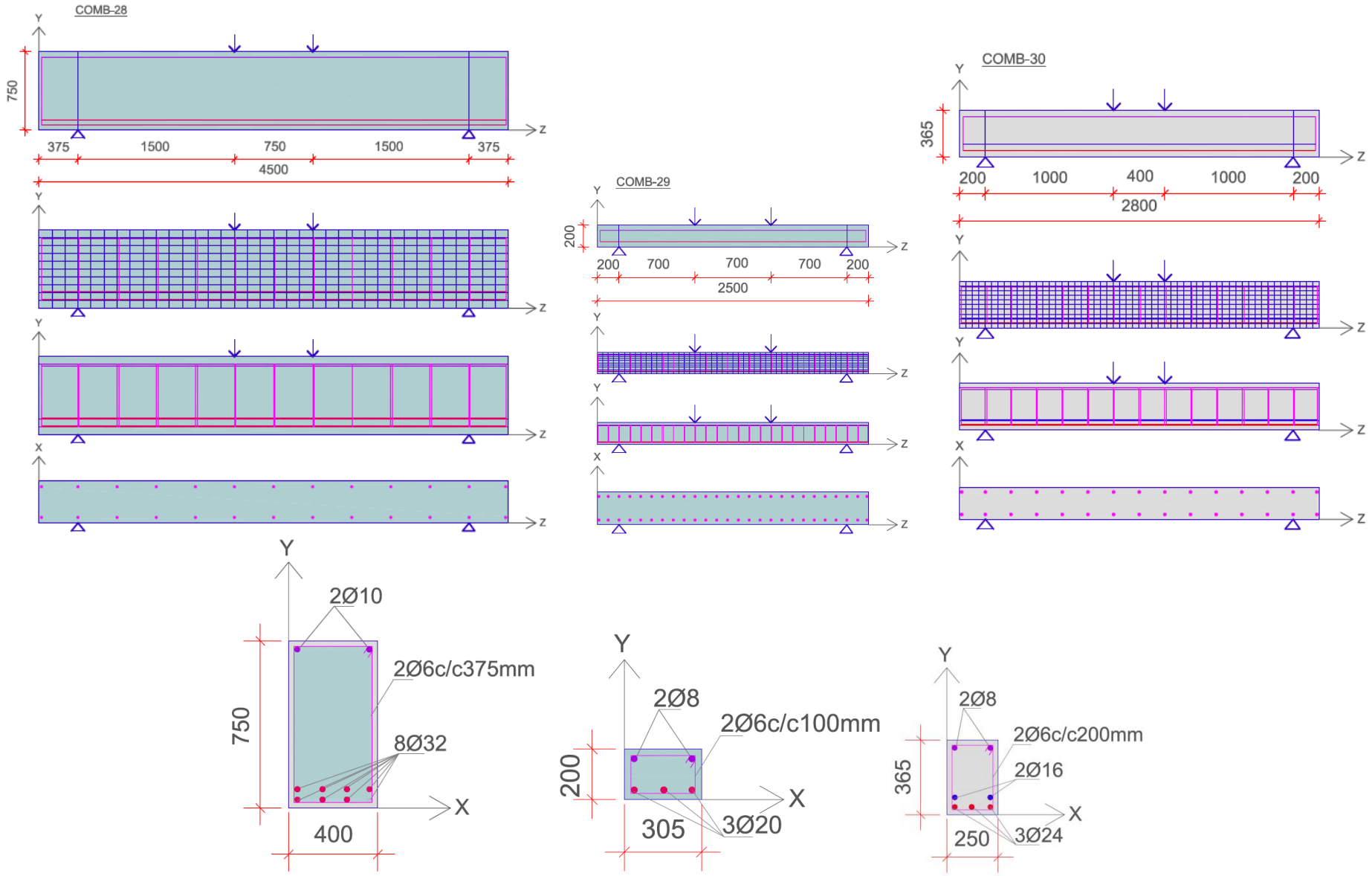
COMB-28
750
375
1500
750
1500
375
4500
COMB-29
200
200
700
700
700
200
2500
COMB-30
365
200
1000
400
1000
200
2800
Y
X
Z
2Ø10
2Ø6c/c375mm
8Ø32
750
400
2Ø8
2Ø6c/c100mm
200
305
3Ø20
2Ø8
2Ø6c/c200mm
2Ø16
365
250
3Ø24

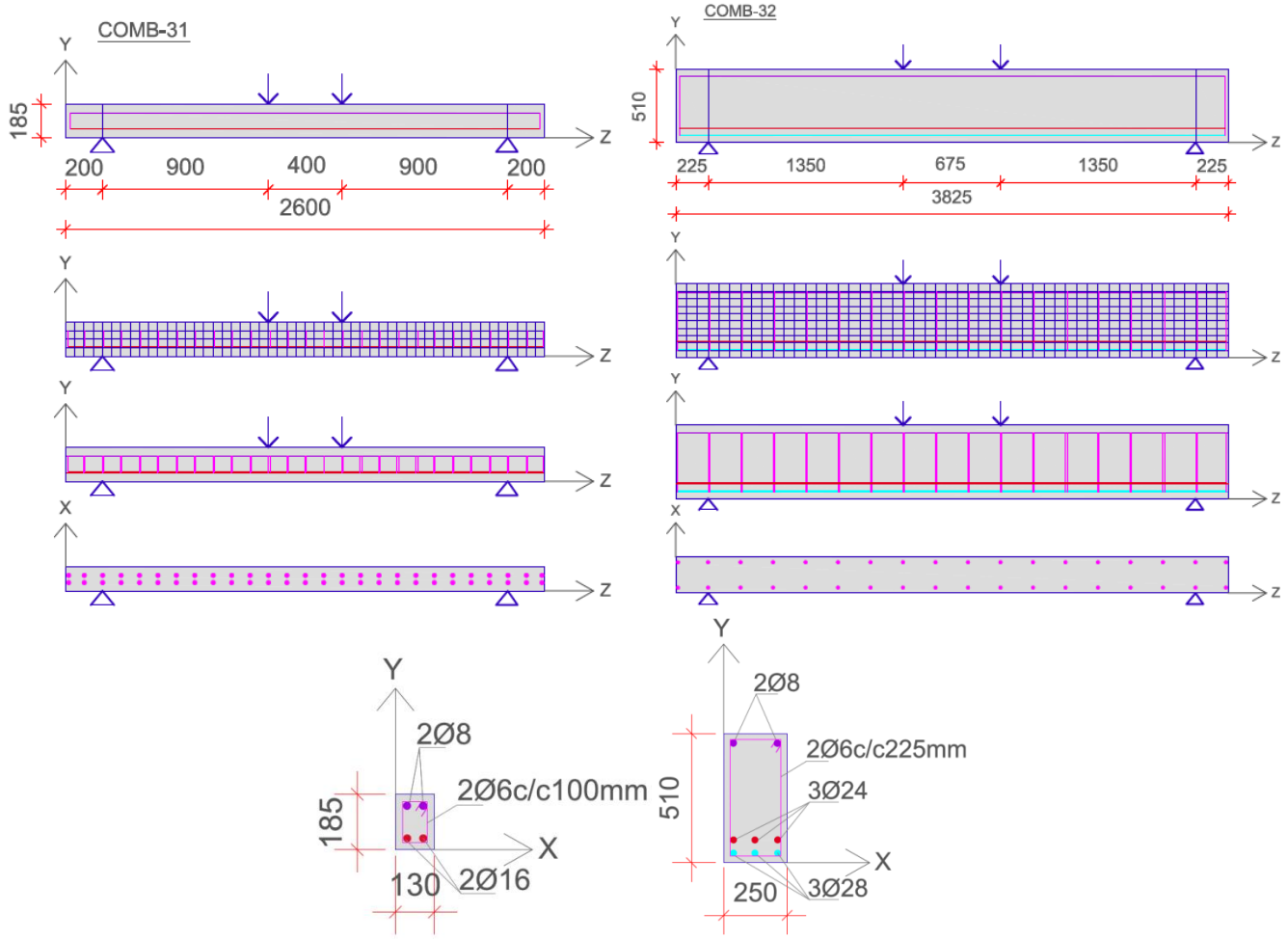
COMB-31
Y
Z
185
200
900
400
900
200
2600
X
COMB-32
510
225
1350
675
1350
225
3825
2Ø8
2Ø6c/c100mm
2Ø16
130
2Ø6c/c225mm
3Ø24
3Ø28
250

APPENDIX B

Analysis Outputs

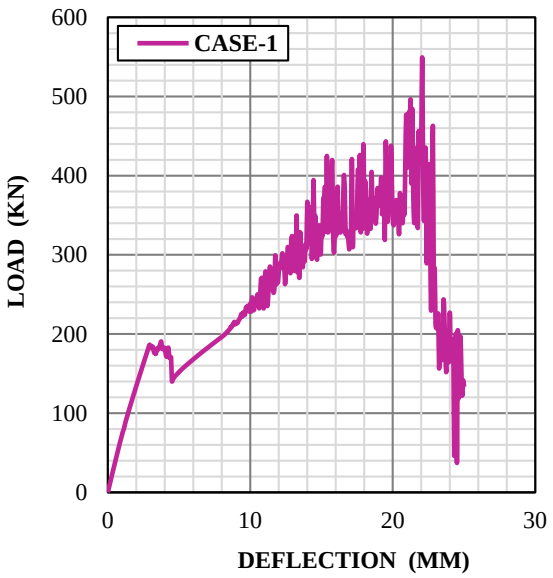
CASE-1
LOAD (KN)
DEFLECTION (MM)
0
100
200
300
400
500
600
0
10
20
30

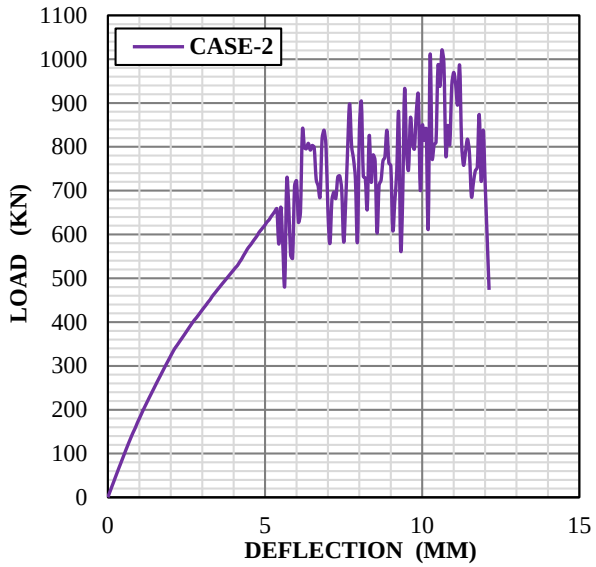
CASE-2
LOAD (KN)
DEFLECTION (MM)
0
100
200
300
400
500
600
700
800
900
1000
1100
0
5
10
15

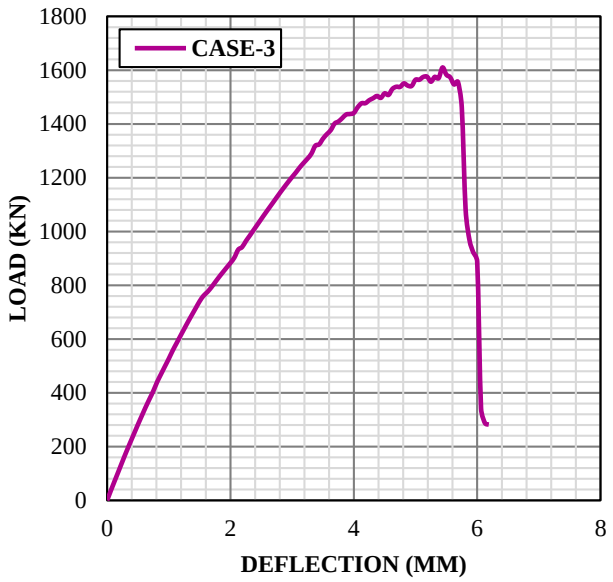
CASE-3
LOAD (KN)
DEFLECTION (MM)
0
200
400
600
800
1000
1200
1400
1600
1800
0
2
4
6
8

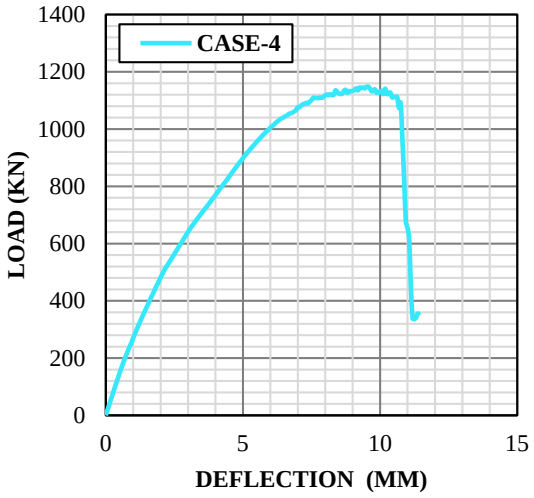
CASE-4
LOAD (KN)
DEFLECTION (MM)
0
200
400
600
800
1000
1200
1400
0
5
10
15

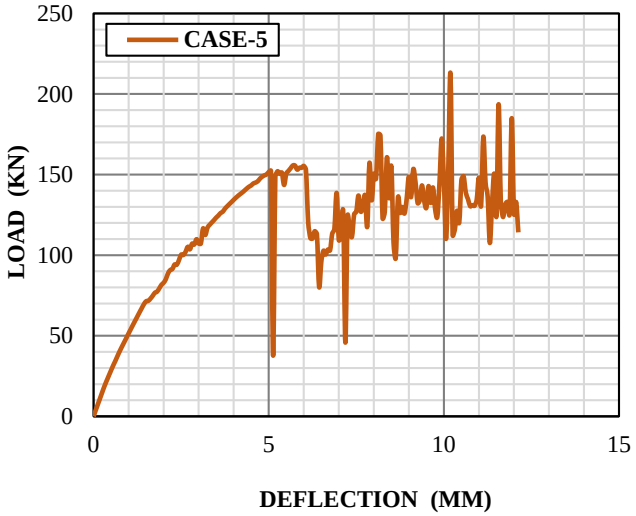
CASE-5
LOAD (KN)
DEFLECTION (MM)
0
50
100
150
200
250
0
5
10
15

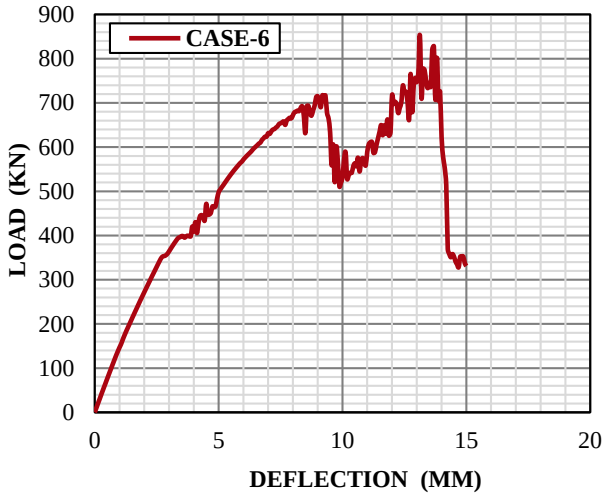
CASE-6
LOAD (KN)
DEFLECTION (MM)
0
100
200
300
400
500
600
700
800
900
0
5
10
15
20

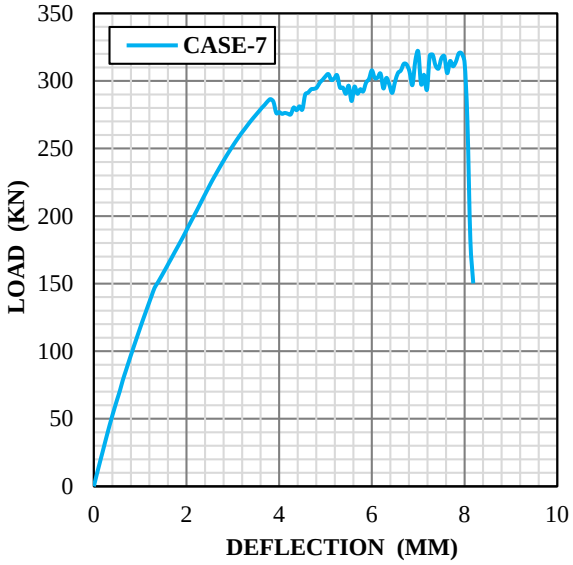
CASE-7
LOAD (KN)
DEFLECTION (MM)
0
50
100
150
200
250
300
350
0
2
4
6
8
10

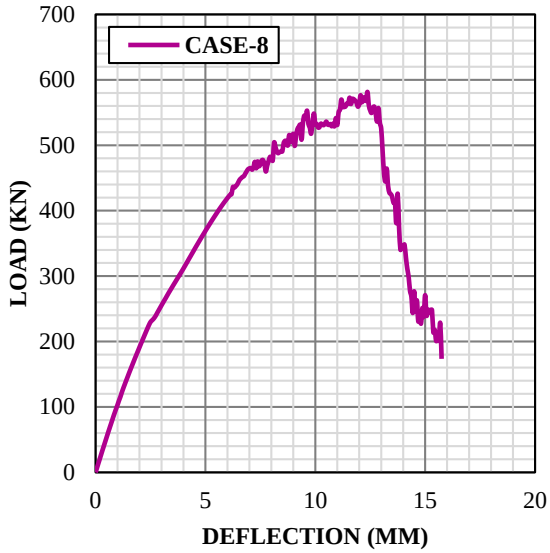
CASE-8
LOAD (KN)
DEFLECTION (MM)
0
100
200
300
400
500
600
700
0
5
10
15
20

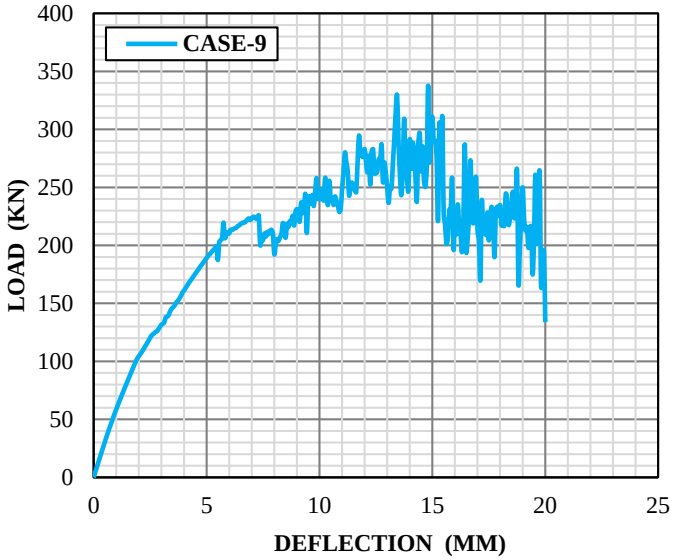
CASE-9
LOAD (KN)
DEFLECTION (MM)
0
50
100
150
200
250
300
350
400
0
5
10
15
20
25

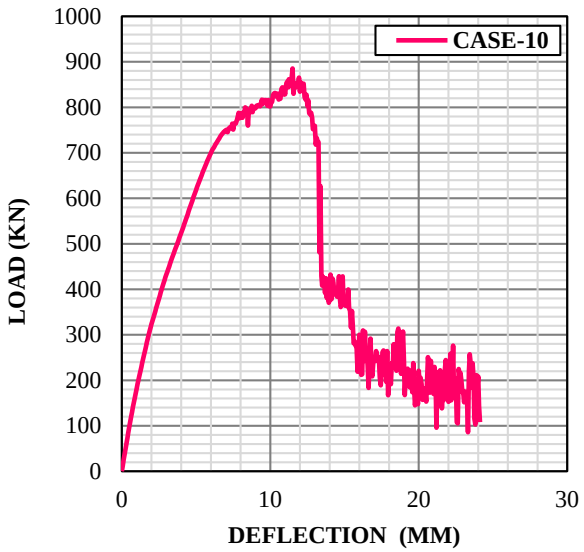
CASE-10
LOAD (KN)
DEFLECTION (MM)
0
100
200
300
400
500
600
700
800
900
1000
0
10
20
30

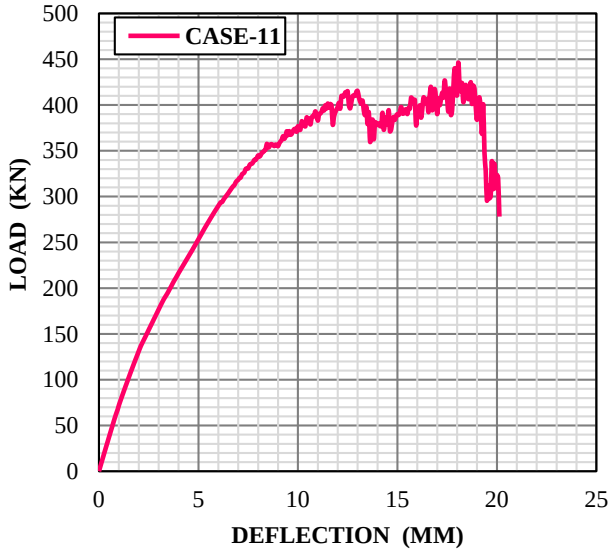
CASE-11
LOAD (KN)
DEFLECTION (MM)
0
50
100
150
200
250
300
350
400
450
500
0
5
10
15
20
25

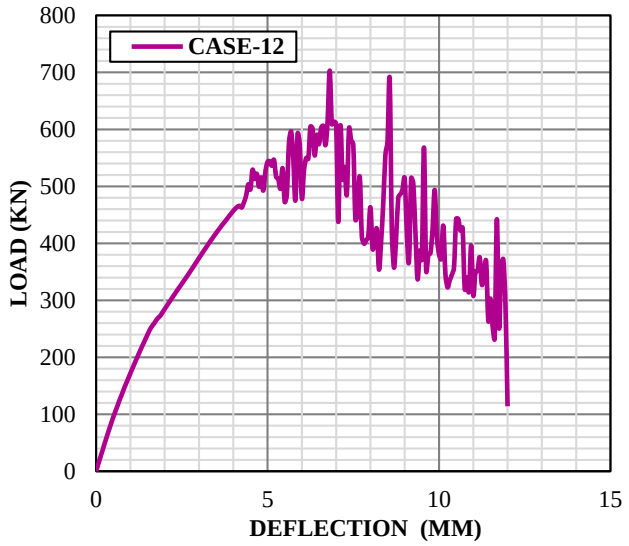
CASE-12
LOAD (KN)
DEFLECTION (MM)
0
100
200
300
400
500
600
700
800
0
5
10
15

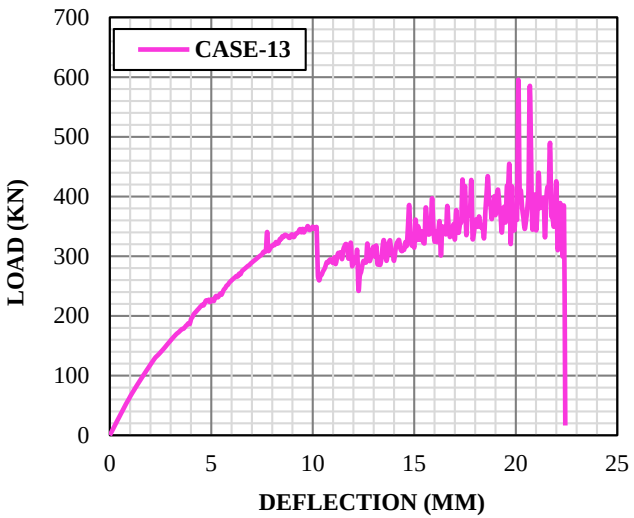
CASE-13
LOAD (KN)
DEFLECTION (MM)
0
100
200
300
400
500
600
700
0
5
10
15
20
25

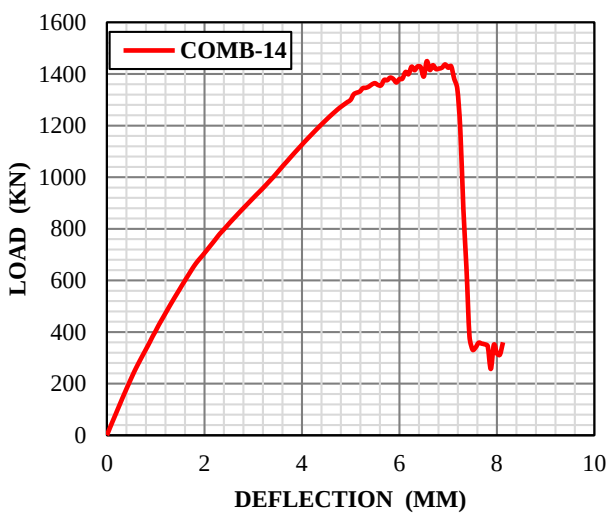
COMB-14
LOAD (KN)
DEFLECTION (MM)
0
200
400
600
800
1000
1200
1400
1600
0
2
4
6
8
10

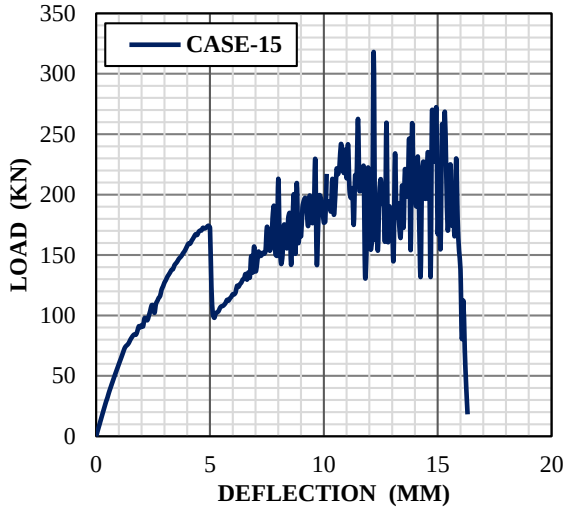
CASE-15
LOAD (KN)
DEFLECTION (MM)
0
50
100
150
200
250
300
350
0
5
10
15
20

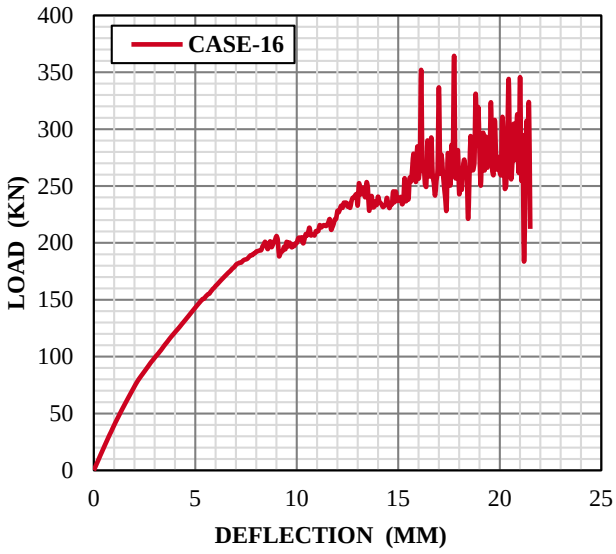
CASE-16
LOAD (KN)
DEFLECTION (MM)
0
50
100
150
200
250
300
350
400
0
5
10
15
20
25

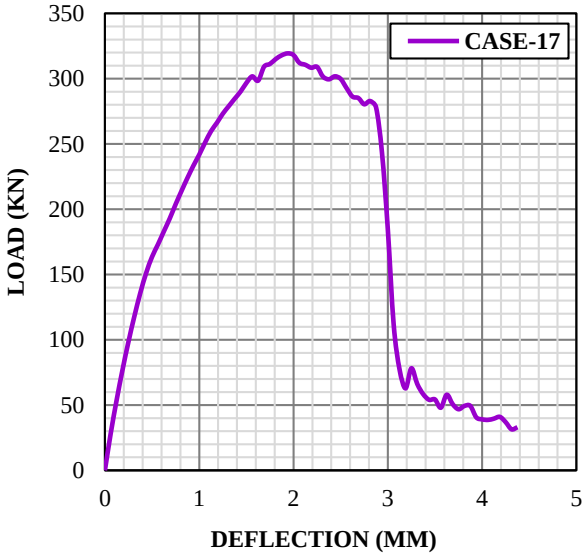
CASE-17
LOAD (KN)
DEFLECTION (MM)
0
50
100
150
200
250
300
350
0
1
2
3
4
5

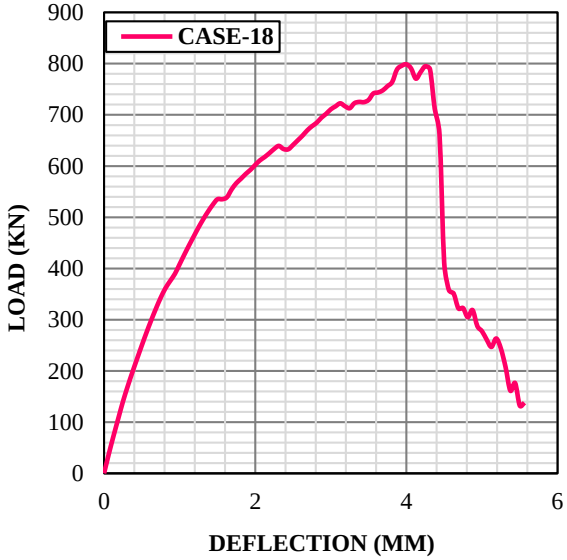
CASE-18
LOAD (KN)
DEFLECTION (MM)
0
100
200
300
400
500
600
700
800
900
0
2
4
6

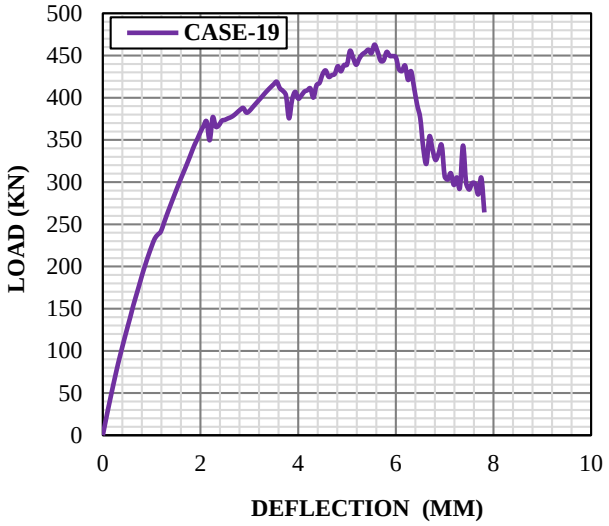
CASE-19
LOAD (KN)
DEFLECTION (MM)

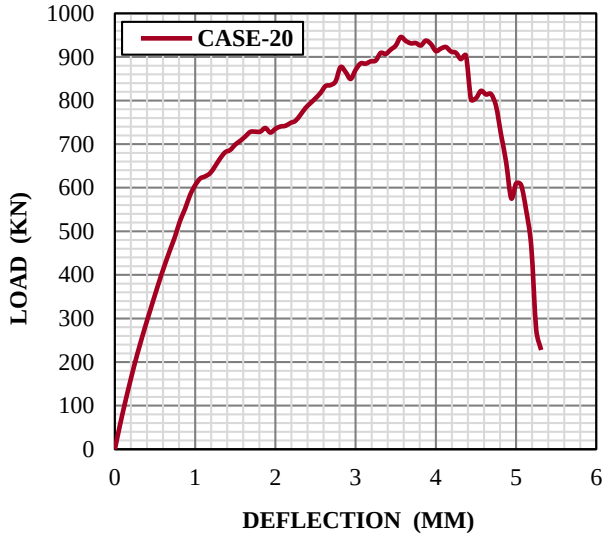
CASE-20
LOAD (KN)
DEFLECTION (MM)

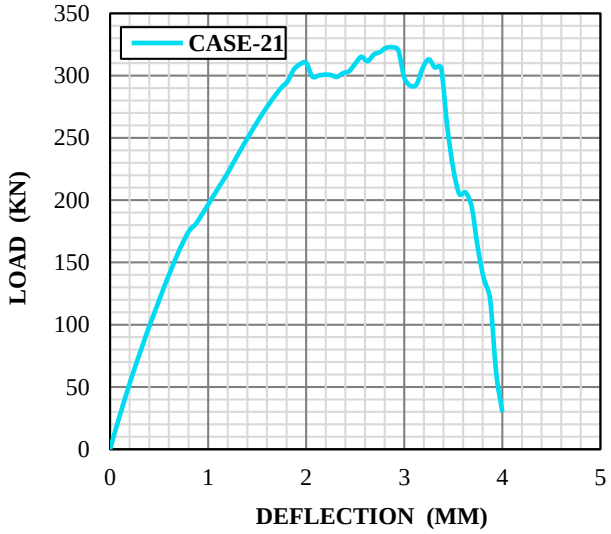
CASE-21
LOAD (KN)
DEFLECTION (MM)

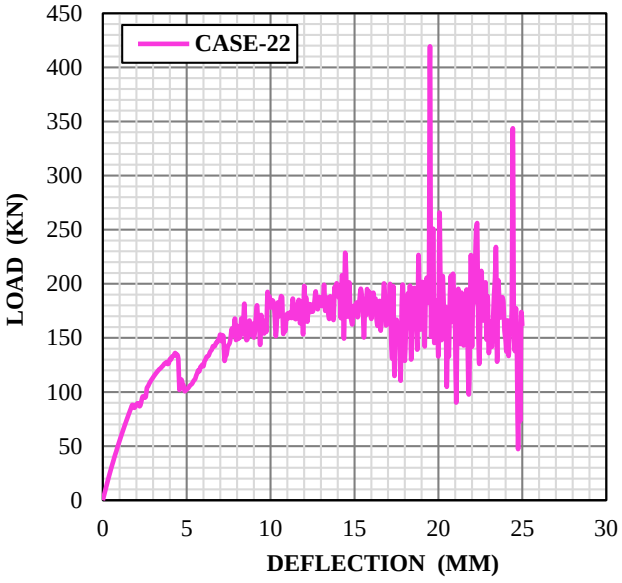
CASE-22
LOAD (KN)
DEFLECTION (MM)

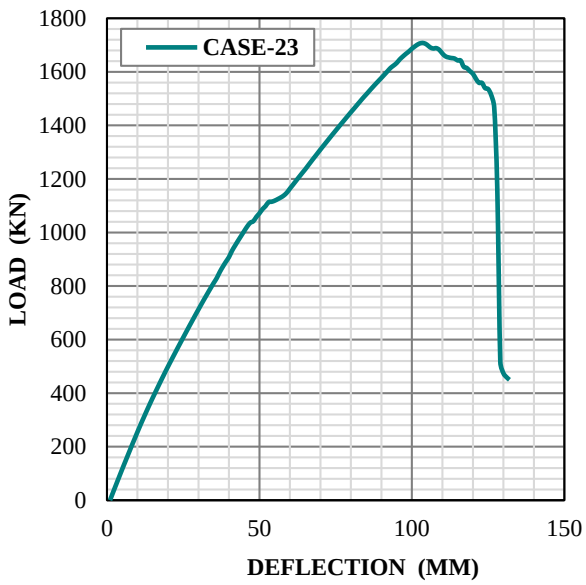
CASE-23
LOAD (KN)
DEFLECTION (MM)

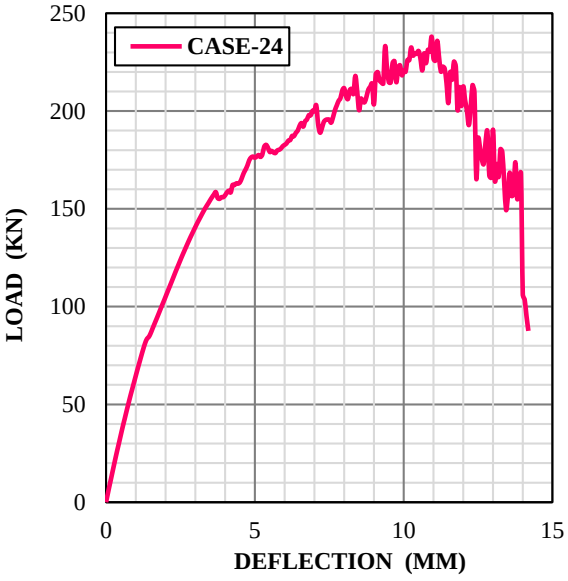
CASE-24
LOAD (KN)
DEFLECTION (MM)

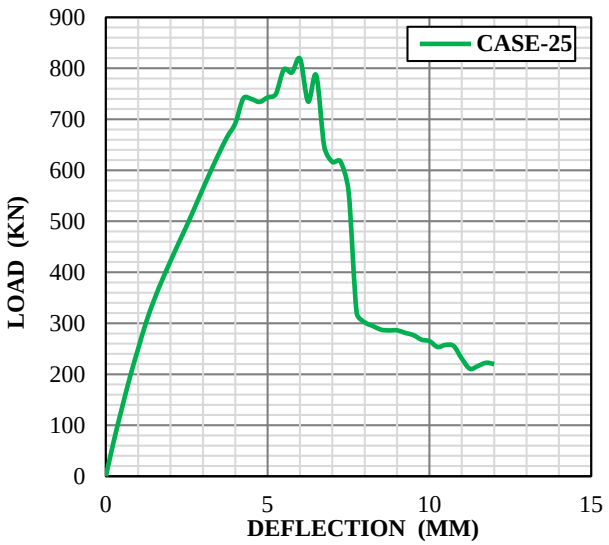
CASE-25
LOAD (KN)
DEFLECTION (MM)
0
100
200
300
400
500
600
700
800
900
0
5
10
15

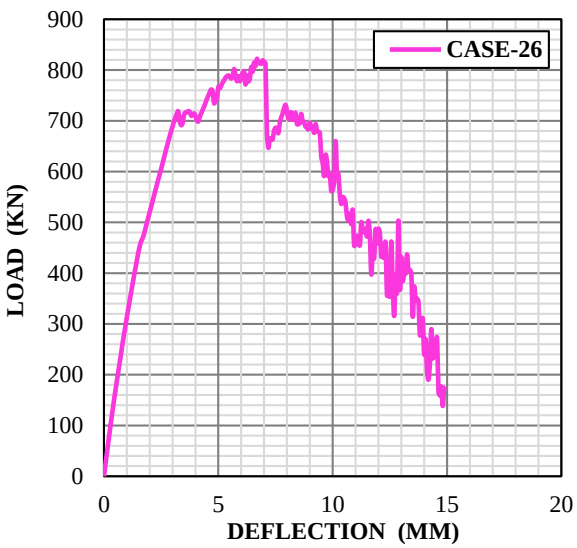
CASE-26
LOAD (KN)
DEFLECTION (MM)
0
100
200
300
400
500
600
700
800
900
0
5
10
15
20

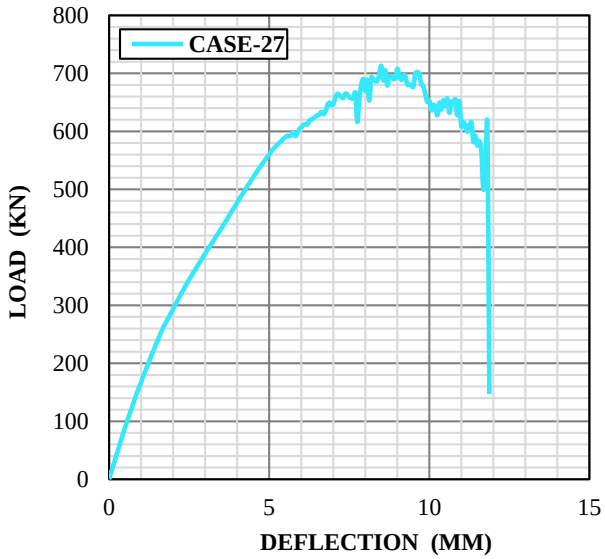
CASE-27
LOAD (KN)
DEFLECTION (MM)
0
100
200
300
400
500
600
700
800
0
5
10
15

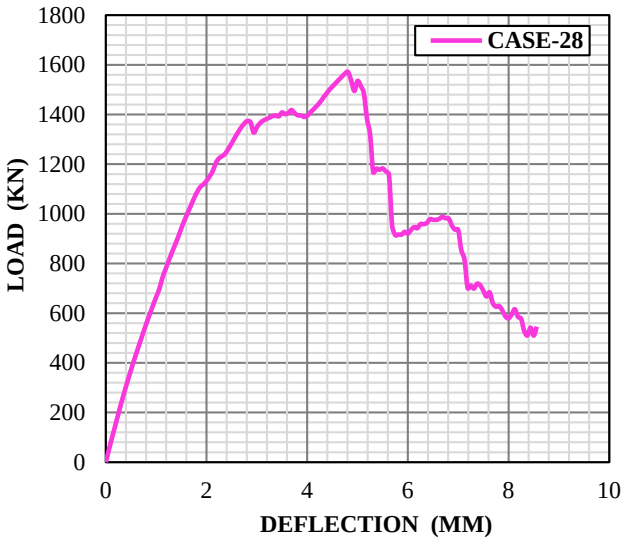
CASE-28
LOAD (KN)
DEFLECTION (MM)
0
200
400
600
800
1000
1200
1400
1600
1800
0
2
4
6
8
10

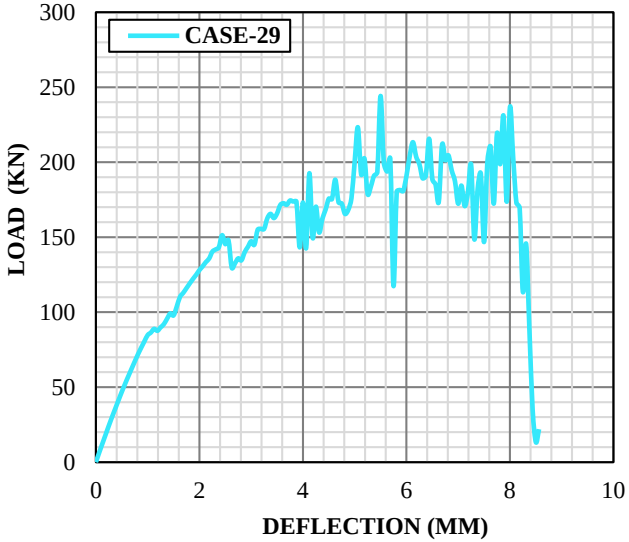
CASE-29
LOAD (KN)
DEFLECTION (MM)
0
50
100
150
200
250
300
0
2
4
6
8
10

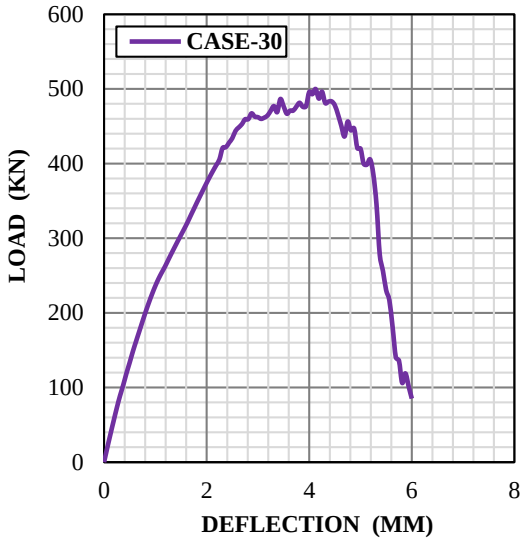
CASE-30
LOAD (KN)
DEFLECTION (MM)
0
100
200
300
400
500
600
0
2
4
6
8

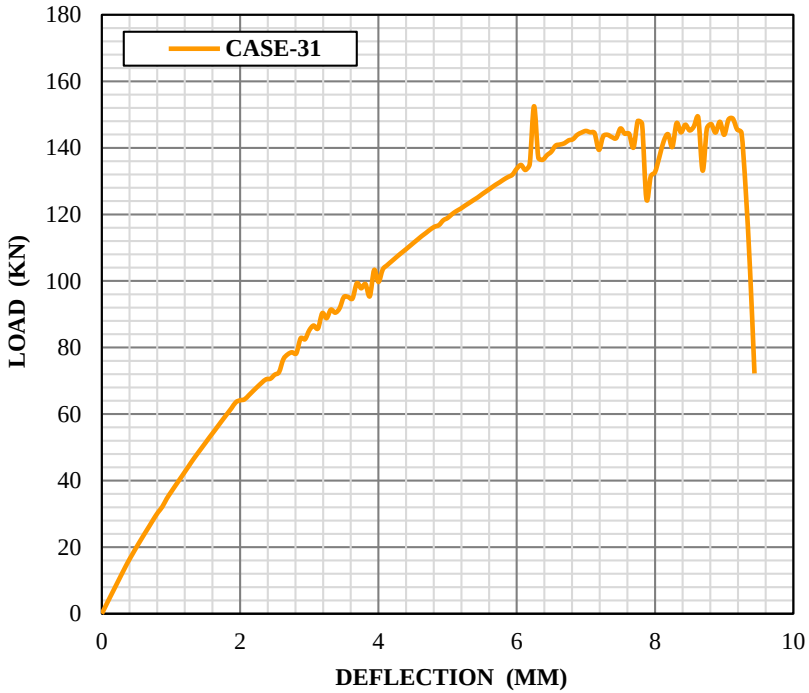
CASE-31
LOAD (KN)
DEFLECTION (MM)
0
20
40
60
80
100
120
140
160
180
0
2
4
6
8
10

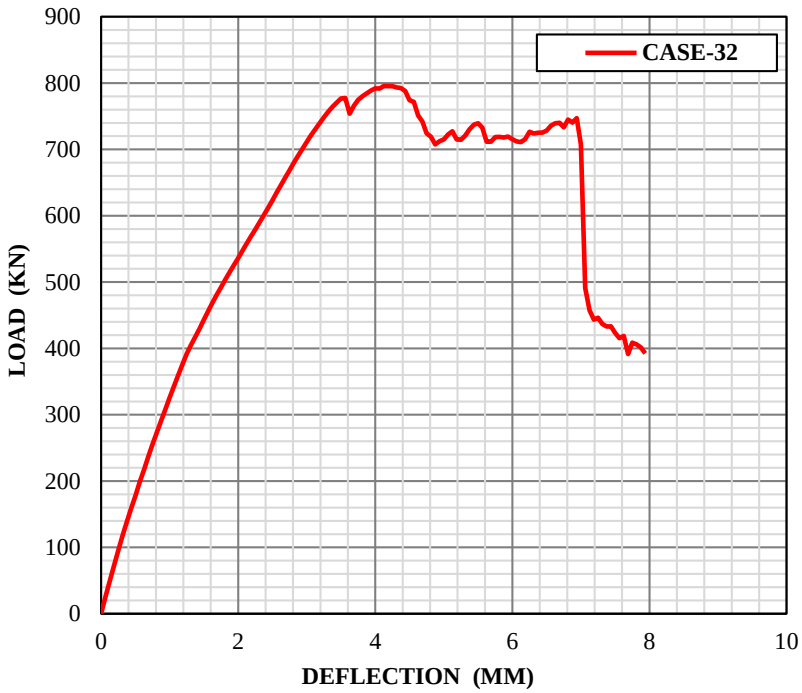
CASE-32
LOAD (KN)
DEFLECTION (MM)
0
100
200
300
400
500
600
700
800
900
0
2
4
6
8
10